UC San Diego

UC San Diego Electronic Theses and Dissertations

Title

KLC1 deficiency alters APP and tau levels and impairs neuronal development

Permalink

https://escholarship.org/uc/item/4wk3z2cf

Author

Killian, Rhiannon Lynn

Publication Date

2011

Peer reviewed|Thesis/dissertation

eScholarship.org Powered by the California Digital Library
University of California

UNIVERSITY OF CALIFORNIA, SAN DIEGO

KLC1 deficiency alters APP and tau levels and impairs neuronal development

A dissertation submitted in partial satisfaction of the requirements for the degree
Doctor of Philosophy

in

Biomedical Sciences

by

Rhiannon Lynn Killian

Committee in charge:

Professor Lawrence S. B. Goldstein, Chair
Professor Don W. Cleveland
Professor Marilyn G. Farquhar
Professor Edward H. Koo
Professor Jean Y. J. Wang

2011

The Dissertation of Rhiannon Lynn Killian is approved, and it is acceptable in quality and form for publication on microfilm and electronically:

Chair

University of California, San Diego

2011

DEDICATION

As the culmination of six years of unceasing effort, I can do no other but dedicate this work to my children, Patrick, Killian and Conley, who I hope will one day understand why I was in the laboratory when they awoke and ‘too busy’ when at home.

EPIGRAPH

It is a popular delusion that the scientific enquirer is under an obligation not to go beyond generalization of observed facts...but anyone who is practically acquainted with scientific work is aware that those who refuse to go beyond the facts, rarely get as far.

Thomas Henry Huxley (1825-95) English biologist

We are in the ordinary position of scientists of having to be content with piecemeal improvements: we can make several things clearer, but we cannot make anything clear.

Frank Plumpton Ramsey (1903-1930) English mathematician

For a successful technology, reality must take precedence over public relations, for Nature cannot be fooled.

Richard Feynman (1918-1988) American physicist

TABLE OF CONTENTS

DEDICATION iv
EPIGRAPH v
TABLE OF CONTENTS vi
LIST OF FIGURES viii
ACKNOWLEDGEMENTS ix
VITA x
ABSTRACT OF THE DISSERTATION xi
CHAPTER 1 1
Introduction 1
Kinesin-1 structure and function 1
Alzheimer's Disease (AD) and axonal transport defects 4
Modeling aspects of AD in mouse and man 7
References 12
CHAPTER 2 19
Kinesin-1C and KLC1 affect neuronal development and APP levels in murine hippocampal neurons 19
Abstract 19
Introduction 21
Materials and Methods 23
Preparation of primary mouse hippocampal cultures 23
Analysis of hippocampal axons 23
Immunofluorescence characterization of primary mouse hippocampal cultures 24
Western blot analysis of protein levels. 25
Quantification of Aβ/P3 26
Results and Discussion 27
Murine KLC1 and Kinesin-1C protein levels in primary hippocampal cultures are related 27
Kinesin-1C and KLC1 may function in hippocampal neuron development 29
Tau levels are unchanged in primary hippocampal neurons with reduced KLC1. 30
Altered extracellular Aβ/p3 levels in Kinesin-1C-/- hippocampal cultures 32
Characterization of KLC1-/- and Kinesin-1C-/- hippocampal primary cultures 34
Conclusions 35
References 44
CHAPTER 3 48
Kinesin light chain 1 reduction impairs human embryonic stem cell neural differentiation and amyloid precursor protein metabolism 48
Abstract 48
Introduction 49
Materials and Methods 51

Cell culture and subcloning of undifferentiated Hues9 hESC lines 51
Flow cytometry 52
Western blot analysis of protein levels 53
Immunofluorescence 54
Neural differentiation of hESC 55
Brightfield imaging of cultures 56
Neural precursor culture, viral transduction and differentiation 56
Aβ and soluble APP (sAPP) quantification 57
Results 57
KLC1 reduction does not alter hESC morphology or pluripotency 57
KLC1 depleted hESC produce cultures containing neural precursors (NPs) 58
Neural precursors with reduced KLC1 do not proliferate normally 60
KLC1-deficient human neural cells exhibit reduced levels of microtubule related proteins 61
Reduced KLC1 alters APP metabolism in human neural cultures derived from hESC 65
Discussion 66
A role for the KLC1 subunit of Kinesin-1 in NP maintenance? 66
KLC1 depletion affects microtubule associated proteins 68
Effect of KLC1 reduction on APP metabolism in human neural cultures. 69
Summary 71
Acknowledgements 71
References 89
CHAPTER 4 94
Discussion 94
Co-regulation of KLC1 and Kinesin-1C protein levels 94
Roles for KLC1 (and Kinesin-1C) in neural development 96
Tau and Kinesin-1 subunits KLC1 and Kinesin-1C 102
Does Kinesin-1C regulate APP levels and metabolism by controlling APP transport? 105
Model for KLC1 functions in neural development and in regulating neuronal Tau and Aβ levels. 111
Prospects for human pluripotent stem cell based systems for modeling human development, biology and disease 113
References 121

LIST OF FIGURES

Figure 1.1. Kinesin-1 is composed of heavy and light chain dimers……..... 9
Figure 1.2. Proteolytic processing of APP..……...…. 10
Figure 1.3. Domain structure of microtubule-associated protein Tau……..... 11
Figure 2.1. Kinesin-1C and KLC1 protein levels are interdependent……..... 37
Figure 2.2. Kinesin-1C-/- and KLC1-/- hippocampal neurons polarize……..... 38
Figure 2.3. Kinesin-1C and KLC1-/- hippocampal neurons exhibit normal Tau... 40
Figure 2.4. APP full length and extracellular γ-secretase products are reduced.... 42
Figure 2.5. Neuronal marker composition of primary hippocampal cultures……. 43
Figure 3.1. Scheme for generating pluripotent stem cell lines with KLC1……..... 72
Figure 3.2. Undifferentiated hESC exhibiting reduced KLC1……... 73
Figure 3.3. Undifferentiated KLC1-suppressed hESC exhibit normal……...… 74
Figure 3.4. Undifferentiated KLC1-reduced hESC display normal localization… 75
Figure 3.5. Normal proportions of undifferentiated hESC with reduced KLC1.... 76
Figure 3.6. Neural induction cultures derived from hESC with reduced KLC1.... 78
Figure 3.7. NP cell surface signatures of neural induction cultures……..……. 80
Figure 3.8. Defective proliferation of NPs derived from KLC1 suppressed hESC 81
Figure 3.9. Scheme for infection and sorting of NPs with lentivirus……..……... 82
Figure 3.10. KLC1 and KHC Kinesin-1C subunits are reduced in neural cultures 83
Figure 3.11. Time-course and morphology of neural cultures derived from……. 84
Figure 3.12. Neuron-like cells derived from PA6 feeder differentiation of KLC1 85
Figure 3.13. Reduced neural microtubule associated markers in neural cultures... 86
Figure 3.14. Human neural cultures with reduced KLC1 exhibit altered APP….. 88
Figure 4.1. Model for how KLC1 reduction in pluripotent stem cells may affect. 117
Figure 4.2. Cell signaling pathways governing proliferation in control and KLC1 118
Figure 4.3. Model of KLC1 Kinesin-1 subunit functions in neural cells……..... 120

ACKNOWLEDGEMENTS

My heartfelt thanks go to the many individuals who have shaped my training. I am eternally grateful to Larry Goldstein for providing a fantastic opportunity for me to conduct science at the cutting edge. I thank my family for their unwavering support and encouragement. I am grateful to my thesis committee members for sharing their expertise and their time. Thanks also to fellow Goldstein lab members for many great conversations and good times. I wish all of you the best.

Chapter 3, in part, has been submitted for publication of the material as it may appear in PLoS ONE. Rhiannon L. Killian, Jessica D. Flippin, Cheryl Herrera, Angels Almenar-Queralt and Lawrence S. B. Goldstein, 2011. The dissertation author was the primary investigator and author of this paper.

VITA

Rhiannon Lynn Killian Nolan

2011	Doctor of Philosophy, Biomedical Sciences, University of California, San Diego
1995-2004	Research Technician, Los Alamos National Laboratory
1993	Bachelor of Science, General Science, Minor in Anthropology, Pennsylvania State University

Publications

Killian, R. L., J. D. Flippin, C. Herrera, A. Almenar-Queralt and L. S. B. Goldstein. Kinesin light chain 1 suppression impairs human embryonic stem cell neural differentiation and amyloid precursor protein metabolism (in revision).

Yuan, S. H., J Martin, J. Elia, J. Flippin, R. I. Paramban, M. P. Hefferan, J. G. Vidal, Y. Mu, **R. L. Killian**, M. A. Israel, N. Emre, S. Marsala, M. Marsala, F. H. Gage, L. S. B. Goldstein, and C. T. Carson. Cell-surface marker signatures for the isolation of neural stem cells, glia and neurons derived from human pluripotent stem cells (2011) PLoS One Mar 2;6(3):e17540.

Shah, S.B., **R. Nolan**, E. Davis, G.B. Stokin, I. Niesman, I. Canto, C. Glabe L.S. Goldstein. Examination of potential mechanisms of amyloid-induced defects in neuronal transport. (2009) Neurobiol Dis. Oct;36(1):11-25.

C Kiss, H Fisher, E. Pesavento, M. Dai, R. Valero, M. Ovecka, **R. Nolan**, L. Phipps, N. Velappan, L. Chasteen, J. Martinez, G. S. Waldo, P. Pavlik, A. R.M. Bradbury (2006) Antibody binding loop insertions as diversity elements. Nucleic Acids Research 34(19):e132.

Goodwin, P. M., **R. L. Nolan** and H. Cai (2004) Single-molecule spectroscopy for nucleic acid analysis: a new approach for disease detection and genomic analysis. Current Pharmaceutical Biotechnology (5)3: 271-8.

Nolan, R. L., H. Cai, J. P. Nolan and P. M. Goodwin (2003) A simple quenching method for fluorescence background reduction and its application to the direct, quantitative detection of specific mRNA. Analytical Chemistry 75(22): 6236-6243.

Lauer, S. L., **R. L. Nolan**, B. Goldstein, J. P. Nolan (2002) Analysis of cholera toxin-ganglioside interactions by flow cytometry. Biochemistry 41:1742-1751.

Ruscetti, T., J. Newman, T. S. Peat, J. Francis, **R. Nolan**, T. C. Terwilliger, S.R. Peterson, B. L. Lehnert (1998) A non-denaturing purification scheme for the DNA-binding domain of poly(ADP-ribose) polymerase, a structure specific DNA-binding protein. Protein Expression and Purification 14:79-86.

ABSTRACT OF THE DISSERTATION

KLC1 deficiency alters APP and tau levels and impairs neuronal development

by

Rhiannon Lynn Killian

Doctor of Philosophy in Biomedical Sciences

University of California, San Diego, 2011

Professor Lawrence S.B. Goldstein

Kinesin-1 is a microtubule-based motor essential for cellular organization and function. Which of three possible heavy chain (KHC) and four possible light chain (KLC) homodimer subunits assemble to form heterotetramers and the unique roles particular Kinesin-1 holoenzymes perform in neural tissues is largely unknown. I characterized functions of neuronally-enriched subunits KLC1 and Kinesin-1C in cultured murine KLC1-/- and Kinesin-1C-/- hippocampal neurons and human embryonic stem cell (hESC)-derived neural cultures. In both mouse and human cultures reduction in KLC1 correlated with reduction in Kinesin-1C; in Kinesin-1C-/- mouse cultures KLC1 levels were reduced, suggesting these subunits may function together. Extending on previous analyses of mice lacking these full length proteins, I

examined the effect of reduction in full KLC1 and Kinesin-1C on mouse neuron development and production of human neural progenitors and neural cultures. I found that while Kinesin-1C and KLC1 may play minor roles in the neuronal development of murine neurons, reduction of KLC1 in hESC impairs proliferative capacity of neural precursor (NP) progeny suggesting that KLC1 may be essential for NP maintenance. Neuron-like cells in neural cultures derived from KLC1-reduced hESC have less microtubule associated proteins (MAPs) and shorter projections, suggesting KLC1 and Kinesin-1C may be required for proper development of human neurons. Analyses of adult mice with reduced full length KLC1 suggest this subunit may also influence levels of Amyloid-β (Aβ) and phosphorylated Tau (pTau), the two principle components of Alzheimer's Disease (AD) hallmark lesions. Therefore I used mouse neurons and KLC1-reduced human neural cultures to evaluate levels of these proteins and the Aβ parent molecule amyloid precursor protein (APP). While I found no difference in Tau levels in murine neurons, in human neural cultures Tau was reduced along with other MAPs, suggesting KLC1 may impact Tau levels via more general effects on microtubules. While no change in APP levels was observed in mouse KLC1-/- neurons, mouse Kinesin-1C-/- neurons and human KLC1-reduced neural cultures exhibited lower extracellular Aβ/p3 which may be due to lower APP levels. Altogether my data suggest that Kinesin-1C and KLC1 may form functional Kinesin-1 holoenzymes that affect proliferation of NPs, neuronal development and APP levels.

CHAPTER 1

Introduction

Kinesin-1 structure and function

Intracellular transport of cellular cargos on microtubules enables fundamental cellular processes such as division, polarization and translocation. The molecular motors kinesin and dynein orchestrate ATP-dependent bidirectional cargo movement on microtubules with most kinesins moving materials in the anterograde direction toward the growing end of microtubules and dyneins transporting cargos in the retrograde direction towards the minus end of microtubules [1]. Structurally, Kinesin-1 is a heterotetramer consisting of pairs of heavy (KHC) and light chains (KLCs; Figure 1.1A) [2]. Each KHC consists of an amino-terminal motor domain, a flexible linker region and a carboxyl-terminal globular region which binds to KLC (Figure 1.1B). KLCs contain an amino-terminal heptad repeat domain which binds KHC, a small linker domain and six tetratricopeptide repeats (TPRs) that associate with cargos

(Figure 1.1C). Functionally, KHC powers movement of attached cargos while KLC has been implicated in regulation of heavy chain activity and in mediation of cargobinding [3]. Mammalian Kinesin-1 can assemble from one of three possible heavy chain gene products: Kinesin-1A, Kinesin-1B or Kinesin-1C (formerly called KIF5A, KIF5B and KIF5C) and at least one of four possible light chains: KLC1, KLC2, KLC3 and KLC4 [4-8]. Thus Kinesin-1 is theoretically capable of assembling into many potentially distinct holoenzymes. However, several studies suggest the holoenzyme is in fact comprised of homodimers [4,6,9-11], but which homodimers associate to form a functional Kinesin-1 is not clear. Both KLC1 and KLC2 can immunoprecipitate Kinesin-1A, Kinesin-1B or Kinesin-1C although KLC2 may be more likely to associate with Kinesin-1B while KLC1 interacts more with Kinesin-1A or Kinesin-1C [4,9].

Many questions remain about how the heavy and light chain subunits assemble and the unique functions these holoenzymes perform in cells. Why is there a need for multiple KHC and KLC Kinesin-1 subunits in mammalian cells? Does it reflect the vital functions carried out by Kinesin-1 such that if one motor is inactivated, there are two others to take over? Or does each subunit have distinct roles within cells? Studies of tissue specific expression patterns and animals with defective Kinesin-1 subunits suggest they may have specialized roles. Kinesin-1B and KLC2 are widely expressed in all tissues; KLC1, Kinesin-1A and Kinesin-1C are enriched in neural tissues; KLC3 has thus far been detected in testes and certain cerebellar neurons, while KLC4 has only as yet been identified at the genomic level [4,8,10,12]. Kinesin-1A-/- mice die at

birth of a breathing abnormality while mice with Cre-induced excision of Kinesin-1A under the control of the Synapsin promoter can survive for several months but are 50% smaller than wildtype, exhibit sensory and larger caliber motor neuron degeneration and abnormal hind leg posture [13]. Interestingly, human point mutations in Kinesin-1A lead to spastic paraplegia characterized by weakness and spasticity in the legs [14]. Kinesin-1B-/- mice die mid-gestation [12]. Kinesin-1C-/- mice have smaller brains and fewer motor neurons than wildtype [10]. KLC1-/- mice are smaller in stature, have reduced white matter in the brain and spinal cord, reduced numbers of motor neurons and axonopathies containing accumulations of cytoskeletal and membrane-bound organelles [15,16]. KLC2, KLC3 and KLC4 mutant mice have not been reported. Differential tissue expression patterns and mutant animal phenotypes suggest that Kinesin-1 subunits may have distinct functions that arise during development and persist in the adult animal.

It is not surprising that highly polarized cells like neurons, which must control the transport of cargoes across a cell that in humans can reach a meter long, express multiple Kinesin-1 subunit isoforms. The general question is how does Kinesin-1 contribute to neuronal development and function? Specific Kinesin-1 subunits have been implicated in the transport of neuronal cargos such as neurofilaments and the mammalian prion protein [17,18]. Several studies in rodent primary hippocampal cultures suggest that Kinesin-1 subunits are required for the proper development of neurons. A truncated constitutively active Kinesin-1C-YFP fusion protein localizes to the tip of the neurite destined to develop into the axon [19]. Suppression of Kinesin-

1B alone, Kinesin-1A, Kinesin-1B and Kinesin-1C or KLC1 and KLC2 decreases the length of cultured rodent neurons [20-22]. Simultaneous siRNA reduction of all three Kinesin-1 motor subunits increases the fraction of neurons with multiple axons [22]. However, it is still unknown which particular subunits are required for these neuronal functions, whether such functions are neuron type dependent and whether these functions can be filled by the other subunits.

Alzheimer's Disease (AD) and axonal transport defects

Alzheimer's Disease is a devastating neurodegenerative disease afflicting millions in the U.S. alone. AD is characterized clinically by progressive memory loss and cognitive decline. Pathologically, AD brains exhibit amyloid plaques [23], neurofibrillary tangles (NFTs) [24,25], synapse loss [26-28], axonal defects [23,29-31] and neurodegeneration [32]. Amyloid plaques are extracellular protein deposits principally comprised of aggregated Aβ peptide predominantly 42 amino acids in length [33,34]. This secreted peptide is produced by proteolysis of the type I membrane protein APP [35-38]. NFTs form inside neurons from aberrantly phosphorylated and mislocalized Tau assembled into paired helical filaments (PHF) [39-43]. Axonal defects manifest as axonal swellings containing accumulations of cytoskeletal proteins, motor proteins and their cargos [44-46], and as we showed recently, Aβ fibrils can induce such swellings in differentiated neuroblastoma cells [47].

About 1% of AD cases are inherited early onset forms (familial AD or FAD) associated with mutations in the APP [48] and Presenilin [49-52] genes. APP is a type I membrane protein of uncertain function [53]. Presenilin is the catalytic component of the intramembrane cleaving γ–secretase, a protease complex also containing Nicastrin, Anterior Pharanx Defective 1 (APH-1) and Presenilin Enhancer 2 (PEN-2) [54]. APP triplication (for example Trisomy 21) also causes AD-like symptoms [55,56]. Although mutations or overexpression of APP and/or presenilin causes FAD, most cases of AD are sporadic with no known cause.

APP is metabolized via α or β cleavage pathways. In the α cleavage pathway, α- and γ-secretases cleave APP to produce amino terminal soluble APP (sAPP-α), internal p3 and APP intracellular domain (AICD) C terminal (Figure 1.2A). In the β cleavage pathway, β- [57] and γ-secretases cut APP to generate sAPP-β, Aβ and AICD (Figure 1.2B). APP metabolism by α vs. β pathways is regulated both by cell type (α secretases are expressed widely while β secretase is enriched in neurons) as well as intracellular location (β secretase is located in and active at the pH of early endosomes and α secretases tend to localize to the cell surface) [58].

APP is transported into axons [59,60] and several studies suggest Kinesin-1 is responsible for this movement. Kinesin-1B antisense treatment of cultured neurons confines endogenous APP to the cell body [61,62] while reduction in the full length KLC1 reduces transport of transfected APP-YFP in mouse hippocampal neurons [16,46]. Further, APP forms a complex with KLC1 [63-65]. Evidence suggests that reduction in full length KLC1 also increases brain levels of transgenic human Aβ in

aged mice [46], suggesting Kinesin-1 function can also affect APP metabolites. This brings up several related questions. Are increased Aβ levels only evident in aged KLC1 animals or is the effect detectible earlier? Are the changes in Aβ levels exclusive to overexpression of human mutant APP or is this a more general phenomenon applicable to endogenous levels in the mouse? Does Kinesin-1 reduction alter Aβ levels in human cells expressing normal endogenous APP? Is the neuronal Kinesin-1C subunit responsible for any observed differences in Aβ levels?

While APP metabolism is responsible for the production of the principle component of amyloid plaques, Tau is the main element in the second AD hallmark lesion – the NFT. No known Tau mutations cause AD, although many Tau mutations lead to frontotemporal dementia with Parkinsonism linked to chromosome 17, another adult-onset disease characterized by dementia [66]. Structurally, Tau is comprised of an amino terminal projection domain and three to four microtubule binding repeats which are flanked by disease-associated phosphorylation sites (Figure 1.2). Functionally, Tau promotes the elongation and stability of microtubules [67-69]. Tau expression is most prominent in neurons and the protein is enriched in the axonal compartment [70], but mislocalizes to cell bodies in Tauopathies such as AD [71].

One study suggests normal axonal Tau transport in rat cortical neurons may be Kinesin-1 dependent [72]. Disruption of Kinesin-1 transport in the KLC1-/- mouse leads to axonopathies in the adult spinal cord which contain hyperphosphorylated Tau. Very recently it was reported that KLC1+/- adult mice expressing transgenic mutant human Tau exhibit higher proportions of cell bodies in the hippocampus and spinal

cord with pTau [73], suggesting reduced Kinesin-1 function may lead to increased hyperphosphorylated Tau. However much remains unknown about this connection. Are increased phosphorylated Tau levels only apparent in aged animals or is the effect detectible earlier? Can we model these changes in a tissue culture system? Are changes in Tau levels more apparent in human neurons expressing endogenous Tau? Is the neuronal Kinesin-1C subunit responsible for any observed differences in Tau levels?

Modeling aspects of AD in mouse and man

Various mice that overexpress mutant human presenilin, APP and/or Tau proteins have been useful in modeling aspects of AD pathogenesis [74,75]. However, none simultaneously recapitulate all the central features of the disease. This may be due to differences between humans and mice in lifespan (humans live ~40X longer) or in endogenous protein sequences or regulation (mouse Aβ does not aggregate and mouse Tau inhibits human Tau NFT formation). Although a human AD model system would be ideal, human AD and control brains are scarce and thus their use in controlled studies is problematic. Hence the development of cultures of human embryonic stem cells (hESC) [76] and more recently induced pluripotent stem cells (iPS) [61,77] offer the opportunity to study aspects of AD pathogenesis in human neural cells. Such pluripotent stem cells (hPSC) can proliferate indefinitely in culture, are genetically malleable, and express proteins under endogenous transcriptional, translational and post-translational control. Further, hPSC are capable of

differentiating into any somatic cell, including neurons, for example using a method we reported earlier this year [78]. Further, tissue culture systems are well-suited to high-throughput drug screens. Therefore I set up a hESC-based tissue culture system to model the effect of KLC1 reduction on neural development, pTau/Tau levels and APP metabolism in neural cultures. To bridge the gap between the well established mouse model and the novel human system and to address whether Aβ and Tau phenotypes in the aged mice are likely to be related to aging or mechanisms conserved between the species, I also examined the effects of reduced full length KLC1 and Kinesin-1C levels on neuronal development, pTau/Tau and APP levels in hippocampal neurons derived from KLC1 and Kinesin-1C mutant mice.

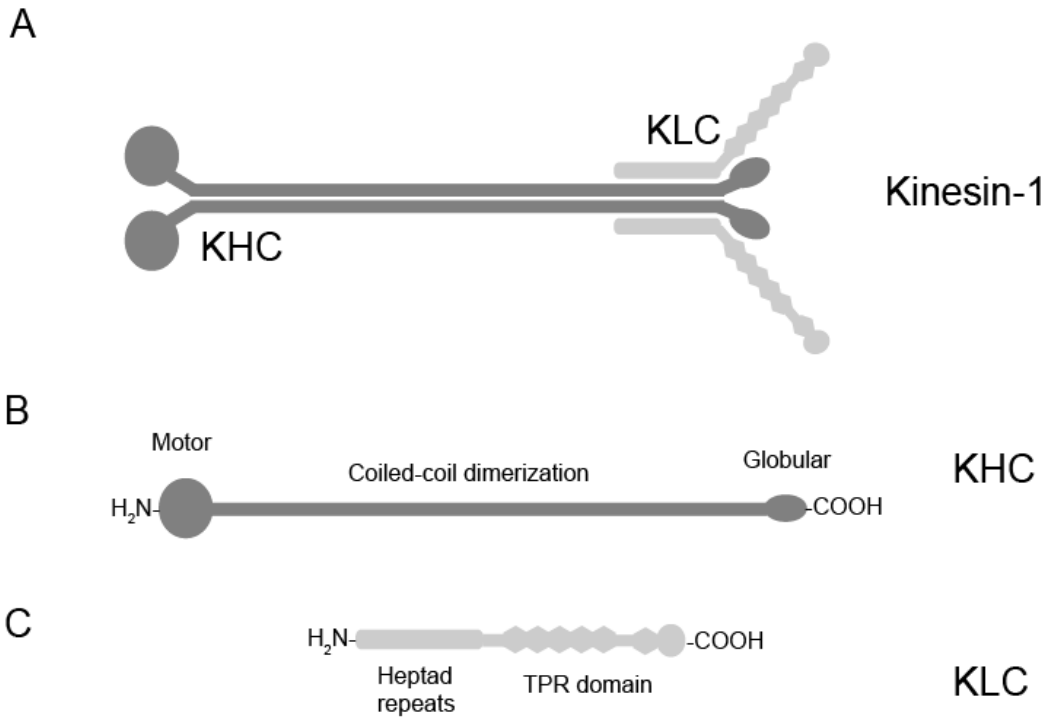


Figure 1.1. Kinesin-1 is composed of heavy and light chain dimers. (A) Pairs of KHCs and KLCs combine to form a functional Kinesin-1 holoenzyme. (B) KHCs have three major structural domains: the microtubule binding and ATP-hydrolyzing motor head, a long coiled-coil dimerization domain which also associates with KLCs, and a globular tail. (C) KLCs consist of a heptad repeat domain which binds the KHC coiled-coil domain, a small linker domain, six imperfect TPR repeats and a variable carboxyl-terminal tail.

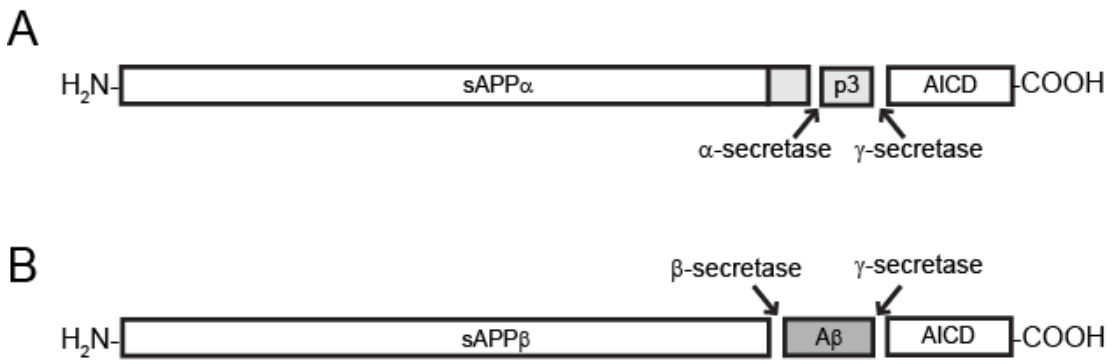


Figure 1.2. Proteolytic processing of APP. APP proteolytic processing by either α- and γ-secretases (A) or β- and γ-secretases (B) produces sAPPα, p3 and AICD (A) or sAPPβ, Aβ (shaded dark grey; B) and AICD fragments, respectively.

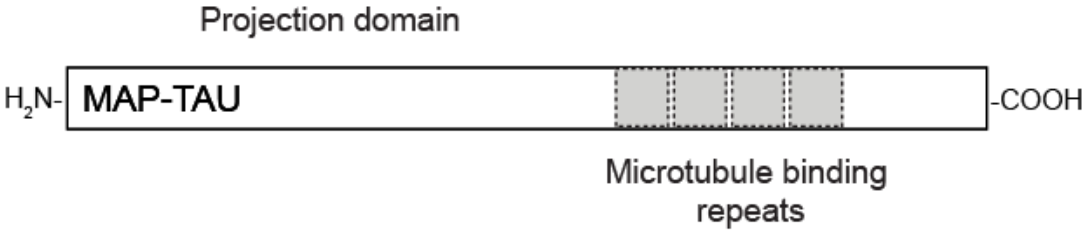


Figure 1.3. Domain structure of microtubule-associated protein Tau. Tau contains an amino-terminal projection domain which protrudes from the microtubule surface when Tau is bound to the microtubule and three to four microtubule binding repeats (grey shading) which associate with microtubules.

References

1. Vale RD (2003) The molecular motor toolbox for intracellular transport. Cell 112: 467-480.

2. Hirokawa N, Pfister KK, Yorifuji H, Wagner MC, Brady ST, et al. (1989) Submolecular domains of bovine brain kinesin identified by electron microscopy and monoclonal antibody decoration. Cell 56: 867-878. doi:10.1016/0092-8674(89)90691-0

3. Verhey KJ, Kaul N, Soppina V (2010) Kinesin Assembly and Movement in Cells. Annu Rev Biophys. Available: http://www.ncbi.nlm.nih.gov/pubmed/21332353. Accessed 15 Mar 2011.

4. Rahman A, Friedman DS, Goldstein LS (1998) Two kinesin light chain genes in mice. Identification and characterization of the encoded proteins. J. Biol. Chem 273: 15395-15403.

5. Cabeza-Arvelaiz Y, Shih LC, Hardman N, Asselbergs F, Bilbe G, et al. (1993) Cloning and genetic characterization of the human kinesin light-chain (KLC) gene. DNA Cell Biol 12: 881-892.

6. Niclas J, Navone F, Hom-Booher N, Vale RD (1994) Cloning and localization of a conventional kinesin motor expressed exclusively in neurons. Neuron 12: 1059-1072.

7. Lamerdin JE, Stilwagen SA, Ramirez MH, Stubbs L, Carrano AV (1996) Sequence analysis of the ERCC2 gene regions in human, mouse, and hamster reveals three linked genes. Genomics 34: 399-409. doi:10.1006/geno.1996.0303

8. Xia C, Rahman A, Yang Z, Goldstein LS (1998) Chromosomal localization reveals three kinesin heavy chain genes in mouse. Genomics 52: 209-213. doi:10.1006/geno.1998.5427

9. DeBoer SR, You Y, Szodorai A, Kaminska A, Pigino G, et al. (2008) Conventional kinesin holoenzymes are composed of heavy and light chain homodimers. Biochemistry 47: 4535-4543. doi:10.1021/bi702445j

10. Kanai Y, Okada Y, Tanaka Y, Harada A, Terada S, et al. (2000) KIF5C, a Novel Neuronal Kinesin Enriched in Motor Neurons. J. Neurosci. 20: 6374-6384.

11. Kamal A, Almenar-Queralt A, LeBlanc JF, Roberts EA, Goldstein LS (2001) Kinesin-mediated axonal transport of a membrane compartment containing beta-

secretase and presenilin-1 requires APP. Nature 414: 643-648. doi:10.1038/414643a

12. Tanaka Y, Kanai Y, Okada Y, Nonaka S, Takeda S, et al. (1998) Targeted disruption of mouse conventional kinesin heavy chain, kif5B, results in abnormal perinuclear clustering of mitochondria. Cell 93: 1147-1158.

13. Xia C-H, Roberts EA, Her L-S, Liu X, Williams DS, et al. (2003) Abnormal neurofilament transport caused by targeted disruption of neuronal kinesin heavy chain KIF5A. J. Cell Biol 161: 55-66. doi:10.1083/jcb.200301026

14. Reid E, Kloos M, Ashley-Koch A, Hughes L, Bevan S, et al. (2002) A Kinesin Heavy Chain (KIF5A) Mutation in Hereditary Spastic Paraplegia (SPG10). Am J Hum Genet 71: 1189-1194.

15. Rahman A, Kamal A, Roberts EA, Goldstein LSB (1999) Defective Kinesin Heavy Chain Behavior in Mouse Kinesin Light Chain Mutants. J Cell Biol 146: 1277-1288.

16. Falzone TL, Stokin GB, Lillo C, Rodrigues EM, Westerman EL, et al. (2009) Axonal Stress Kinase Activation and Tau Misbehavior Induced by Kinesin-1 Transport Defects. J. Neurosci. 29: 5758-5767. doi:10.1523/JNEUROSCI.0780-09.2009

17. Uchida A, Alami NH, Brown A (2009) Tight Functional Coupling of Kinesin-1A and Dynein Motors in the Bidirectional Transport of Neurofilaments. Mol. Biol. Cell 20: 4997-5006. doi:10.1091/mbc.E09-04-0304

18. Encalada SE, Szpankowski L, Xia C-H, Goldstein LSB (2011) Stable Kinesin and Dynein assemblies drive the axonal transport of Mammalian prion protein vesicles. Cell 144: 551-565. doi:10.1016/j.cell.2011.01.021

19. Jacobson C, Schnapp B, Banker GA (2006) A Change in the Selective Translocation of the Kinesin-1 Motor Domain Marks the Initial Specification of the Axon. Neuron 49: 797-804. doi:10.1016/j.neuron.2006.02.005

20. Ferreira A, Niclas J, Vale RD, Banker G, Kosik KS (1992) Suppression of kinesin expression in cultured hippocampal neurons using antisense oligonucleotides. J. Cell Biol 117: 595-606.

21. Kimura T, Watanabe H, Iwamatsu A, Kaibuchi K (2005) Tubulin and CRMP-2 complex is transported via Kinesin-1. J. Neurochem 93: 1371-1382. doi:10.1111/j.1471-4159.2005.03063.x

22. Konishi Y, Setou M (2009) Tubulin tyrosination navigates the kinesin-1 motor domain to axons. Nat. Neurosci 12: 559-567. doi:10.1038/nn.2314

23. Terry RD, Gonatas NK, Weiss M (1964) Ultrastructural studies in Alzheimer's presenile dementia. Am. J. Pathol 44: 269-297.

24. Terry RD (1963) The fine structure of neurofibrillary tangles in Alzheimer's Disease. J. Neuropathol. Exp. Neurol 22: 629-642.

25. Kidd M (1963) Paired helical filaments in electron microscopy of Alzheimer's Disease. Nature 197: 192-193.

26. Perdahl E, Adolfsson R, Alafuzoff I, Albert KA, Nestler EJ, et al. (1984) Synapsin I (protein I) in different brain regions in senile dementia of Alzheimer type and in multi-infarct dementia. J. Neural Transm 60: 133-141.

27. Hamos JE, DeGennaro LJ, Drachman DA (1989) Synaptic loss in Alzheimer's disease and other dementias. Neurology 39: 355-361.

28. Masliah E, Terry RD, DeTeresa RM, Hansen LA (1989) Immunohistochemical quantification of the synapse-related protein synaptophysin in Alzheimer disease. Neuroscience Letters 103: 234-239. doi:10.1016/0304-3940(89)90582-X

29. Krigman MR, Feldman RG, Bensch K (1965) Alzheimer's presenile dementia. A histochemical and electron microscopic study. Lab. Invest 14: 381-396.

30. Gonatas NK, Anderson W, Evangelista I (1967) The contribution of altered synapses in the senile plaque: an electron microscopic study in Alzheimer's dementia. J. Neuropathol. Exp. Neurol 26: 25-39.

31. Masliah E, Mallory M, Deerinck T, DeTeresa R, Lamont S, et al. (1993) Re-evaluation of the structural organization of neuritic plaques in Alzheimer's disease. J. Neuropathol. Exp. Neurol 52: 619-632.

32. Terry RD, Peck A, DeTeresa R, Schechter R, Horoupian DS (1981) Some morphometric aspects of the brain in senile dementia of the Alzheimer type. Ann. Neurol 10: 184-192. doi:10.1002/ana.410100209

33. Glenner GG, Wong CW (1984) Alzheimer's disease: initial report of the purification and characterization of a novel cerebrovascular amyloid protein. Biochem. Biophys. Res. Commun 120: 885-890.

34. Masters CL, Simms G, Weinman NA, Multhaup G, McDonald BL, et al. (1985) Amyloid plaque core protein in Alzheimer disease and Down syndrome. Proc Natl Acad Sci U S A 82: 4245-4249.

35. Seubert P, Vigo-Pelfrey C, Esch F, Lee M, Dovey H, et al. (1992) Isolation and quantification of soluble Alzheimer's beta-peptide from biological fluids. Nature 359: 325-327. doi:10.1038/359325a0

36. Haass C, Schlossmacher MG, Hung AY, Vigo-Pelfrey C, Mellon A, et al. (1992) Amyloid beta-peptide is produced by cultured cells during normal metabolism. Nature 359: 322-325. doi:10.1038/359322a0

37. Shoji M, Golde TE, Ghiso J, Cheung TT, Estus S, et al. (1992) Production of the Alzheimer amyloid beta protein by normal proteolytic processing. Science 258: 126-129.

38. Kang J, Lemaire HG, Unterbeck A, Salbaum JM, Masters CL, et al. (1987) The precursor of Alzheimer's disease amyloid A4 protein resembles a cell-surface receptor. Nature 325: 733-736. doi:10.1038/325733a0

39. Grundke-Iqbal I, Iqbal K, Tung YC, Quinlan M, Wisniewski HM, et al. (1986) Abnormal phosphorylation of the microtubule-associated protein tau (tau) in Alzheimer cytoskeletal pathology. Proc. Natl. Acad. Sci. U.S.A 83: 4913-4917.

40. Ihara Y, Nukina N, Miura R, Ogawara M (1986) Phosphorylated tau protein is integrated into paired helical filaments in Alzheimer's disease. J. Biochem 99: 1807-1810.

41. Nukina N, Ihara Y (1986) One of the antigenic determinants of paired helical filaments is related to tau protein. J. Biochem 99: 1541-1544.

42. Kosik KS, Joachim CL, Selkoe DJ (1986) Microtubule-associated protein tau (tau) is a major antigenic component of paired helical filaments in Alzheimer disease. Proc. Natl. Acad. Sci. U.S.A 83: 4044-4048.

43. Wood JG, Mirra SS, Pollock NJ, Binder LI (1986) Neurofibrillary tangles of Alzheimer disease share antigenic determinants with the axonal microtubule-associated protein tau (tau). Proc. Natl. Acad. Sci. U.S.A 83: 4040-4043.

44. Yagishita S (1978) Morphological investigations on axonal swellings and spheroids in various human diseases. Virchows Arch A Pathol Anat Histol 378: 181-197.

45. Su JH, Cummings BJ, Cotman CW (1993) Identification and distribution of axonal dystrophic neurites in Alzheimer's disease. Brain Res 625: 228-237.

46. Stokin GB, Lillo C, Falzone TL, Brusch RG, Rockenstein E, et al. (2005) Axonopathy and Transport Deficits Early in the Pathogenesis of Alzheimer's Disease. Science 307: 1282-1288. doi:10.1126/science.1105681

47. Shah SB, Nolan R, Davis E, Stokin GB, Niesman I, et al. (2009) Examination of potential mechanisms of amyloid-induced defects in neuronal transport. Neurobiol. Dis 36: 11-25. doi:10.1016/j.nbd.2009.05.016

48. Goate A, Chartier-Harlin M-C, Mullan M, Brown J, Crawford F, et al. (1991) Segregation of a missense mutation in the amyloid precursor protein gene with familial Alzheimer's disease. Nature 349: 704-706. doi:10.1038/349704a0

49. Rogaev EI, Sherrington R, Rogaeva EA, Levesque G, Ikeda M, et al. (1995) Familial Alzheimer's disease in kindreds with missense mutations in a gene on chromosome 1 related to the Alzheimer's disease type 3 gene. Nature 376: 775-778. doi:10.1038/376775a0

50. Sherrington R, Rogaev EI, Liang Y, Rogaeva EA, Levesque G, et al. (1995) Cloning of a gene bearing missense mutations in early-onset familial Alzheimer's disease. Nature 375: 754-760. doi:10.1038/375754a0

51. Levy-Lahad E, Wasco W, Poorkaj P, Romano DM, Oshima J, et al. (1995) Candidate gene for the chromosome 1 familial Alzheimer's disease locus. Science 269: 973-977.

52. Campion D, Flaman JM, Brice A, Hannequin D, Dubois B, et al. (1995) Mutations of the presenilin I gene in families with early-onset Alzheimer's disease. Hum. Mol. Genet 4: 2373-2377.

53. Thinakaran G, Koo EH (2008) Amyloid Precursor Protein Trafficking, Processing, and Function. Journal of Biological Chemistry 283: 29615 -29619. doi:10.1074/jbc.R800019200

54. De Strooper B (2003) Aph-1, Pen-2, and Nicastrin with Presenilin Generate an Active [gamma]-Secretase Complex. Neuron 38: 9-12. doi:10.1016/S0896-6273(03)00205-8

55. Burger PC, Vogel FS (1973) The development of the pathologic changes of Alzheimer's disease and senile dementia in patients with Down's syndrome. Am. J. Pathol 73: 457-476.

56. Rovelet-Lecrux A, Hannequin D, Raux G, Meur NL, Laquerriere A, et al. (2006) APP locus duplication causes autosomal dominant early-onset Alzheimer disease with cerebral amyloid angiopathy. Nat Genet 38: 24-26. doi:10.1038/ng1718

57. Vassar R, Bennett BD, Babu-Khan S, Kahn S, Mendiaz EA, et al. (1999) Beta-secretase cleavage of Alzheimer's amyloid precursor protein by the transmembrane aspartic protease BACE. Science 286: 735-741.

58. Ling Y, Morgan K, Kalsheker N (2003) Amyloid precursor protein (APP) and the biology of proteolytic processing: relevance to Alzheimer's disease. The International Journal of Biochemistry & Cell Biology 35: 1505-1535. doi:10.1016/S1357-2725(03)00133-X

59. Koo EH, Sisodia SS, Archer DR, Martin LJ, Weidemann A, et al. (1990) Precursor of amyloid protein in Alzheimer disease undergoes fast anterograde axonal transport. Proc. Natl. Acad. Sci. U.S.A 87: 1561-1565.

60. Kaether C, Skehel P, Dotti CG (2000) Axonal membrane proteins are transported in distinct carriers: a two-color video microscopy study in cultured hippocampal neurons. Mol. Biol. Cell 11: 1213-1224.

61. Yamazaki T, Selkoe DJ, Koo EH (1995) Trafficking of cell surface beta-amyloid precursor protein: retrograde and transcytotic transport in cultured neurons. J. Cell Biol 129: 431-442.

62. Ferreira A, Caceres A, Kosik KS (1993) Intraneuronal compartments of the amyloid precursor protein. J. Neurosci 13: 3112-3123.

63. Kamal A, Stokin GB, Yang Z, Xia CH, Goldstein LS (2000) Axonal transport of amyloid precursor protein is mediated by direct binding to the kinesin light chain subunit of kinesin-I. Neuron 28: 449-459.

64. Inomata H, Nakamura Y, Hayakawa A, Takata H, Suzuki T, et al. (2003) A scaffold protein JIP-1b enhances amyloid precursor protein phosphorylation by JNK and its association with kinesin light chain 1. J. Biol. Chem 278: 22946-22955. doi:10.1074/jbc.M212160200

65. Matsuda S, Matsuda Y, D'Adamio L (2003) Amyloid beta protein precursor (AbetaPP), but not AbetaPP-like protein 2, is bridged to the kinesin light chain by the scaffold protein JNK-interacting protein 1. J. Biol. Chem 278: 38601-38606. doi:10.1074/jbc.M304379200

66. Buée L, Bussière T, Buée-Scherrer V, Delacourte A, Hof PR (2000) Tau protein isoforms, phosphorylation and role in neurodegenerative disorders. Brain Research Reviews 33: 95-130. doi:10.1016/S0165-0173(00)00019-9

67. Witman GB, Cleveland DW, Weingarten MD, Kirschner MW (1976) Tubulin requires tau for growth onto microtubule initiating sites. Proc. Natl. Acad. Sci. U.S.A 73: 4070-4074.

68. Cleveland DW, Hwo SY, Kirschner MW (1977) Purification of tau, a microtubule-associated protein that induces assembly of microtubules from purified tubulin. J. Mol. Biol 116: 207-225.

69. Cleveland DW, Hwo SY, Kirschner MW (1977) Physical and chemical properties of purified tau factor and the role of tau in microtubule assembly. J. Mol. Biol 116: 227-247.

70. Binder LI, Frankfurter A, Rebhun LI (1986) Differential localization of MAP-2 and tau in mammalian neurons in situ. Ann. N. Y. Acad. Sci 466: 145-166.

71. Augustinack JC, Schneider A, Mandelkow E-M, Hyman BT (2002) Specific tau phosphorylation sites correlate with severity of neuronal cytopathology in Alzheimer's disease. Acta Neuropathol 103: 26-35.

72. Utton MA, Noble WJ, Hill JE, Anderton BH, Hanger DP (2005) Molecular motors implicated in the axonal transport of tau and {alpha}-synuclein. J Cell Sci 118: 4645-4654. doi:10.1242/jcs.02558

73. Falzone TL, Gunawardena S, McCleary D, Reis G, Goldstein LSB (2010) Kinesin-1 transport reductions enhance human tau hyperphosphorylation, aggregation and neurodegeneration in animal models of tauopathies. Hum Mol Genet. Available: http://www.ncbi.nlm.nih.gov/pubmed/20817925. Accessed 8 Sep 2010.

74. Eriksen JL, Janus CG (2007) Plaques, tangles, and memory loss in mouse models of neurodegeneration. Behav. Genet 37: 79-100. doi:10.1007/s10519-006-9118-z

75. Ashe KH, Zahs KR (2010) Probing the Biology of Alzheimer's Disease in Mice. Neuron 66: 631-645. doi:10.1016/j.neuron.2010.04.031

76. Thomson JA, Itskovitz-Eldor J, Shapiro SS, Waknitz MA, Swiergiel JJ, et al. (1998) Embryonic Stem Cell Lines Derived from Human Blastocysts. Science 282: 1145-1147. doi:10.1126/science.282.5391.1145

77. Yu J, Vodyanik MA, Smuga-Otto K, Antosiewicz-Bourget J, Frane JL, et al. (2007) Induced Pluripotent Stem Cell Lines Derived from Human Somatic Cells. Science 318: 1917-1920. doi:10.1126/science.1151526

78. Yuan SH, Martin J, Elia J, Flippin J, Paramban RI, et al. (2011) Cell-surface marker signatures for the isolation of neural stem cells, glia and neurons derived from human pluripotent stem cells. PLoS ONE 6: e17540. doi:10.1371/journal.pone.0017540

CHAPTER 2

Kinesin-1C and KLC1 affect neuronal development and APP levels in murine hippocampal neurons

Abstract

The microtubule-based molecular motor Kinesin-1 performs vital functions in maintaining intracellular transport in neurons. The Kinesin-1 holoenzyme is a heterotetramer of two heavy chains (KHCs) and two light chains (KLCs). In mammals there are three possible KHCs (Kinesin-1A, Kinesin-1B, Kinesin-1C) and four possible KLCs (KLC1, KLC2, KLC3, KLC4), but which KHCs and KLCs assemble together and the specific functions of these holoenzymes is not well known. Similarities in expression patterns and in mutant animal phenotypes as well as co-immunoprecipitation studies suggest KLC1 and Kinesin-1C may function together in neurons. Defective microtubule-based neuronal transport is associated with neurodegenerative diseases such as AD, a condition characterized pathologically by aggregates of Aβ and Tau. Experimental induction of axonal transport defects via

genetic reduction in full length KLC1 causes abnormal deposits of Aβ and Tau in adult mice. Kinesin-1 subunits are also implicated in neuronal polarization in developing neurons in culture, but it is not known specifically whether KLC1 or Kinesin-1C subunits are required. We tested whether hippocampal neurons from KLC1-/- or Kinesin-1C-/- mice exhibit normal axon polarization and whether changes in AD-associated molecules APP and Tau levels are altered in these young neurons. Interestingly, we found that loss of full length KLC1 or Kinesin-1C reduces protein levels of the other subunit in hippocampal cultures, suggesting protein levels of Kinesin-1C and KLC1 are co-regulated. We also found that developing Kinesin-1C-/- and KLC1-/- axons are longer than wildtype and have lower fractions of neurons with multiple axons than wildtype, suggesting that these subunits may play a role in the development of hippocampal neurons. In addition, hippocampal cultures from Kinesin-1C-/- but not KLC1-/- mice exhibited reduced extracellular γ–secretase metabolites Aβ and p3, which was likely attributable to concomitant reduction in APP in the cells, suggesting Kinesin-1C may regulate APP levels. Tau levels in hippocampal neurons were not different between Kinesin-1C-/-, KLC1-/- and wildtype mice, suggesting that changes in Tau observed previously in adult KLC1 animals may be age, cell type or environment dependent. Altogether these data suggest Kinesin-1C and KLC1 may work together to function in neuronal development and in regulating levels of APP.

Introduction

Molecular motor proteins enable vital eukaryotic cellular functions such as division, migration and intracellular trafficking. Kinesin-1 is a widely expressed microtubule based motor that transports cargos in the anterograde direction towards the growing end of microtubules. Structurally, Kinesin-1 is a heterotetramer consisting of homodimers of KHCs and KLCs [1]. Each KHC contains an amino-terminal motor domain, a long flexible linker region and a carboxyl-terminal globular region which binds to KLC. Functionally, KHC powers movement of attached cargos along microtubules. KLCs contain an amino-terminal heptad repeat domain which binds KHC, a small linker domain and six tetratricopeptide repeat (TPR) that associate with cargos. KLC has been implicated in regulation of heavy chain activity and in mediation of cargo binding [2]. Mammalian Kinesin-1 can be comprised of three possible heavy chain gene products: Kinesin-1A, Kinesin-1B or Kinesin-1C (formerly called KIF5A, KIF5B and KIF5C) and at least four possible light chains: KLC1, KLC2, KLC3 and KLC4 [3-7]. Kinesin-1B and KLC2 are widely expressed in all tissues; KLC1, Kinesin-1A and Kinesin-1C are enriched in neural tissues. KLC3 has only been detected in testes and certain cerebellar neurons, while KLC4 has only as yet been identified at the genomic level [3,7-9]. Although it seems clear that KHC and KLC subunits form homodimers [3,5,8,10,11], less is known about how these homodimers assemble into the holoenzyme, although immunoprecipitation experiments suggest KLC1 prefers Kinesin-1A and Kinesin-1C and KLC2 Kinesin-1B [3,10]. Previous reports show that both Kinesin-1C-/- and KLC1-/- animals have

reductions in motor neuron populations; KLC1-/- and Kinesin-1C-/- hippocampal neurons exhibit similarly impaired transport of the mammalian prion protein in hippocampal neurons [8,12,13] and KLC1 protein levels are reduced in murine Kinesin-1C-/- brains (Chun-Hong Xia doctoral dissertation “Functional analysis of mouse neuronal kinesin heavy chains”, University of California San Diego 2000), suggesting these two Kinesin-1 subunits may form functional holoenzymes. Work in primary rodent neurons using anti-sense and RNA interference targeting Kinesin-1 subunits suggest Kinesin-1 may also have important functions early in neuronal polarization [14-16], but it is not known whether these functions specifically require KLC1 or Kinesin-1C.

Alzheimer’s disease (AD), the most common form of dementia among the elderly, is associated pathologically with amyloid plaques and neurofibrillary tangles. These lesions are comprised of protein deposits of the APP cleavage fragment called Aβ and hyperphosphorylated Tau (pTau) protein, respectively. Several studies support a role for Kinesin-1 in the transport of APP in cultured primary neurons [12,17-19]. Interestingly, previous reports show that reduced function of KLC1 leads to increased pTau and transgenic human Aβ in aged mice [12,17], but it is still not known if the pathology observed in the adult mice occurs is aging related or if Kinesin-1C perturbations also affect Tau or Aβ levels . Therefore I used murine primary hippocampal neurons isolated from Kinesin-1C-/- and KLC1-/- neonates to test whether loss of function of KLC1 or Kinesin-1C causes early defects in neurons which might lead to the AD-like phenotypes observed in aged KLC1 mutant mice.

Materials and Methods

Preparation of primary mouse hippocampal cultures

Hippocampal cultures were prepared from newborn or embryonic day 18-21 wildtype, KLC1-/- [20] and Kinesin-1C-/- [13] animals. Pups were decapitated and the heads immersed in ice cold Hank's balanced salt solution supplemented with 0.08% glucose and 7 mM HEPES (HBSS++). Hippocampi were dissected and washed twice with cold HBSS++, then treated for 15 min at 37°C with papain (Worthington) in PBS (Invitrogen) supplemented with 0.625% glucose (Sigma), 0.025% BSA (Sigma), 0.025% cysteine (Sigma) and 0.008% DNAse I (grade II; Boehringer). Hippocampi were washed twice with DMEM with 10% FBS, dissociated by trituration and plated on poly-lysine coated plates or coverslips. Media was changed to neurobasal with B27 and GlutaMAX (Invitrogen) one hour after plating.

Analysis of hippocampal axons

Axons of Stage 3 [21] hippocampal neurons aged 3 days *in vitro* were identified by enrichment of Tau-1 compared to MAP2 immunofluorescence staining. The NeuronJ plug-in of ImageJ was used to trace and quantify axon length per cell [22]. Neurons with multiple axons were manually counted.

Immunofluorescence characterization of primary mouse hippocampal cultures

Cells incubated 3 or 11 days *in vitro* were rinsed once with PBS and fixed in 4% paraformaldehyde in PBS with 0.12M sucrose for 30 minutes at 37°C. Following a PBS rinse, cells were permeabilized in 0.1% Triton X-100 for 10 minutes and blocked for one hour at room temperature using 2.5% FBS, 0.75% BSA in PBS for NeuN or 10% FBS, 3% BSA for all other antibodies. Cells were incubated overnight at 4°C with NeuN (Millipore; 1:250), rabbit polyclonal MAP2 (Millipore, 1:1000) or Tau-1 (Millipore, 1:1000) antibodies and rinsed three times in PBS. AlexaFluor 568 goat anti-mouse IgG (H+L) and AlexaFluor 488 goat anti-rabbit IgG (H+L) secondary antibodies (Invitrogen) were used at 1:750 dilution for 45 minutes at room temperature with 0.1 micrograms/ml 4′,6′-diamidino-2-phenylindole (DAPI) nuclei stain, rinsed several times and mounted on slides with Prolong Gold anti-fade reagent (Invitrogen). Specificity of secondary antibody staining was verified using secondary only controls. Images were collected using a Zeiss Axioplan microscope equipped with a Zeiss Plan Neofluor 10X/0.30 NA or 40X/0.75 NA objectives, DAPI, FITC or Texas Red filters, a CoolSNAPcf camera (Roper Scientific) and MetaMorph (Molecular Devices) software. To determine the fraction of neurons in the hippocampal cultures, NeuN and DAPI nuclei were quantified using Image J (NIH) and the Image-based tool for counting nuclei (ITCN) plug-in. A minimum of 4 mice and 850 nuclei were analyzed for each genotype.

Western blot analysis of protein levels.

Quantitative Western blots were performed on tissue culture lysates to compare protein levels between genotypes. The bicinchoninic acid (Pierce) protein assay was used to measure the protein content of each sample relative to a bovine serum albumin standard curve prepared in cell disruption buffer (PARIS kit, Ambion). Equal protein amounts were separated in MES buffer alongside Novex Sharp pre-stained markers (Invitrogen) on NUPAGE 4-12% Bis Tris precast gels (Invitrogen) and transferred to nitrocellulose (Whatman Protran 0.45 micron pore size). Membranes were blocked with 5% milk in Tris-buffered saline with 0.1% Tween-20 (TBST) for 30 minutes at room temperature. Primary antibodies (APP C-terminus, 1:300 Zymed/Invitrogen, Actin C4 1:20,000 Millipore, GAPDH 1:1000 Ambion, Rab-5 1:300 Synaptic Systems, α-Tubulin DM1a 1:50,000 Sigma, β-III-Tubulin rabbit TUJ1 1:1000 Covance, MAP2 rabbit Millipore 1:500, Rab-3 Synaptic Systems 1:300, NSE rabbit Millipore 1:500, CP13 (Tau phosphorylated at Ser202) 1:300 Peter Davies, Tau-5 1:500 Invitrogen, PHF1(Tau phosphorylated at Ser396 and Ser404) Peter Davies 1:500, Tau46.1 1:500 Sigma) were prepared in 5% BSA in TBS and incubated with membranes overnight at 4°C. Excess primary antibodies were washed out with TBST. LiCor infrared fluorescent secondary antibodies were diluted 1:6000-1:20,000 in 2.5% milk in TBST and incubated with the blots in the dark for 1 hour at room temperature. Blots were washed with TBST and then TBS prior to imaging. LiCor Odyssey infrared imager was used to measure pixel intensities of bands. For each antibody, detector settings were set to the maximum or one half unit below

saturation to ensure measurements were recorded within the linear range. For each protein band, background subtracted integrated intensity values were calculated using the odyssey software. Since absolute integrated intensity values vary for the same samples on different blots, samples within a blot were plotted relative to wildtype samples and these normalized values were used to compare between replicate blots. Linearity of antibody response was verified over the range of 1-10 μg. Images were inverted to display black bands on white background.

Quantification of Aβ/P3

Meso Scale Discovery electrochemiluminescence sandwich immunoassays were used to measure γ–secretase APP cleavage products Aβ and P3. To measure secreted Aβ/P3 peptides from mouse hippocampal cultures, media was collected, protease inhibitors added and the samples frozen on dry ice. Media samples were thawed and assayed relative to known amounts of Aβ peptides (Meso Scale Discovery) prepared in unconditioned media. Aβ-38, 40 and 42 specific antibodies were used as capture antibodies, but Aβ-38 and -42 were not reliably detected. The monoclonal mouse antibody 4G8 recognizing amino acids 17-24 of the Aβ region was used for detection. Picogram per milliliter Aβ and p3 values were adjusted to the total protein content of the lysate and expressed relative to wildtype.

Results and Discussion

Murine KLC1 and Kinesin-1C protein levels in primary hippocampal cultures are related

I confirmed the absence of full length KLC1 in lysates from KLC1-/- compared to wildtype primary hippocampal neurons by Western blot (Figure 2.1A-B). C-H Xia reported in her dissertation ("Functional analysis of mouse neuronal kinesin heavy chains", University of California San Diego 2000) substantial reduction in KLC1 levels in Kinesin-1C-/- brain lysates. Therefore, I examined levels of the Kinesin-1C motor subunit in KLC1-/- hippocampal cultures. Interestingly, KLC1-/- hippocampal neurons had 50% less Kinesin-1C than wildtype (Figure 2.1A, C) as measured by Western blot, suggesting levels of the KLC1 and Kinesin-1C subunits may be correlated in primary hippocampal neurons of KLC1-/- mice as well as in adult Kinesin-1C-/- brain. I also evaluated KLC1 levels in Kinesin-1C-/- primary hippocampal cultures. Primary hippocampal cultures from Kinesin-1C-/- neonates have background levels of Kinesin-1C (Figure 2.1D, E). Paralleling the reduction observed in KLC1 Kinesin-1C-/- in brain lysates (C-H. Xia thesis), KLC1 levels in Kinesin-1C-/- hippocampal neurons were substantially reduced - to only 25% wildtype levels (Figure 2.1D, E). This data, taken together with previous results describing co-immunoprecipitation of Kinesin1-C and KLC1 [3,10,23], similar tissue expression profiles [3,7,8] and defects in KLC1-/- and Kinesin-1C-/- mice [12,24] suggests the hypothesis that the Kinesin-1C and KLC1 subunits may form functional Kinesin-1C/KLC1 holoenzymes in neurons.

How Kinesin-1C and KLC1 levels are co-regulated is as yet unknown. It is possible that regulatory mechanisms occur at the mRNA or protein level. Given the strong reduction of KLC1 in the Kinesin-1C-/- it is puzzling that Kinesin-1C levels are not more reduced in KLC1-/- cultures. KHC can exist as a homodimer and perform functions independent of KLCs [2]. Perhaps there are KLC1-dependent and KLC1-independent pools of Kineisn-1C and the Kinesin-1C still present in the KLC1-/- cultures is KLC1 independent. It is also of note that the KLC1-/- mice were made by genomic targeting of the linker between the KLC1 amino-terminal KHC–binding heptad repeat domain and the carboxyl terminal TPR domain (Figure 1.1). This strategy resulted in a frame shift mutation in this linker region that truncates the encoded protein before translation of the carboxyl-terminal TPR domains. This truncated protein is detectable by Western in KLC1-/- embryonic stem cells, KLC1-/- brain and KLC1-/- sciatic nerve and by immunofluorescence in differentiated KLC1-/- embryonic stem cells, KLC1-/- sciatic nerve and KLC1-/- dorsal root ganglia and a sciatic nerve ligation assay suggests it is transported in axons with KHC (Amena Rahman doctoral dissertation “Analysis of Kinesin Light Chain in Mouse”, University of California, San Diego 1997). Since the truncated KLC1 fragment present in KLC1-/- mice contains the entire heptad repeat KHC binding domain, it is capable of associating with KHC [25]. If this truncated KLC1 binds Kinesin-1C, it may stabilize Kinesin-1C levels. This scenario would support a Kinesin-1C-KLC1 co-regulatory mechanism operating at the translational level. Such a phenomenon has been

described for protein phosphatase 2A: siRNA-induced reduction of the A or C subunit in *Drosophila* cells leads to protein destabilization of the entire heterotrimer [26].

Kinesin-1C and KLC1 may function in hippocampal neuron development

Primary rodent hippocampal neurons display a distinct development pattern when placed in culture. Soon after plating, they form lamellipodia (Stage 1) that grow into distinct minor processes (Stage 2; several hours), one of which typically elongates rapidly and becomes the axon (Stage 3; days 2-3) [21]. Previous studies report that primary rodent neurons challenged with acute reduction in KHCs or KLCs exhibit 40-50% reduced axon lengths and an increased frequency of neurons with multiple axons [14-16]. I tested whether the KLC1 or Kinesin-1C subunits contribute to these processes by analyzing axon lengths and numbers in developing Kinesin-1C-/-, KLC1-/- and wildtype primary hippocampal neurons stained with Tau-1 and MAP2 antibodies, whose epitopes are enriched in axons and dendrites, respectively [27-29]. After three days *in vitro* the neurons typically exhibited a single longer Tau-1 enriched axon (Figure 2.2A arrowheads), although rare cells with two axons were also observed. Interestingly, smaller proportions of Kinesin-1C (2.1%) and KLC1-/- (1.5%) polarized neurons exhibited multiple axons than wildtype (6.0%; Figure 2.2B), while a previous study found an increased appearance of multiple Tau positive axons in neurons treated with either siRNA or dominant negative Kinesin-1 constructs simultaneously targeting Kinesin-1A, Kinesin-1B and Kinesin-1C, suggesting that different subunits have distinct roles in this process.

I tested whether loss of full length KLC1 or Kinesin-1 affects axon length in Kinesin-1C-/- or KLC1-/- relative to stage 3 neurons. The average Kinesin-1C-/- or KLC1-/- axon was 20% longer than wildtype (Figure 2.2C). Previous studies reported 40-50% reduced neurite length in neurons treated with anti-sense oligonucleotides specific for Kinesin-1B, siRNA or carboxyl-terminal dominant negative KHC targeting Kinesin-1A, Kinesin-1B and Kinesin-1C or siRNA targeting both KLC1 and KLC2 [14-16]. Since antisense to Kinesin-1B alone or inhibition of all three KHCs shortens neurite lengths by half, Kinesin-1B may normally function to lengthen the axon. In contrast, when Kinesin-1C and KLC1 are reduced genetically, the axon lengthens, suggesting that, when present, they may exert a force that shortens the axon. Therefore these data may fit a model where Kinesin-1B and Kinesin-1C/KLC1 have opposing functions in modulating the length of developing hippocampal neurites.

Tau levels are unchanged in primary hippocampal neurons with reduced KLC1.

AD is associated with brain neurofibrillary tangles consisting of aggregated hyperphosphorylated MAP-Tau protein. Recent studies in mice suggested that reducing KLC1 levels increases human mutant transgenic and endogenous mouse pTau levels in neural tissues [12,30]. I tested whether reduced KLC1 function alone can affect endogenous mouse Tau levels early in primary neurons isolated from the mouse neonate hippocampus – a brain region adversely affected in AD. I used Western blotting to test levels of Tau and pTau relative to Actin in Kinesin-1C-/-,

KLC1-/- and wildtype neuronal cultures. I used Tau antibodies to both phosphorylation -independent and -dependent epitopes located upstream and downstream of the microtubule binding repeats (Figure 2.3A; repeats shaded in gray). I found that Tau levels were invariant across genotypes regardless of the antibody used (Figure 2.3B-C). Accordingly the ratio of phosphorylated to non-phosphorylated Tau was not different between the genotypes (Figure 2.3D), suggesting that reduced KLC1 or Kinesin-1C function does not affect overall Tau levels in primary hippocampal cultures from neonates.

Two previous studies suggested that KLC1 reductions may perturb Tau. In the first, 18 month old KLC1-/- mice exhibited accumulations of endogenous pTau in spinal cord axonopathies [12]. In the second, pTau accumulations in cell bodies in the brain and spinal cord were compared between KLC1+/+ and KLC1+/- transgenic mice expressing human mutant Tau [30]. More cell bodies in the hippocampus of KLC1+/- compared to KLC1+/+ mice had pTau accumulations at 9 months of age but not at earlier or later time points. Larger numbers of pTau-positive cell bodies within the spinal cord of KLC1+/- compared to KLC1+/+ were evident at 12 and 15 months but not earlier [30]. Together with my data these results suggest that KLC1 or Kinesin-1C impairments do not universally perturb Tau in young neurons. However, such Kinesin-1 impairments may, with aging, result in aberrant accumulations of Tau in specific neural regions.

Altered extracellular Aβ/p3 levels in Kinesin-1C-/- hippocampal cultures

AD is associated with brain plaques principally comprised of Aβ, a proteolytic cleavage product of the amyloid precursor protein, which can also generate an alternative peptide fragment called p3 (Figure 2.4A). Previous work suggests that reduced KLC1 function in transgenic mice expressing a human APP familial Alzheimer's mutant increases levels of Aβ in adult mice [17]. I tested whether reduced KLC1 function can trigger changes in extracellular endogenous mouse γ–secretase cleavage products Aβ or p3. Because the hippocampus is one of the brain regions impaired in AD, I used primary mouse hippocampal cultures to test this hypothesis. I examined extracellular levels of γ–secretase products p3 and Aβ using a detection antibody which binds to both. I found no statistically significant difference in extracellular Aβ and p3 in KLC1-/- compared to wildtype (Figure 2.4B). However, Kinesin-1C-/- cultures contained almost 40% less extracellular γ–secretase peptide products than wildtype (Figure 2.4B), suggesting that while reduction of full length KLC1 alone does not alter extracellular mouse γ-secretase products in hippocampal cultures, substantial reduction of both KLC1 and Kinesin-1C may impair production, decrease secretion or increase degradation of these products. To gain insight into the reduced generation of extracellular Aβ and p3 in Kinesin-1C-/- hippocampal cultures, I used Western blotting to assess levels of full length APP relative to Actin in the motor mutants compared to wildtype. Full length APP levels mirrored those of its extracellular γ secretase cleavage products: APP was reduced - by ~24% - in Kinesin-1C-/-, but not in KLC1-/- cultures (Figure 2.4C-D). Indeed there were no statistically

significant differences between genotypes in the ratio of extracellular Aβ and p3 peptides to APP in the lysate (Figure 2.4E). These data suggest that significant reductions in Kinesin-1C and KLC1, but not in full length KLC1 alone, may lower extracellular γ–secretase peptide levels via a reduction in total APP.

Numerous studies suggest transport of APP is Kinesin-1 dependent. Two studies noted fewer and slower anterograde moving APP-YFP vesicles in KLC1-/- and KLC1+/- hippocampal neurons, suggesting the KLC1 subunit influences APP transport [12,17]. An absence of endogenous APP within neurites of Kinesin-1B anti-sense treated hippocampal primary neurons cultured 30 days *in vitro* suggests that Kinesin-1B may transport APP [19]. However, based on co-immunoprecipitation of low density iodixanol gradient mouse brain membrane fractions, Szodorai et al (2009) contend that APP is transported by Kinesin-1C and not Kinesin-1B [31]. If Kinesin-1C transports APP, loss of Kinesin-1C may prevent the axon-dependent secretase cleavage of APP to produce γ–secretase products, the secretion of these products, or the secretion of molecules that alter extracellular Aβ degradation. However my data suggest that the reductions in hippocampal culture extracellular γ–secretase products may simply be due to a reduction in the APP substrate. Examination of APP-YFP live transport in Kinesin-1C-/- primary hippocampal neurons would shed light on whether Kinesin-1C subunit transports APP and if reduced levels of Aβ and p3 are related to impaired transport of APP or reduced APP.

Characterization of KLC1-/- and Kinesin-1C-/- hippocampal primary cultures

To verify that the primary hippocampal cultures from wildtype, KLC1-/- and Kinesin-1C mice have similar compositions I used IF to quantify the proportion of neurons and Western blotting to assay the total levels of commonly used neuron markers β-III-Tubulin, MAP2 and NSE. I quantified the percent of cells positive by immunofluorescence for the neuronal marker NeuN, which stains most neurons [32] compared to total DAPI-stained nuclei (Figure 2.5A-B). I found no statistically significant difference between the percent of NeuN+ neurons in wildtype and either Kinesin-1C-/- or KLC1-/- cultures (Figure 2.5B), suggesting that reduction of full length KLC1 or Kinesin-1C does not affect the percent of cells that are neurons in hippocampal cultures. Using Western blots, I tested the relative levels of α-Tubulin and neuron markers MAP2, β-III-Tubulin and NSE relative to Actin in KLC1-/- and Kinesin-1C-/- compared to wildtype hippocampal cultures. Levels of α-Tubulin in Kinesin-1C-/- and KLC1-/- hippocampal cultures were similar to wildtype (Figure 2.5C-D). Levels of the neuronal markers MAP2 and β-III-Tubulin were also comparable to wildtype in Kinesin-1C-/- and KLC1-/- hippocampal cultures (Figure 2.5E, F). Interestingly, levels of NSE were reduced relative to wildtype in Kinesin-1C-/-, but not KLC1-/- hippocampal cultures (Figure 2.5G). NSE is a soluble protein distributed throughout the cell body and processes of neurons [33]. Experiments in squid axoplasm suggest that squid enolase mRNA is present in axons [34]. Kinesin-1C has been suggested to be a motor responsible for the transport of mRNA into the

dendritic compartment of vertebrate neurons [24,35]. One possibility is that Kinesin-1C participates in the transport of NSE mRNA and when transport is compromised, less protein is made locally which contributes to reduced levels overall. On the other hand, data collected in the rabbit visual system suggests NSE protein is actively transported into axons [36], but the motor has not been identified. Thus a second possibility is that Kinesin-1C transports NSE protein and faulty transport leads to reduced overall levels. Overall my data suggest that although KLC1 reduction has no affect on the fraction of neurons in hippocampal cultures, in conjunction with the total loss of Kinesin-1C it may alter the level of a subset of neuronal proteins within these cells, including APP and NSE.

Conclusions

I tested whether KLC1-/- primary hippocampal neurons exhibit early defects associated with aberrant Tau or APP which could lead to the pathology observed in aged KLC1+/- and KLC1-/- mice. I found that these cultures contained similar fractions of neurons as wildtype but the KLC1-/- neurons exhibited longer axon lengths and reduced proportions of polarized neurons with multiple axons. Further, I observed no statistically significant differences in endogenous levels of Tau, APP or APP γ–secretase products Aβ and p3 in KLC1-/- compared to wildtype hippocampal cultures. As KLC1-/- hippocampal neurons exhibit no overt Tau or Aβ abnormalities it seems likely that other factors may be necessary to drive the pathology in adult

animals. Such factors could include aging, neural tissue type, and/or the presence of human, overexpressed and/or mutant Tau or APP.

I also report that mutant Kinesin-1C-/- hippocampal neurons have substantially reduced levels of KLC1-/- suggesting the hypothesis that Kinesin-1C and KLC1 associate into functional Kinesin-1 holoenzymes. Interestingly, compared to wildtype, Kinesin-1C-/- hippocampal neurons have longer axons and reduced fractions of polarized neurons with multiple axons, suggesting Kinesin-1C may play a role in neuronal development. While I observed no differences in protein levels of α- or β-III-Tubulin, MAP2 or Tau between wildtype and Kinesin-1C-/- cultures, I did find reduced total levels of NSE. Kinsein-1C-/- compared to wildtype neurons also had lower levels of extracellular γ-secretase products Aβ and p3 and less full length APP in the lysate. Overall, my data suggest that Kinesin-1C has specific functions in primary hippocampal neurons. How Kinesin-1C modulates neurite development and levels of NSE and APP is unknown. Experiments scrutinizing the localization and transport of specific mRNA and proteins such as APP in neurons with reduced Kinesin-1 subunits will shed light on the specialized role these subunits in neurons.

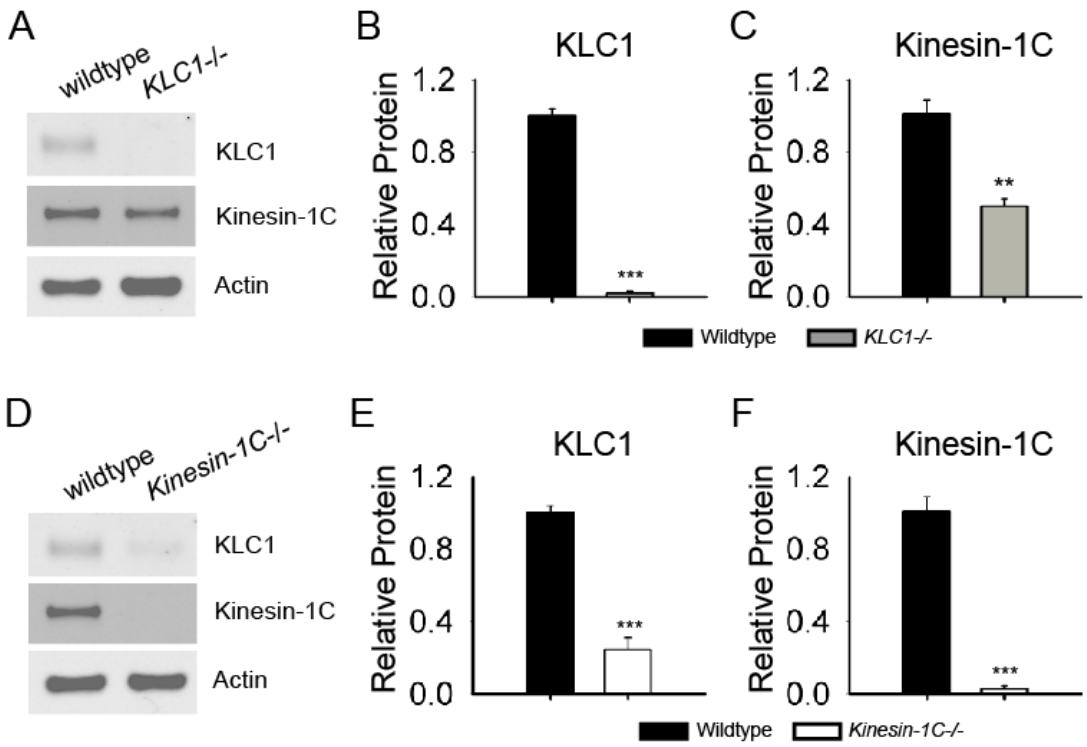


Figure 2.1. Kinesin-1C and KLC1 protein levels are interdependent in primary hippocampal mouse cultures. (A-C) Wildtype and KLC1-/- primary hippocampal cells were harvested after 11 days *in vitro* and the protein analyzed by Western blotting. (A) Representative immunoblots showing KLC1, Kinesin-1C and Actin in wildtype and KLC1-/- hippocampal culture lysates. (B-C) Quantification of Actin-normalized KLC1 (B) and Kinesin-1C (C) levels for n=6 wildtype and n=3 KLC1-/-. (D-F) Wildtype and Kinesin-1C-/- primary hippocampal cells were harvested after 11 days *in vitro* and the protein analyzed by Western blotting. (D) Representative immunoblots showing KLC1, Kinesin-1C and Actin in wildtype or Kinesin-1C-/- hippocampal culture lysates. (E-F) Quantification of Actin-normalized KLC1 (E) and Kinesin-1C (F) levels for n=6 wildtype and n=6 Kinesin-1C-/-. (B, D) **$p < 0.01$, ***$p<0.001$ by 2 tailed t-test compared to wildtype. Error bars indicate standard error of the mean.

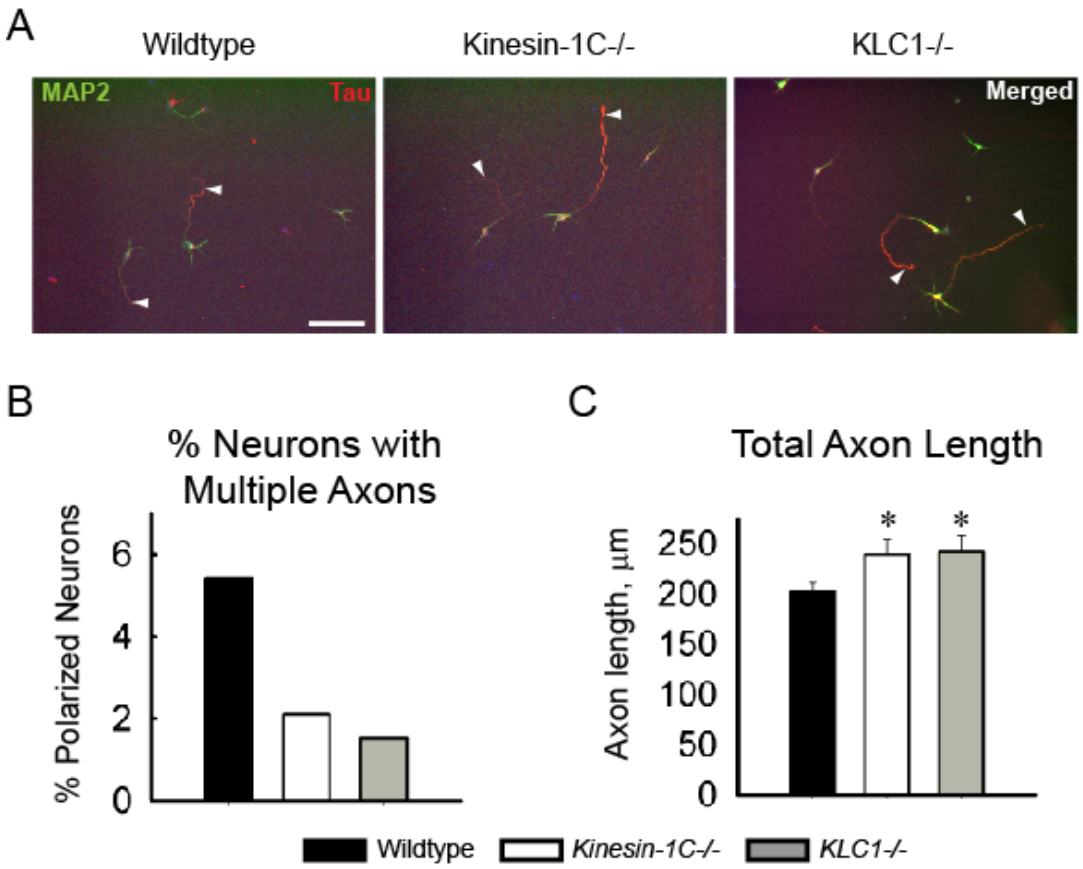


Figure 2.2. Kinesin-1C-/- and KLC1-/- hippocampal neurons polarize abnormally. Wildtype, KLC1-/- and Kinesin-1C-/- hippocampal neurons were cultured for 3 *in vitro* and stained for neuronal polarity markers Tau-1 and MAP2 which are enriched in axons and dendrites, respectively. (A) Representative images of wildtype, Kinesin-1C-/- and KLC1-/-neurons. Arrowheads indicate axons. Scale bar 100 microns (B) Percentage of polarized neurons with multiple axons. (C) Quantification of axon lengths in wildtype, Kinesin-1C and KLC1-/- neurons. *p < 0.05 by two-tailed t-test compared to wildtype. (B-C) based on n=129 wildtype, n=95 and Kinesin-1C and n=131 KLC1-/- neurons.

Figure 2.3. Kinesin-1C and KLC1-/- hippocampal neurons exhibit normal Tau levels. (A) Diagram of Tau primary sequence showing locations of antibody epitopes relative to microtubule binding domains (in grey). (B-D) Wildtype, Kinesin-1C-/- and KLC1-/- primary hippocampal cells were cultured for 11 days *in vitro*, harvested and the protein analyzed by Western blotting. (B) Representative immunoblots showing CP13, Tau-5, PHF1, Tau-46.1 and Actin. (C) Quantification of Actin-normalized CP13 (n=17 wildtype, n=8 Kinesin-1C-/- and n=12 KLC1-/-), Tau-5 (n=17 wildtype, n=8 Kinesin-1C-/- and n=12 KLC1-/-), PHF1 (n=13 wildtype, n=6 Kinesin-1C-/- and n=8 KLC1-/-) and Tau-46.1 (n=13 wildtype, n=6 Kinesin-1C-/- and n=8 KLC1-/-) levels relative to wildtype. (D) Ratios of phosphorylated Tau (CP13 and PHF1) relative to adjacent phosphorylation-independent epitopes (Tau-5 and Tau-46.1, respectively). CP13/Tau-5: n=17 wildtype, n=8 Kinesin-1C-/- and n=12 KLC1-/-; PHF1/Tau-46.1 n=13 wildtype, n=6 Kinesin-1C-/- and n=8 KLC1-/-. There were no statistically significant differences between genotypes by 2 tailed t-test compared to wildtype. Error bars indicate standard error of the mean.

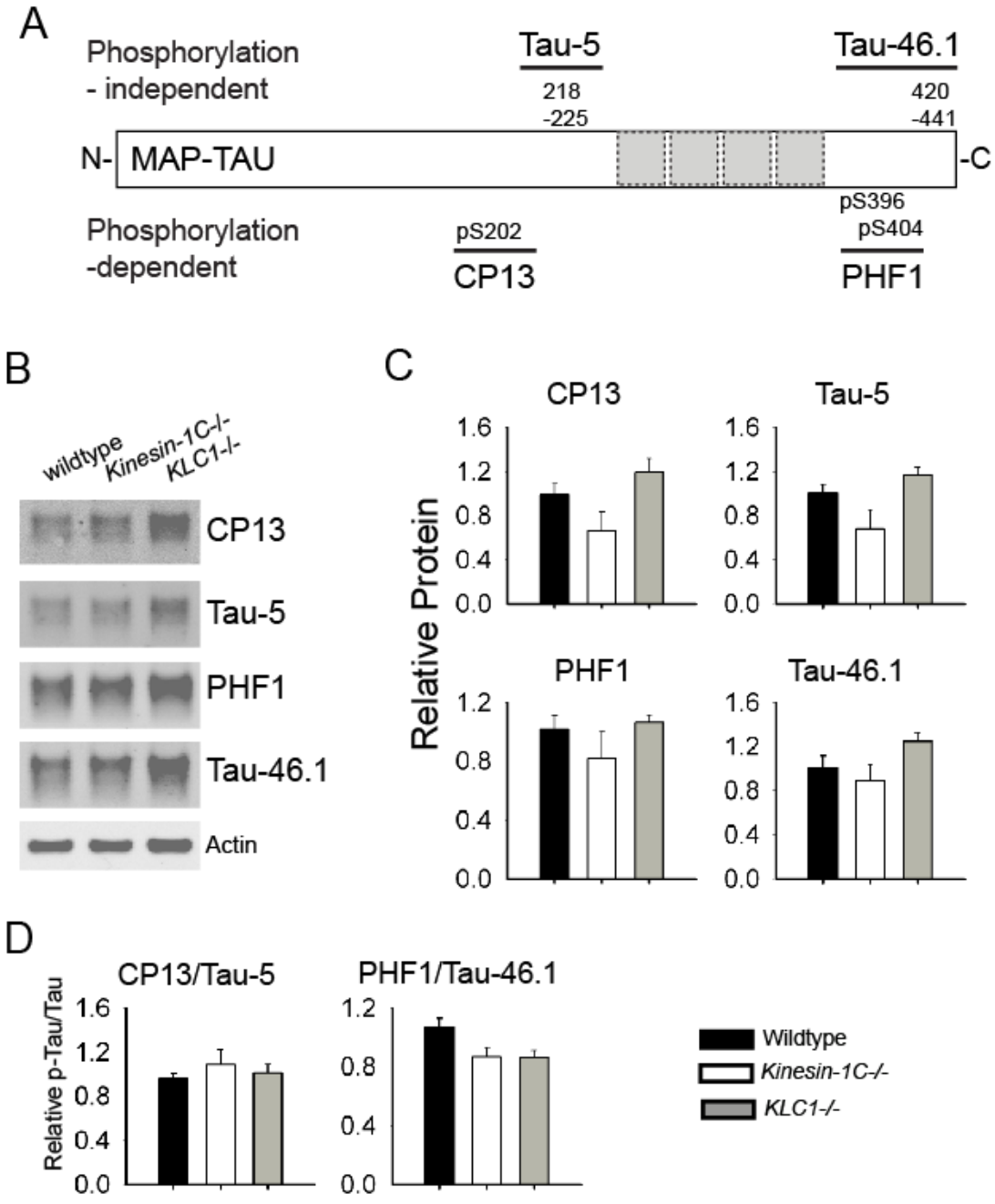
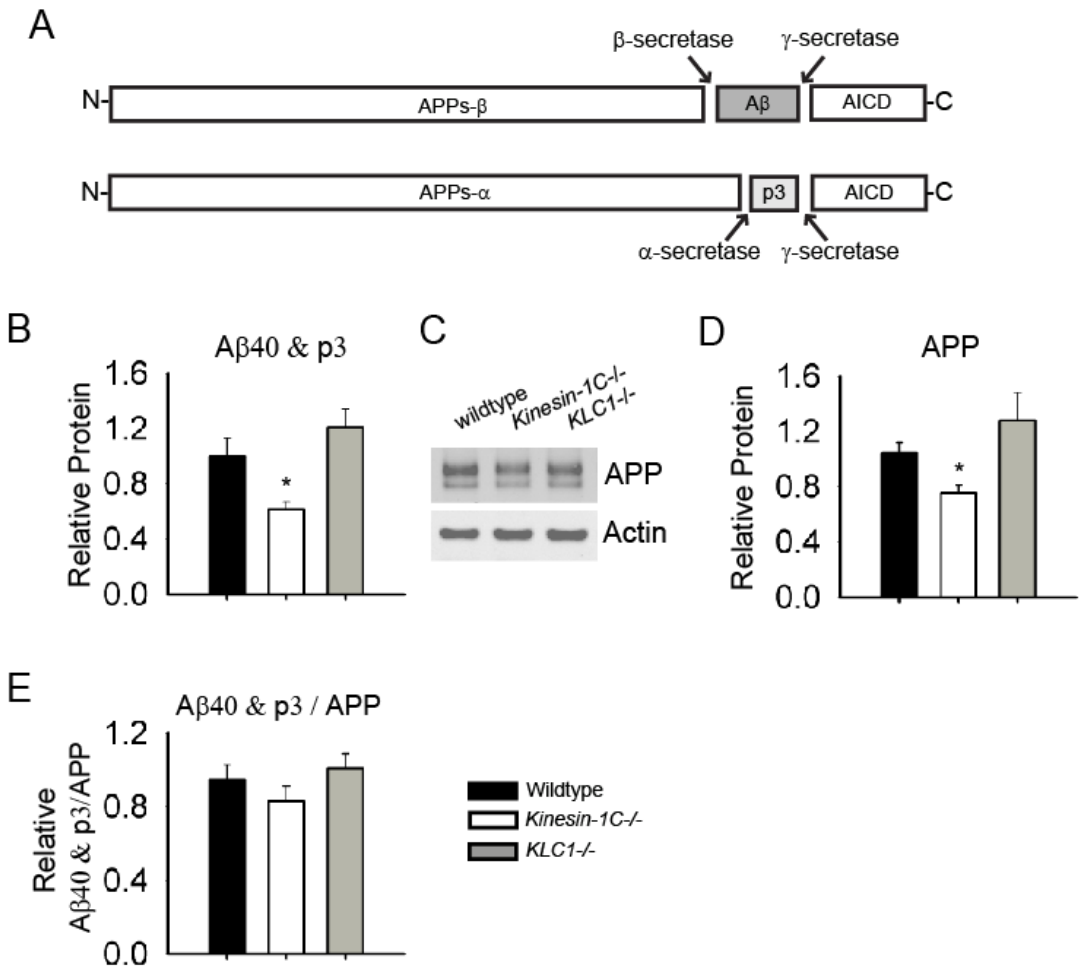

A
Phosphorylation
- independent
Tau-5
218
-225
Tau-46.1
420
-441
N-
MAP-TAU
-C
pS396
pS404
Phosphorylation
-dependent
pS202
CP13
PHF1
B
wildtype
Kinesin-1C-/-
KLC1-/-
CP13
Tau-5
PHF1
Tau-46.1
Actin
C
CP13
Tau-5
PHF1
Tau-46.1
Relative Protein
1.6
1.2
0.8
0.4
0.0
D
CP13/Tau-5
PHF1/Tau-46.1
Relative p-Tau/Tau
Wildtype
Kinesin-1C-/-
KLC1-/-

Figure 2.4. APP full length and extracellular γ–secretase products are reduced in Kinesin-1C but not KLC1 hippocampal cultures.
(A) APP proteolytic processing by either β-and γ-secretases or α- and γ-secretases produces secreted peptides Aβ (shaded dark grey) and p3 (light grey shading) peptides, respectively (B-E). Wildtype, Kinesin-1C-/- and KLC1-/- primary hippocampal cells were cultured for 11 days *in vitro*. Cells and conditioned media were harvested. (B) Levels of extracellular p3 and Aβ 40 amino acids in length detected in media conditioned by wildtype, Kinesin-1C-/- and KLC1-/- primary hippocampal cultures using 4G8 (Aβ amino acids 17-24) detection antibody and normalized to the total protein in the corresponding lysate. Intracellular Aβ peptides or extracellular Aβ of lengths 42 and 38 amino acids were not reliably detected. n=12 wildtype, n=8 Kinesin-1C-/- and n=10 KLC1-/-. (C-E) Hippocampal lysates were analyzed by Western blot. (C) Representative immunoblots for full length APP using a C- terminal antibody in wildtype, Kinesin-1C-/- and KLC1-/- primary hippocampal cultures. The APP carboxyl terminal cleavage fragments were not detectable. (D) Quantification of full length APP levels relative to Actin (n=17 wildtype, n=8 Kinesin-1C-/- and n=12 KLC1-/-). (E) Ratio of protein normalized extracellular γ–secretase products Aβ and p3 to Actin normalized APP in the lysate (n=12 wildtype, n=8 Kinesin-1C-/- and n=10 KLC1-/-). *$p<0.05$, by 2-tailed t-test. Error bars indicate standard error of the mean.


A
β-secretase
γ-secretase
N-
APPs-β
Aβ
AICD
-C
N-
APPs-α
p3
AICD
-C
α-secretase
γ-secretase
B
Aβ40 & p3
Relative Protein
1.6
1.2
0.8
0.4
0.0
*
C
wildtype
Kinesin-1C-/-
KLC1-/-
APP
Actin
D
APP
Relative Protein
1.6
1.2
0.8
0.4
0.0
*
E
Aβ40 & p3 / APP
Relative Aβ40 & p3/APP
1.2
0.8
0.4
0.0
Wildtype
Kinesin-1C-/-
KLC1-/-

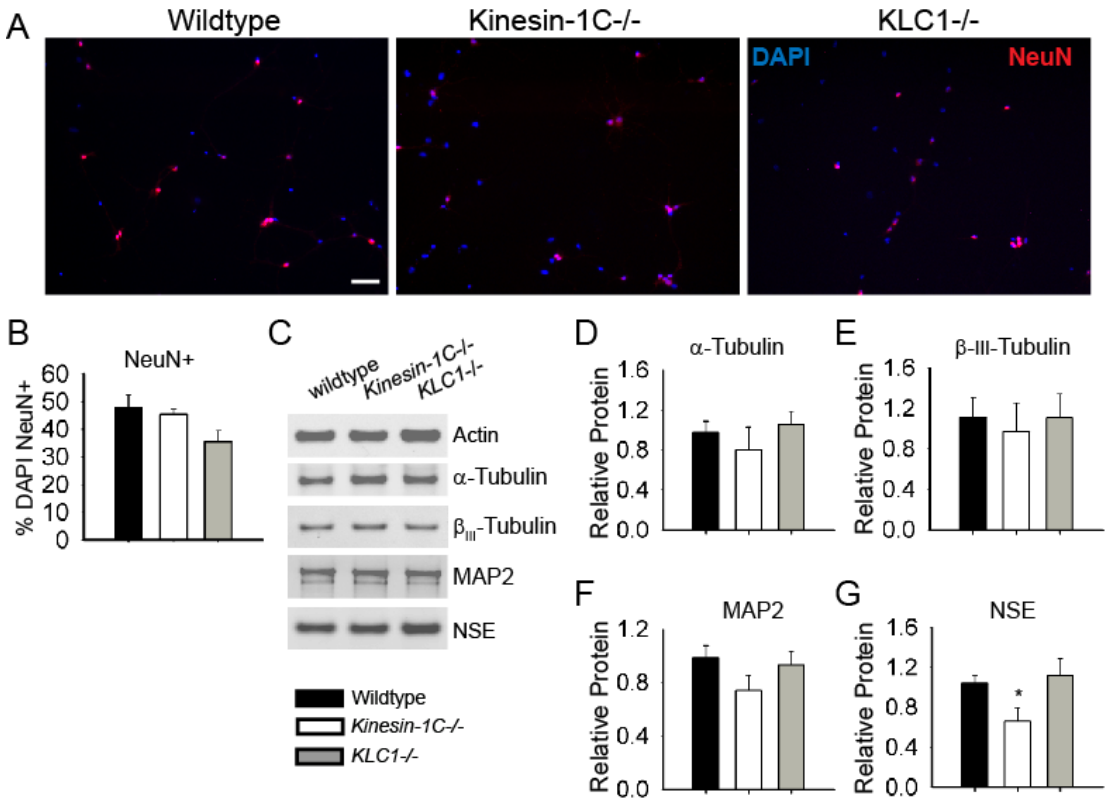


Figure 2.5. Neuronal marker composition of primary hippocampal cultures from wildtype KLC1-/- and Kinesin-1C-/- neonates. (A-B) Wildtype, KLC1-/- and Kinesin-1C-/- hippocampal neurons were cultured 11 days *in vitro* and stained for DAPI and the nuclear neuron marker NeuN. (A) Representative immunofluorescence images of wildtype, KLC1-/- and Kinesin-1C-/- hippocampal neurons stained with DAPI nuclei stain (blue) and NeuN (red). Scale bar 50 um. (B) Quantification of NeuN+ cells compared to total cells (=DAPI). n=6 wildtype, n=4 Kinesin-1C-/- and n=6 KLC1-/- mice; n=1347 wildtype, 896 Kinesin-1C-/- and 1919 KLC1-/- total DAPI nuclei. (C-G) Wildtype, Kinesin-1C-/- and KLC1-/- primary hippocampal cells were cultured for 11 days *in vitro* and then harvested. Protein was analyzed by Western blotting. (C) Representative immunoblots of Actin, α-Tubulin , β-III-Tubulin, MAP2, and NSE. (D-G) Quantification of protein levels relative to wildtype and normalized to Actin for α-Tubulin (D; n=15 wildtype, n=8 Kinesin-1C-/- and n=10 KLC1-/-), β-III-Tubulin (E; n=11 wildtype, n=6 Kinesin-1C-/- and n=10 KLC1-/-), MAP2 (F; n=15 wildtype, n=8 Kinesin-1C-/- and n=10 KLC1-/-) and NSE (G; n=17 wildtype, n=8 Kinesin-1C-/- and n=12 KLC1-/-). *$p < 0.05$ by 2 tailed t-test compared to wildtype. Error bars indicate standard error of the mean.

References

1. Hirokawa N, Pfister KK, Yorifuji H, Wagner MC, Brady ST, et al. (1989) Submolecular domains of bovine brain kinesin identified by electron microscopy and monoclonal antibody decoration. Cell 56: 867-878. doi:10.1016/0092-8674(89)90691-0

2. Verhey KJ, Kaul N, Soppina V (2010) Kinesin Assembly and Movement in Cells. Annu Rev Biophys. Available: http://www.ncbi.nlm.nih.gov/pubmed/21332353. Accessed 15 Mar 2011.

3. Rahman A, Friedman DS, Goldstein LS (1998) Two kinesin light chain genes in mice. Identification and characterization of the encoded proteins. J. Biol. Chem 273: 15395-15403.

4. Cabeza-Arvelaiz Y, Shih LC, Hardman N, Asselbergs F, Bilbe G, et al. (1993) Cloning and genetic characterization of the human kinesin light-chain (KLC) gene. DNA Cell Biol 12: 881-892.

5. Niclas J, Navone F, Hom-Booher N, Vale RD (1994) Cloning and localization of a conventional kinesin motor expressed exclusively in neurons. Neuron 12: 1059-1072.

6. Lamerdin JE, Stilwagen SA, Ramirez MH, Stubbs L, Carrano AV (1996) Sequence analysis of the ERCC2 gene regions in human, mouse, and hamster reveals three linked genes. Genomics 34: 399-409. doi:10.1006/geno.1996.0303

7. Xia C, Rahman A, Yang Z, Goldstein LS (1998) Chromosomal localization reveals three kinesin heavy chain genes in mouse. Genomics 52: 209-213. doi:10.1006/geno.1998.5427

8. Kanai Y, Okada Y, Tanaka Y, Harada A, Terada S, et al. (2000) KIF5C, a Novel Neuronal Kinesin Enriched in Motor Neurons. J. Neurosci. 20: 6374-6384.

9. Tanaka Y, Kanai Y, Okada Y, Nonaka S, Takeda S, et al. (1998) Targeted disruption of mouse conventional kinesin heavy chain, kif5B, results in abnormal perinuclear clustering of mitochondria. Cell 93: 1147-1158.

10. DeBoer SR, You Y, Szodorai A, Kaminska A, Pigino G, et al. (2008) Conventional kinesin holoenzymes are composed of heavy and light chain homodimers. Biochemistry 47: 4535-4543. doi:10.1021/bi702445j

11. Kamal A, Stokin GB, Yang Z, Xia CH, Goldstein LS (2000) Axonal transport of amyloid precursor protein is mediated by direct binding to the kinesin light chain subunit of kinesin-I. Neuron 28: 449-459.

12. Falzone TL, Stokin GB, Lillo C, Rodrigues EM, Westerman EL, et al. (2009) Axonal Stress Kinase Activation and Tau Misbehavior Induced by Kinesin-1 Transport Defects. J. Neurosci. 29: 5758-5767. doi:10.1523/JNEUROSCI.0780-09.2009

13. Encalada SE, Szpankowski L, Xia C-H, Goldstein LSB (2011) Stable Kinesin and Dynein assemblies drive the axonal transport of Mammalian prion protein vesicles. Cell 144: 551-565. doi:10.1016/j.cell.2011.01.021

14. Ferreira A, Niclas J, Vale RD, Banker G, Kosik KS (1992) Suppression of kinesin expression in cultured hippocampal neurons using antisense oligonucleotides. J. Cell Biol 117: 595-606.

15. Kimura T, Watanabe H, Iwamatsu A, Kaibuchi K (2005) Tubulin and CRMP-2 complex is transported via Kinesin-1. J. Neurochem 93: 1371-1382. doi:10.1111/j.1471-4159.2005.03063.x

16. Konishi Y, Setou M (2009) Tubulin tyrosination navigates the kinesin-1 motor domain to axons. Nat. Neurosci 12: 559-567. doi:10.1038/nn.2314

17. Stokin GB, Lillo C, Falzone TL, Brusch RG, Rockenstein E, et al. (2005) Axonopathy and Transport Deficits Early in the Pathogenesis of Alzheimer's Disease. Science 307: 1282-1288. doi:10.1126/science.1105681

18. Yamazaki T, Selkoe DJ, Koo EH (1995) Trafficking of cell surface beta-amyloid precursor protein: retrograde and transcytotic transport in cultured neurons. J. Cell Biol 129: 431-442.

19. Ferreira A, Caceres A, Kosik KS (1993) Intraneuronal compartments of the amyloid precursor protein. J. Neurosci 13: 3112-3123.

20. Rahman A, Kamal A, Roberts EA, Goldstein LSB (1999) Defective Kinesin Heavy Chain Behavior in Mouse Kinesin Light Chain Mutants. J Cell Biol 146: 1277-1288.

21. Dotti CG, Sullivan CA, Banker GA (1988) The establishment of polarity by hippocampal neurons in culture. J. Neurosci 8: 1454-1468.

22. Meijering E, Jacob M, Sarria J-CF, Steiner P, Hirling H, et al. (2004) Design and validation of a tool for neurite tracing and analysis in fluorescence microscopy images. Cytometry A 58: 167-176. doi:10.1002/cyto.a.20022

23. Kamal A, Almenar-Queralt A, LeBlanc JF, Roberts EA, Goldstein LS (2001) Kinesin-mediated axonal transport of a membrane compartment containing beta-secretase and presenilin-1 requires APP. Nature 414: 643-648. doi:10.1038/414643a

24. Kanai Y, Dohmae N, Hirokawa N (2004) Kinesin Transports RNA: Isolation and Characterization of an RNA-Transporting Granule. Neuron 43: 513-525. doi:10.1016/j.neuron.2004.07.022

25. Gauger AK, Goldstein LS (1993) The Drosophila kinesin light chain. Primary structure and interaction with kinesin heavy chain. J. Biol. Chem 268: 13657-13666.

26. Silverstein AM, Barrow CA, Davis AJ, Mumby MC (2002) Actions of PP2A on the MAP kinase pathway and apoptosis are mediated by distinct regulatory subunits. Proceedings of the National Academy of Sciences of the United States of America 99: 4221 -4226. doi:10.1073/pnas.072071699

27. Binder LI, Frankfurter A, Rebhun LI (1986) Differential localization of MAP-2 and tau in mammalian neurons in situ. Ann. N. Y. Acad. Sci 466: 145-166.

28. Cáceres A, Banker GA, Binder L (1986) Immunocytochemical localization of tubulin and microtubule-associated protein 2 during the development of hippocampal neurons in culture. J. Neurosci 6: 714-722.

29. Dotti CG, Banker GA, Binder LI (1987) The expression and distribution of the microtubule-associated proteins tau and microtubule-associated protein 2 in hippocampal neurons in the rat in situ and in cell culture. Neuroscience 23: 121-130.

30. Falzone TL, Gunawardena S, McCleary D, Reis G, Goldstein LSB (2010) Kinesin-1 transport reductions enhance human tau hyperphosphorylation, aggregation and neurodegeneration in animal models of tauopathies. Hum Mol Genet. Available: http://www.ncbi.nlm.nih.gov/pubmed/20817925. Accessed 8 Sep 2010.

31. Szodorai A, Kuan Y-H, Hunzelmann S, Engel U, Sakane A, et al. (2009) APP anterograde transport requires Rab3A GTPase activity for assembly of the transport vesicle. J. Neurosci 29: 14534-14544. doi:10.1523/JNEUROSCI.1546-09.2009

32. Mullen RJ, Buck CR, Smith AM (1992) NeuN, a neuronal specific nuclear protein in vertebrates. Development 116: 201-211.

33. Marangos PJ, Schmechel DE (1987) Neuron specific enolase, a clinically useful marker for neurons and neuroendocrine cells. Annu. Rev. Neurosci 10: 269-295. doi:10.1146/annurev.ne.10.030187.001413

34. Chun JT, Gioio AE, Crispino M, Giuditta A, Kaplan BB (1996) Differential compartmentalization of mRNAs in squid giant axon. J. Neurochem 67: 1806-1812.

35. Falley K, Schütt J, Iglauer P, Menke K, Maas C, et al. (2009) Shank1 mRNA: dendritic transport by kinesin and translational control by the 5'untranslated region. Traffic 10: 844-857. doi:10.1111/j.1600-0854.2009.00912.x

36. Erickson PF, Moore BW (1980) Investigation of the axonal transport of three acidic, soluble proteins (14-3-2, 14-3-3, and S-100) in the rabbit visual system. J. Neurochem 35: 232-241.

CHAPTER 3

Kinesin light chain 1 reduction impairs human embryonic stem cell neural differentiation and amyloid precursor protein metabolism

Abstract

The etiology of sporadic Alzheimer disease (AD) is largely unknown, although evidence implicates the pathological hallmark molecules amyloid-β (Aβ) and phosphorylated Tau (pTau). Work in animal models suggest that altered axonal transport caused by Kinesin-1 dysfunction perturbs levels of both Aβ and pTau in neural tissues, but the relevance of Kinesin-1 dependent functions to the human disease is unknown. To begin to address this issue, we generated human embryonic stem cells (hESC) expressing reduced levels of the Kinesin light chain 1 (KLC1) Kinesin-1 subunit to use as a source of human neural cultures. Despite reduction of KLC1, undifferentiated hESC were apparently normal. Neural induction cultures derived from KLC1-suppressed hESC contained neural rosettes and cells exhibiting a neural precursor (NP) cell surface marker signature, but exhibited reduced cell density.

When KLC1-suppressed NPs were sorted from neural induction cultures, unlike control cells, they failed to proliferate. Nevertheless, neural cultures containing neuron markers were obtained from KLC1-suppressed hESC by further differentiation of unsorted neural induction cultures. These cultures exhibited reduced levels of microtubule-associated neural proteins, including Tau. Interestingly these KLC1-deficient neural cultures also secrete less Aβ, a metabolite of the Amyloid Precursor Protein (APP), supporting the previously established connection between Kinesin-1 and Aβ. These data suggest that Kinesin-1 is required for normal human neural differentiation and ensuring proper metabolism of AD-associated molecules APP and Tau.

Introduction

Normal cellular organization and function requires intracellular transport driven by molecular motors. Kinesin-1 is a microtubule-based motor, moving cargos towards the plus end of microtubules [1,2] in neurons and in other cell types. Kinesin-1 is composed of a pair of heavy chains (KHCs), which use ATP hydrolysis to power movement on microtubules, and a pair of light chains (KLCs), which regulate KHC activity and mediate cargo attachment [3]. Mammalian Kinesin-1 is assembled from three KHC gene products - Kinesin-1A, -1B or 1C (formerly KIF5A, KIF5B or KIF5C, respectively) and four KLCs (KLC1, KLC2, KLC3, or KLC4) [4-8].

Kinesin-1 plays important roles in the nervous system. In mice Kinesin-1 subunits have tissue specific expression patterns: Kinesin-1B and KLC2 are ubiquitously expressed while Kinesin-1A, Kinesin-1C and KLC1 are enriched in

neural tissue [7-10]. Mutations in Kinesin-1 subunits in flies and mice can lead to smaller body sizes [11-13]. Kinesin-1 mutant mice exhibit reductions in brain size and/or white matter tracts [9,14] and cultured primary neurons with reduced Kinesin-1 subunits have shorter neurites [15-17]. Further, Kinesin-1 mutants exhibit loss of specific neuron populations [9,13,14]. These observations suggest that specific Kinesin-1 subunits may have multiple functions in nervous system development.

Kinesin-1 is a major anterograde motor driving transport into the axons of neurons and faulty axonal transport may contribute to neurodegenerative diseases [18]. AD is characterized pathologically by the presence of brain amyloid plaques and neurofibrillary tangles, the principle components of which are the APP proteolytic cleavage product Aβ and the axonal microtubule associated protein (MAP) Tau. APP is transported to synapses in a Kinesin-1 dependent manner and associates closely with KLC [19-22]. Tau also interacts with Kinesin-1 and may be transported in the axon by Kinesin-1 [23]. KLC1 mutant mice have hyperphosphorylated Tau [14,24] and APP transgenic mice with reduced KLC1 function exhibit earlier and accentuated brain amyloid plaques [25]. Together these data suggest that Kinesin-1 can modulate APP and Tau function but this is challenging to test in human neurons.

Progress in understanding human development and disease is limited by a lack of appropriate human model systems. While model organisms and human immortalized cells will continue to provide useful information, species or cell type differences restrict their utility [26]. Human embryonic stem cells [27] offer important benefits for modeling human development and disease - they proliferate indefinitely in

culture, are genetically malleable, are capable of differentiating into any cell type, and express proteins under endogenous transcriptional, translational and post-translational control.

We engineered hESC to express reduced levels of KLC1 as a source of neural cells to examine whether Kinesin-1 deficiency impairs human neural differentiation or endogenous human APP metabolism.

Materials and Methods

Cell culture and subcloning of undifferentiated Hues9 hESC lines

DNA oligonucleotides targeting KLC1 exon 2 (Forward 5`-TGTAATTTGGTGGAGGAGAATTCAAGAGATTCTCCTCCACCAAATTACTTTTTTC-3` and Reverse 5`-TCGAGAAAAAAGTAATTTGGTGGAGGAGAATCTCTTGAATTCTCCTCCACCAAATTACA -3` were subcloned as described [28] into pSicoR, or a modified pSico derived plasmid lacking the CMV-GFP cassette (Figure 3.1A). Vesicular stomatitis virus G protein pseudotyped lentivirus was prepared at the University of California, San Diego Vector Development lab to a titer of 10^8 colony forming units/ml.

Undifferentiated Hues9 hESC lines were maintained as described [29]. To derive Hues9 lines with reduced KLC1 Hues9 were exposed to lentivirus encoding KLC1 shRNA and plated at limiting dilution. Single hESC colonies were expanded and viral insertion confirmed by PCR. Cell karyotypes were obtained from Cell Line Genetics (Madison, WI).

Flow cytometry

Pluripotency of undifferentiated Hues9 lines was assessed by flow cytometry analysis of Oct-4 and TRA-1-81 expression. Cells were dissociated with accutase (Invitrogen), fixed in 4% paraformaldehyde, permeabilized, incubated with primary antibodies (direct conjugates from BD) and suspended to 1-2 X 10^6 cells/ml in sort buffer (1% FBS, 2.5 mM EDTA, 25 mM HEPES in PBS).

Neural induction cultures were dissociated with a 1:1 mixture of accutase and accumax. Antibodies (BD) were added to a final cell concentration of 1-5 X 10^7cells /ml. Labeled cells were sorted at 2.5-5.0 X 10^6 cells/ml in NP sort media (NP media - DMEM/F12, GlutaMAX, B27, N2, penicillin/streptomycin (all from Invitrogen) and 20 ng/ml bFGF (Peprotech) - supplemented with 10% FBS and 0.5mM EDTA).

Cells were analyzed or sorted on a BD Biosciences FACSAria cytometer using a 100 micron diameter ceramic nozzle and 20 pounds psi sheath pressure. Single stained cells or CompBeads (BD) and FACSDiva software were used to calculate compensation values prior to analysis. Doublets were excluded from analysis with gates on forward and side scatter bivariate plots of pulse height relative to width (Figure 3.5A and Figure 3.7A). Antibody positivity was defined by comparison to unstained controls. Analysis was conducted offline using FCS Express (De Novo Software).

Western blot analysis of protein levels

Tissue culture lysates were prepared using PARIS kit (Ambion) buffer supplemented with protease (cocktail set I, Calbiochem) and phosphatase (Halt, Pierce) inhibitors. The BCA assay (Pierce) was used to estimate the protein content. Equal protein amounts were separated in MES buffer alongside Novex Sharp pre-stained markers (Invitrogen) on NUPAGE 4-12% acrylamide precast gels (Invitrogen) and then transferred to nitrocellulose (0.2 or 0.45 um pore size Immobilon Millipore). Membranes were blocked in 5% BSA in tris buffered saline with 0.1% Tween-20. Primary antibodies (KLC1 H75 1:500 Santa Cruz Biotechnology; Kinesin-1C 1:500 C.H. Xia (unpublished); Actin C4 1:100,000 Millipore; GFAP 1:500 Dako; NSE 1:1000 Millipore; MAP2 AP20 1:1000; α-Tubulin DM1A 1:50,000 Sigma; β-III-Tubulin TUJ1 1:1000 Covance; pNF-H and pNF-M SMI31 1:1000 Covance; Tau Tau-46.1 1:500 Sigma; pTau PHF1 1:500 Peter Davies, The Feinstein Institute for Medical Research; APP N terminus LN27 1:250 Invitrogen; APP C terminus 1:250 Zymed/Invitrogen; 1:250 SOD1 Santa Cruz Biotechnology; GAPDH, 1:3000 Ambion) were prepared in 5% BSA and incubated with membranes overnight at 4°C. Fluorescent secondary antibodies (LiCor) were diluted 1:6000-15,000. LiCor Odyssey infrared imager was used to measure pixel intensities of bands at detector settings set one half unit below saturation. For each protein band, background subtracted integrated intensity values were calculated using the Odyssey software. Since absolute integrated intensity values vary for the same samples on different blots, samples within a blot were plotted relative to control and these normalized values were used to

average replicates from separate blots. Linearity of antibody response was verified over the range of 1-10 μg. To show protein bands in the conventional manner with dark bands on a light background, grayscale images were inverted in the figures.

Immunofluorescence

Cells were fixed in 4% paraformaldehyde/0.12M sucrose. For intracellular staining of Oct-4, KLC1, Sox1 and Nestin, cells were permeabilized with 0.1% Triton X-100, blocked with 10% FBS in PBS, and incubated with KLC1 (H75 rabbit IgG, 1:400, Santa Cruz Biotechnology), Octamer-4 (Oct-4; C10 mouse IgG2b 1:300, Santa Cruz Biotechnology), Sex determining region Y-box 1 (Sox1; mouse IgG 1:1000, BD Biosciences) or Nestin (rabbit IgG, 1:2000, Millipore) primary antibodies. Secondary antibodies AlexaFluor 568 goat anti-rabbit IgG (H+L) or AlexaFluor 568 goat anti-mouse IgG (H+L) antibodies (both from Invitrogen) were used at 1:750 with 0.1 mg/ml 4′,6′-diamidino-2-phenylindole (DAPI; Sigma) nuclei stain prior to mounting on slides with Prolong Gold anti-fade reagent (Invitrogen). Specificity of secondary antibody staining was verified using secondary only controls. For cell surface Tumor Rejection Antigen (TRA-1-81) staining, cells were fixed and blocked as above and AlexaFluor 647 conjugated TRA-1-81 primary antibody (BD Biosciences) was used at 1:10. Fluorescence images were collected using a Zeiss Axioplan microscope equipped with a Zeiss Plan Neofluor 20X/0.50 NA objective, Texas Red and Cy5 filters, a CoolSNAPcf camera (Roper Scientific) and MetaMorph (Molecular Devices) software.

To quantify the percent of Sox1 or Nestin-positive cells, Sox1, Nestin and DAPI, the Image-based Tool for Counting Nuclei (University of California – Santa Barbara Center for Bio-Image Informatics) plug-in of ImageJ (NIH) was used to count the number of Sox1, Nestin and DAPI-positive cells per image. Care was taken to ensure that the best possible input parameters were used so that the algorithm identified cells that would also be manually judged positive. The proportion of Sox1 and Nestin-positive nuclei was calculated from a total of 932 DAPI nuclei. Technical replicates were used to calculate the standard error of the mean.

Neural differentiation of hESC

For differentiating hESC using the embryoid body (EB) method [30], hESC on confluent 10 cm plates were dispase treated (BD; 1:50 in hESC media), scraped and transferred to bacteriological grade Petri dishes in hESC media lacking FGF2 but containing 1 mM Rho-associated protein kinase inhibitor (Y27632 or trans-4-[(1R)-1-Aminoethyl]-N-4-pyridinylcyclohexanecar boxamide dihydrochloride; Calbiochem). On day 5, EBs were plated onto matrigel (BD) treated tissue culture plate in insulin, transferrin and selenium (ITS) media (Dulbecco's minimum essential medium (DMEM)/F12, penicillin streptomycin (both from Invitrogen) and ITS supplement, Sigma). Media was replenished every other day thereafter.

For PA6 feeder differentiation, mouse PA6 stromal cells [31] were co-cultured with hESC as described [32]. In brief, PA6 cells were plated at 6400 cells/cm^2 in growth media (high glucose DMEM, FBS, glutamine, penicillin and streptomycin).

The following day hESC were seeded onto the PA6 feeder at 13 cells/cm^2 (for control and *shKLC1-1*) or 50 cells/cm^2 (*shKLC1-2*) in PA6 differentiation media. The media was exchanged on day 6 and every other day thereafter.

Brightfield imaging of cultures

To track morphology of the cells, cultures were imaged using a Nikon Eclipse TS100 and a Sony Power Shot G3. The camera was set to landscape mode, manual focus and images were collected with 5.7X zoom. A micrometer was used to calibrate the images.

Neural precursor culture, viral transduction and differentiation

Sorted Hues9-derived NPs were grown on polyornithine and laminin coated plates in NP media. Media was exchanged every other day and cultures were split every 3-4 days. When nearly confluent, Hues9 derived NPs were transduced with virus containing CMV-GFP reporter cassette and U6-shKLC1 or U6-shLUC control shRNA and centrifuged at 800 x *g* for 45 min at room temperature. Following expansion for 1-2 passages, cells were subjected to fluorescence activated cell sorting to enrich for GFP+ cells and cultured.

To differentiate NPs to neurons, NPs were plated on polyornithine and laminin coated plates in NP media and grown until they reached 70% confluence. FGF was removed and NP media supplemented with 20 ng/ml BDNF (Peprotech), 20 ng/ml GDNF (Peprotech) and 0.5 mM dibutyryl cAMP (N6,2′-O-Dibutyryladenosine 3′,5′-cyclic monophosphate sodium salt; Sigma). Media was exchanged every 2-3 days.

Aβ and soluble APP (sAPP) quantification

To measure secreted Aβ and sAPP from hESC derived neural cultures, cultures were differentiated as described and the media changed completely 24 hours before harvest. Media was collected and supplemented with protease inhibitors. Cells were scraped in homogenization buffer (20 mM Tris pH 7.4, 1 mM EDTA, 1 mM EGTA, 250 mM sucrose, protease and phosphatase inhibitors) and homogenized. Aβ-40, -42 and -38 and sAPP-α and -β were quantified in media or lysate solubilized in 1% Triton X-100 using multiplex Meso Scale Discovery electrochemiluminescence immunoassays with human specific antibodies according to kit instructions. The data were normalized to the total protein in the lysate. Since the fraction of neurons may differ between cultures, APP cleavage product levels were normalized to neuron-specific enolase (NSE) in the lysate.

Results

KLC1 reduction does not alter hESC morphology or pluripotency

To obtain undifferentiated KLC1-deficient hESC, we transduced Hues9 hESCs [29] with lentivirus [33] coding for a KLC1-specific shRNA (referred to here as *shKLC1-1* or *shKLC1-2;* Figure 3.1A-B) [28]. Using limiting dilution plating single colonies were obtained, expanded and screened by PCR for the insert (Figure 3.1C-D). Reduced KLC1 levels of *shKLC1-1* and *shKLC1-2* compared to control cells were confirmed by both immunofluorescence (Figure 3.2A) and immunoblot (Figure 3.2B).

We tested whether subcloned undifferentiated hESC exhibited normal colony morphology, karyotype and pluripotency marker expression. Cell clusters from control and shKLC1 lines exhibited well-bordered colony morphology typical of pluripotent stem cells (Figure 3.3A, arrows). Normal karyotypes suggest neither the subcloning process nor KLC1 reduction caused gross cytogenetic instability (Figure 3.3B). Fluorescence micrographs of Oct-4 (Figure 3.4A) and TRA-1-81(Figure 3.4B) revealed normal cellular distributions of Oct-4 in the nucleus and TRA-1-81 on the cell surface in control and KLC1 reduced cells suggesting depletion of KLC1 has no obvious effect on localization of these two pluripotency markers. Using flow cytometry, we found similar proportions of *shKLC1-1*, *shKLC1-2* and control cells expressing both Oct-4 and TRA-1-81 (Figure 3.5B, events colored blue). Collectively these data suggest that undifferentiated pluripotent cells with 70-80% reduced KLC1 exhibit apparently normal colony morphology, karyotypes and pluripotency marker expression.

KLC1 depleted hESC produce cultures containing neural precursors (NPs)

Defects in specific Kinesin-1 subunits can cause reductions in overall body size and/or neural tissue as well as loss of specific neuron types [9,12-14] in animal models. NPs are the cells that divide and give rise to neurons or glia. Therefore, we examined the NPs produced in neural induction cultures derived from control and KLC1-reduced hESC. We used two different methods for inducing hESC to differentiate to neuroectoderm. In the first, feeder cells are used to stimulate

differentiation (Figure 3.6A, top). These mouse stromal PA6 feeder cells can also be used to generate more mature neural cultures containing markers of neurons and glia [32]. In the second, nonadherent floating cell clusters, called embryoid bodies (EBs), are generated and plated in neuralizing media (Figure 3.6A, bottom). Since human neural differentiation from hESC generally follows human embryonic developmental principles [34], we analyzed NPs at 18 days from the undifferentiated hESC state, during the developmental equivalent of the neural tube stage. Bright-field imaging of day 18 cultures from both the PA6 feeder (Figure 3.6B, top panels) and EB methods (Figure 3.6B, bottom panels) revealed that control, *shKLC1-1* and *shKLC1-2* hESC derived differentiation cultures contained 'rosette' cell cluster structures (Figure 3.6B arrowheads and insets) which resemble the neural tube and are typically found in neural induction cultures [35], suggesting that hESC with reduced KLC1 are capable of generating NP cells. Interestingly, both types of neural induction cultures from hESC with reduced KLC1 had smaller colonies suggesting reduced overall cell densities (Figure 3.6B). We confirmed that KLC1-suppressed hESC produced reduced neural induction culture cell densities by quantifying cell densities in day 18 EB neural induction cultures (Figure 3.6C).

Flow cytometry is a useful tool for identifying stem cell populations [36]. To determine whether expression of KLC1 shRNA in undifferentiated hESC affects the proportion of neural precursor (NP) cells within both types of neural induction cultures, we used flow cytometry to survey the population of control, *shKLC1-1* and *shKLC1-2* progeny exhibiting high levels of CD184 and CD24 and low levels of

CD271 and CD44, a cell surface signature characteristic of cells which differentiate into neurons and glia ($CD184^{hi}CD24^{hi}CD271^{lo}CD44^{lo}$; Figure 3.7)[30]. Interestingly, while ~40% of control cells in EB neural induction cultures exhibited this $CD184^{hi}CD24^{hi}CD271^{lo}CD44^{lo}$ NP signature only ~8% of control cells in PA6 feeder neural induction cultures expressed this marker combination (Compare black bars between Figure 3.7C and Figure 3.7D; see also Figure 3.7B). Thus the EB compared to the PA6 differentiation method produces a higher proportion of control cells exhibiting the $CD184^{hi}CD24^{hi}CD271^{lo}CD44^{lo}$ NP signature. The effect of KLC1 reduction on the proportion of NPs generated was also dependent on the neural induction method. EB differentiated cultures derived from KLC1-suppressed compared to control hESC had ~50% reduced fraction of $CD184^{hi}CD24^{hi}CD271^{lo}CD44^{lo}$ cells (Figure 3.7C), but levels of KLC1 had no significant effect on the proportions of $CD184^{hi}CD24^{hi}CD271^{lo}CD44^{lo}$ cells when hESC were differentiated using the PA6 feeder method (Figure 3.7D). Thus the effect of KLC1 reduction on the $CD184^{hi}CD24^{hi}CD271^{lo}CD44^{lo}$ NP population is neural induction method dependent.

Neural precursors with reduced KLC1 do not proliferate normally

To address whether KLC1 levels affect NP function, we sorted NPs from neural induction cultures derived from hESC with normal or reduced KLC1. Since EB compared to PA6 feeder neural induction cultures produced a higher proportion of control NPs (Figure 3.7C compared to Figure 3.7D), we sorted cells with the

$CD184^{hi}CD24^{hi}CD271^{lo}CD44^{lo}$ NP cell surface signature from day 18 EB neural induction cultures. Regardless of KLC1 levels, sorted NP cells appeared morphologically similar initially (Figure 3.8A). However NP cells with reduced KLC1 failed to multiply while NP cells differentiated from control hESC proliferated, expressed NP markers Sox1 and Nestin (Figure 3.8B-C) and differentiated to cultures containing highly polarized cells resembling neurons (Figure 3.8D). To confirm that KLC1 suppression prevents normal NP propagation in homogeneous NP cultures, we transduced control hESC derived EB NP cells with lentivirus containing a GFP reporter and either shRNA to KLC1 (shKLC1) or a control luciferase shRNA (shLUC) and sorted GFP positive cells (Figure 3.9). GFP positive shLUC NP cells proliferated and maintained high levels of GFP expression seven passages later (data not shown). In contrast, GFP sorted shKLC1 NPs did not proliferate. Taken together these data suggest cellular defects induced by reduction in KLC1 can affect differentiation to and impair proliferation of some $CD184^{hi}CD24^{hi}CD271^{lo}CD44^{lo}$ NP populations.

KLC1-deficient human neural cells exhibit reduced levels of microtubule related proteins

Several lines of evidence suggest that neurons with impaired Kinesin-1 may be smaller. KLC1 mutant mice have reduced white matter in the brain and spinal cord [14], Kinesin-1C mutant mice have smaller brains [9] and Kinesin-1 dysfunction reduces neurite lengths [15-17,37,38]. We tested whether human neurons with depleted Kinesin-1 were similarly impaired. The PA6 feeder method produced similar

proportions of cells exhibiting the $CD184^{hi}CD24^{hi}CD271^{lo}CD44^{lo}$ NP cell surface signature regardless of KLC1 hESC levels (Compare Figures 3.7C and 3.7D) and can be used to generate more mature neuronal cultures [32]. Therefore I used this method to differentiate control and KLC1-suppressed hESC for seven weeks.

To confirm reduction in KLC1 in PA6 feeder cultures differentiated for seven weeks, I used Western blotting to assess KLC1 protein levels in control *shKLC1-1*, and *shKLC1-2* differentiation culture lysates. I observed that KLC1 levels in *shKLC1-1* and *shKLC1-2* were reduced to 46% and 2% of control levels, respectively (Figure 3.10), suggesting that knockdown is maintained for at least seven weeks of PA6 feeder differentiation. Previous experiments in *M. musculus* (See Figure 2.1) and *D. melanogaster* (unpublished data) suggested that genetic reductions in KLC can lead to reduction in KHC and vice versa. When I examined Kinesin-1C levels in human neural cultures I found reduced Kinesin-1C in KLC1-suppressed differentiation cultures - to 47% and 20% of control (Figure 3.10).

We examined the morphology over time of control, *shKLC1-1* and *shKLC1-2* PA6 feeder differentiation cultures using bright field imaging. By *in vitro* differentiation day nine, hESC derived cell clusters peppered the feeder cell monolayer (Figure 3,11, left panels). By differentiation day 22 these hESC-derived cell clusters had expanded in size and sprouted axon-like projections, which persisted at least until differentiation week seven (compare middle and right panels of Figure 3.11). While all lines followed this differentiation progression, *shKLC1-1* and *shKLC1-2* appeared to exhibit reduced cell density over the course of the

differentiation (Figure 3.11 and Figure 3.12) and less extensive and shorter projections in polarized cells at the time of harvest (Figure 3.11, arrows in right-most panel and Figure 3.12). The *shKLC1-2* line, which expresses the least KLC1 protein (Figure 3.10), was most affected (Figure 3.11, bottom panel and Figure 3.12), suggesting that reduced levels of KLC1 impair neural differentiation.

Since we observed apparent defects in neural differentiation of hESC with reduced KLC1 by bright field imaging we estimated the relative proportion of neurons and glia in control and *shKLC1-1* seven week PA6 feeder differentiation cultures by assessing relative levels of neuron marker Neuron Specific Enolase (NSE) and glial marker Glial Fibrillary Acidic Protein (GFAP) by Western blot. We were unable to include *shKLC1-2* neuronal differentiation cultures in this analysis because of limited material. Since mouse PA6 feeder cells may linger in hESC differentiation cultures, we assessed the relative contribution of these feeder cells by comparing levels of "housekeeping" proteins Actin, Glyceraldehyde 3-Phosphate Dehydrogenase (GAPDH) and Superoxide Dismutase (SOD1) in PA6 feeder cells cultured for seven weeks in the presence or absence of control or *shKLC1-1* hESC. Mouse and human SOD1 and GAPDH proteins have different electrophoretic mobilities so the presence or absence of the mouse and human bands can indicate the contribution of mouse PA6 cells compared to human protein. The mouse SOD1 and GAPDH bands were easily detectable in PA6 feeder cell lysates, but not in samples derived from PA6 cells co-cultured with either control or *shKLC1-1* hESC (Figure 3.13A), suggesting minimal PA6 mouse cell contamination within the differentiation cultures. Since these cultures

also contained other hESC differentiation progeny, we used the ubiquitously expressed protein Actin to normalize between samples. We found no significant difference in either NSE or GFAP levels between control and *shKLC1-1* differentiation cultures (Figure 3.13B-C), suggesting that the proportions of neurons and glia within control and *shKLC1-1* PA6 differentiation cultures were similar.

Our imaging data suggest that human neuron-like cells produced in PA6 differentiation cultures from hESC with reduced KLC1 may have shorter projections than control cells (Figure 3.11 right-most panel and Figure 3.12). To test whether KLC1-suppressed hESC produce neuron-like cells with normal proportions of the microtubule components enriched in neurites, we compared levels of Actin-normalized α-Tubulin, β-III-Tubulin, the dendrite marker microtubule associated protein 2 (MAP2) and axonal markers phosphorylated neurofilament (pNF; heavy – pNF-H and medium - pNF-M chains) and full length Tau (using both phosphorylation-dependent and -independent antibodies) in PA6 control and *shKLC1-1* hESC differentiation cultures cultured seven weeks *in vitro*. Interestingly, *shKLC1-1* compared to control differentiation cultures had 25-30% less microtubule subunits α-Tubulin and β-III-Tubulin (an isoform enriched in neurons) and MAP2 (Figure 3.13B-C). Axonal markers pNF-H and pNF-M were also reduced by 25-35% while Tau was down by > 60%, regardless of phosphorylation state (Figure 3.13B-C). These observations suggest that pluripotent cells with reduced KLC1 are capable of differentiation to neuron-like progeny, but these progeny may be smaller due to shorter projections.

Reduced KLC1 alters APP metabolism in human neural cultures derived from hESC

Because APP metabolism is linked to AD, it is important to understand how it is regulated in human neurons at endogenous levels. APP associates closely with KLC1 and its axonal transport is Kinesin-1 dependent [19-22]. Reduction of full length murine KLC1 in adult mice expressing transgenic human familial AD-associated APP perturbs brain Aβ levels [25]. Aβ is produced by the sequential cleavage of APP by β-secretase and then γ-secretase, while APP cleavage by the α-secretase prevents formation of Aβ peptides (Figure 3.14A). To assess whether human KLC1 depletion alters APP metabolism in human neural cultures, we measured levels of full length APP and its extracellular metabolites in control or shKLC1-1 hESC PA6 differentiation cultures aged seven weeks. To account for possible differences in the fraction of neurons between cultures we normalized the values to NSE. While levels of full length APP (Figure 3.14B-C) or soluble intracellular Aβ (Figure 3.14E) in control compared to shKLC1-1 PA6 feeder cultures were not significantly different, secreted extracellular Aβ levels were substantially reduced in KLC1-suppressed neural cultures (Figure 3.14D). Regardless of KLC1 levels, 99% of the Aβ40 detected was found in the extracellular fraction. We also tested if PA6 differentiation cultures derived from shKLC1-1 compared to control hESC have similar levels of extracellular sAPPβ or sAPPα fragments. We discovered that although KLC1 depletion did not affect extracellular levels of sAPPα, KLC1 depleted neural cultures had less extracellular sAPPβ than control (Figure 3.14F). These results suggest that KLC1

deficiency in human neurons may perturb APPβ, but not APPα cleavage of endogenous APP.

Discussion

A role for the KLC1 subunit of Kinesin-1 in NP maintenance?

Previous studies suggest important functions for Kinesin-1 subunits in the development and maintenance of the nervous system of animal models. Tissue expression patterns of Kinesin-1 subunits show that Kinesin-1A, Kinesin-1B, Kinesin-1C, KLC1 and KLC2 are widely expressed in neural tissues [7-10]. Mice lacking full length Kinesin-1A, Kinesin-1B and KLC1 exhibit moderate to severe growth retardation and Kinesin-1C mice have smaller brains than wildtype suggestive of cell proliferation defects [9,10,12,13]. Previous studies in our lab showed that KLC1 deficient mice also display phenotypes associated with AD [14,24,25]. Therefore, we tested for NP defects in human neural induction cultures with perturbed KLC1. Since overexpression of KLC1 leads to non-physiological cellular aggregation of the protein which is difficult to interpret, we tested the effect of reduced endogenous KLC1 [17,39]. We found neural induction cultures derived from KLC1-suppressed compared to control hESC have reduced overall cell densities. This observation parallels the reduced body sizes observed in *D. melanogaster khc* and *M. Musculus* KLC1 and KHC mutant animals [11-13]. Our data also show that both NPs sorted from KLC1-suppressed neural induction cultures and control NPs infected with lentivirus coding for shRNA to KLC1 fail to proliferate. These data suggest the hypothesis that KLC1

reduction may suppress NP proliferation capacity. Given the neural expression of other Kinesin-1 subunits and the growth retardation defects observed in Kinesin-1A, Kinesin-1B and Kinesin-1C mutant mice, it is possible these other subunits may also have important functions in NP maintenance.

Previous work has demonstrated that different neural induction methods give rise to different neuron types [34,40-44]. We observed that the proportion of control cells exhibiting the NP cell surface signature depended on the neural induction method employed to generate them. The simplest explanation is that the NP subtypes that arise and their local cellular environments are fundamentally different between EB and PA6 feeder neural induction cultures. This possibility is supported by reports suggesting PA6 feeder cells produce neurons most resembling neural crest derivatives while EB methods are capable of generating cells similar to forebrain and spinal cord motor neurons [40,41,44]. A second possibility is that the EB culture system supports the formation of larger or larger numbers of NP producing environments with greater diversity in NP subtypes than the PA6 feeder system.

Our observation that the proportion of NPs produced by the EB cultures is affected by KLC1 knockdown, while the NPs from the PA6 feeder method are not, further underscores the difference between these neural induction methods. The hypothesis that EB and PA6 neural induction cultures produce different NP types may explain why NPs in EB, but not PA6 feeder cultures are susceptible to KLC1 suppression. However, why are the NP proportions in EB cultures derived from hESC with suppressed KLC1 only partially reduced compared to control? Do the EB

cultures produce multiple NP subtypes, a subset of which is KLC1–dependent? Or does KLC1 suppression lead to reduced proportions of all NPs in these cultures? If KLC1 function is required for proliferation or determination of certain but not all types of NPs, this suggests KLC1 function may be required for the normal production of some subsets of neurons. If true this may account for why motor neuron numbers in particular are reduced in KLC1 mutant mice [14]. The discovery of additional cell signatures distinguishing between NP subtypes and their use with both flow and image-based quantitative cytometry, will be an important advance for standardizing culture and differentiation conditions for these types of experiments.

KLC1 depletion affects microtubule associated proteins

Since KLC1 mutant animals exhibit neural defects, we tested whether reduced KLC1 impairs the differentiation of hESC to neural cells. We found that the neural microtubule-associated markers β-III-Tubulin, MAP2, pNF and Tau are reduced in KLC1 suppressed compared to control cultures. Intriguingly, previous studies suggest that Kinesin-1 may transport Tubulin, thereby regulating cell size and shape [16,45,46]. If Kinesin-1 reduction impairs transport of microtubules into neuronal projections, it may cause reductions in cell size, neurite length and levels of MAPs such as MAP2, pNF and Tau. Indeed several studies report reductions in neurite length in KHC or KLC-depleted cultured rodent hippocampal neurons [15-17] and in the dendrites of neurons in *C elegans* and *Drosophila* [37,38]. Reductions in cell size may also partially account for body size reductions observed in Kinesin-1 mutant flies and

mice and the reduced white matter tracts observed in the KLC1 mutant mouse. Alternatively, reduced levels of neural MAPs in the KLC1 suppressed human neural cultures may be due to fewer neurons, although this seems less likely for two reasons. First, we found no apparent reduction in the proportion of NP cells derived from hESC with normal or reduced KLC1 in PA6 feeder derived mixed neural cultures at 18 days *in vitro*. Second, neither NSE levels nor the fraction of neuronal (β-III isoform as a fraction of the more widely expressed α-Tubulin) Tubulin were different in neural cultures derived from hESC with normal or KLC1-depleted hESC.

Effect of KLC1 reduction on APP metabolism in human neural cultures.

We found that neural cultures derived from KLC1-reduced hESC have less Aβ compared to control, supporting a functional connection between Kinesin-1 and APP trafficking and/or metabolism. The exact nature of this connection is unknown. However, evidence suggests that Kinesin-1 may transport APP within axons of neurons [20,25,47]. The intracellular location of APP is thought to affect its metabolism with α-secretase cleavage likely occurring at the plasma membrane and β-secretase cleavage in endosomal compartments [48]. Once produced, sAPP and Aβ peptides are secreted [49] and may be degraded by proteases, such as Neprilysin, in the extracellular milieu [50]. Kinesin-1 based axonal transport defects could disrupt any or all of these processes. Our data imply no net effect on extracellular levels of sAPPα in neural cultures derived from hESC with depleted compared to control KLC1 levels, suggesting this cleavage pathway may be normal. However, extracellular levels

of β-cleavage pathway products sAPPβ and Aβ are both reduced in the KLC1-suppressed compared to control hESC derived neural cultures, suggesting the APPβ cleavage pathway is disrupted by impaired Kinesin-1. The reduced extracellular Aβ from KLC1-reduced hESC derived human neural cultures agrees with reports of reduced amyloid plaque loads following mechanical disruptions in axonal transport in the perforant pathway of APP transgenic mice [51]. Experiments in better defined human neural cultures will be a first step to understanding the nature of this effect in human neurons.

Work in transgenic mice expressing a familial AD mutant APP suggests that axonal transport perturbations arising from reduced KLC1 function lead to earlier and increased brain Aβ production and plaque deposits [25]. Compared to mice with normal Kinesin-1, animals with reduced KLC1 function also have more Tau in neural tissues [14,24]. Here we find that human Kinesin-1 depletion in hESC-derived neural cultures reduces endogenous levels of Tau and Aβ. It is unclear why Kinesin-1 disruption in human neural cultures reduces Aβ and Tau while in mouse brain, these proteins are increased. Possible explanations include species specific differences, modes of KLC1 perturbation, neuron type or maturity or differences in production or turnover. Nonetheless, together our data support functional connections between Kinesin-1 and levels of Tau and Aβ.

Summary

To examine the effect of Kinesin-1 dysfunction on neural differentiation and APP metabolism in human neural cultures, we generated hESC with reduced KLC1. Unexpectedly, we discovered cell proliferation defects in specific populations of NPs in neural induction cultures derived from KLC1-suppressed hESC. Neurons in more mature neural differentiation cultures derived from KLC1-suppressed hESC appear smaller than normal and have less amyloidogenic APP cleavage products. Because impaired APP metabolism is linked to AD the model we have generated can be used to define the essential function(s) of KLC1 in NPs and their progeny as well as to comprehend its role in regulating the production, transport and turnover of APP and Tau. This knowledge will have important implications for human neurodevelopmental and neurodegenerative diseases.

Acknowledgements

We thank Jeremy Chau and Alfonso Reyes for technical support and Sandra Encalada for critical review of work. Chapter 3, in part, has been submitted for publication of the material as it may appear in PLoS ONE. Rhiannon L. Killian, Jessica D. Flippin, Cheryl Herrera, Angels Almenar-Queralt and Lawrence S. B. Goldstein, 2011. The dissertation author was the primary investigator and author of this paper.

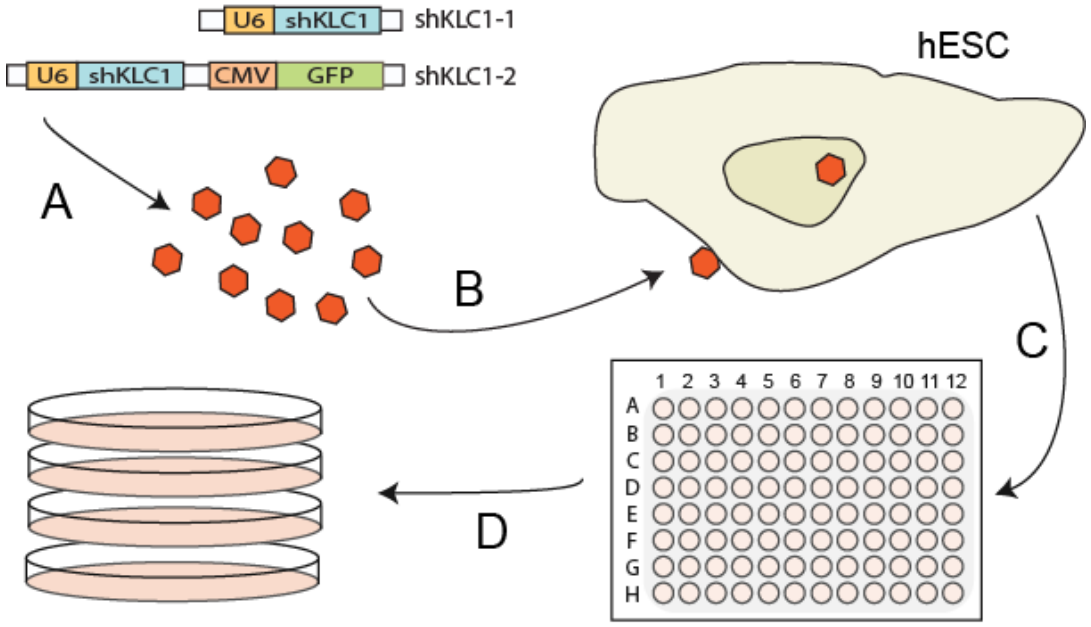


Figure 3.1. Scheme for generating pluripotent stem cell lines with KLC1 knockdown. (A) A lentiviral vector encoding a shRNA targeted to KLC1 (shKLC1) was packaged into lentiviral particles. (B) Dissociated Hues9 hESC cells were exposed to the virus and (C) plated at limiting dilution. Wells containing single colonies were expanded (D) and screened by PCR for the presence of viral elements.

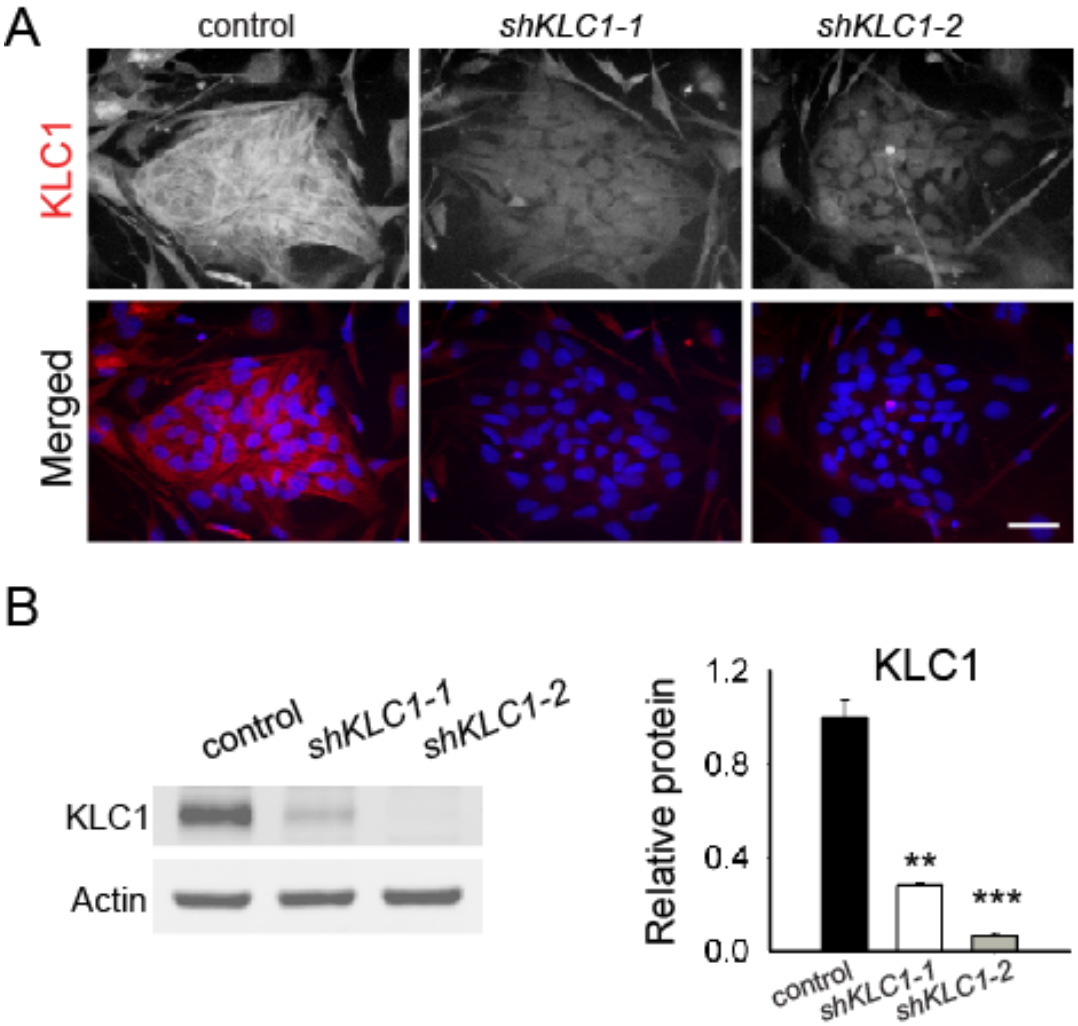


Figure 3.2. Undifferentiated hESC exhibiting reduced KLC1. (A) Immunofluorescence staining of KLC1 in undifferentiated hESC control, *shKLC1-1* and *shKLC1-2* colonies. Merged images show overlay of KLC1 (red) and DAPI-stained nuclei (blue). Scale bar 50 micrometers. (B) Equal protein from undifferentiated control, *shKLC1-1* and *shKLC-2* culture lysates were analyzed by Western blot for KLC1 and Actin. Bar graph shows Actin normalized KLC1 levels relative to control. n=3; **p < 0.01, ***p<0.001 by 2-tailed t-test compared to control.

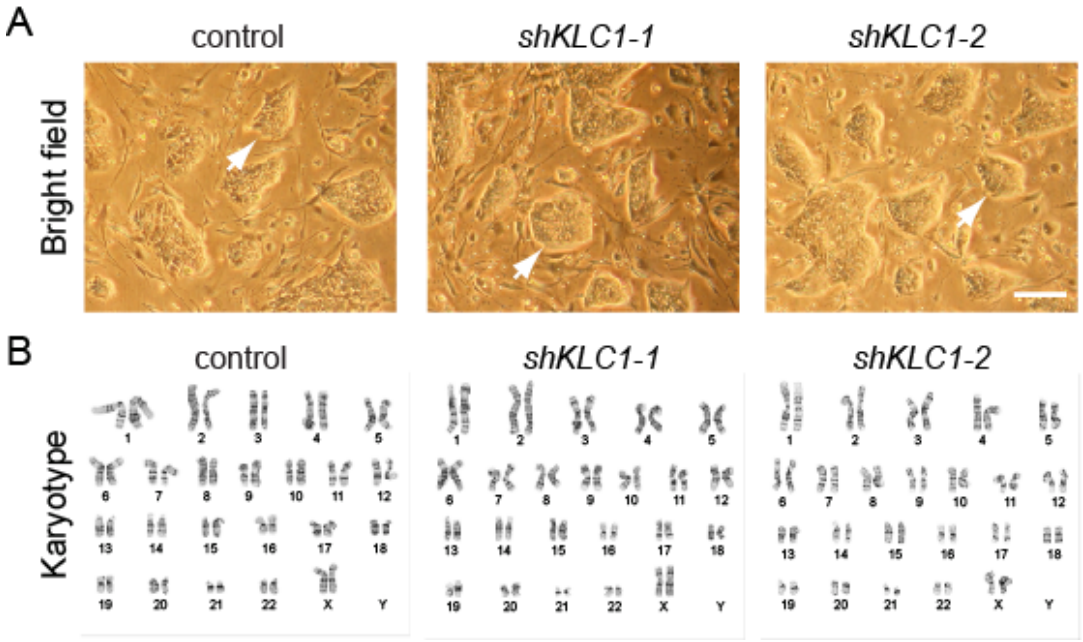


Figure 3.3. Undifferentiated KLC1-suppressed hESC exhibit normal morphology and karyotypes. (A) Representative images of control, *shKLC1-1* and *shKLC1-2* undifferentiated hESC cultures showing bordered colony morphology typical of pluripotent cells (arrows). Scale bar 200 micrometers. (B) Metaphase chromosome spreads of Hues9 passage 41: 46,XX,inv(9)(p12q13), *shKLC1-1* passage 42: 46,XX,inv(9) and *shKLC1-2* passage 44: 46,XX,inv(9)(p12q13).

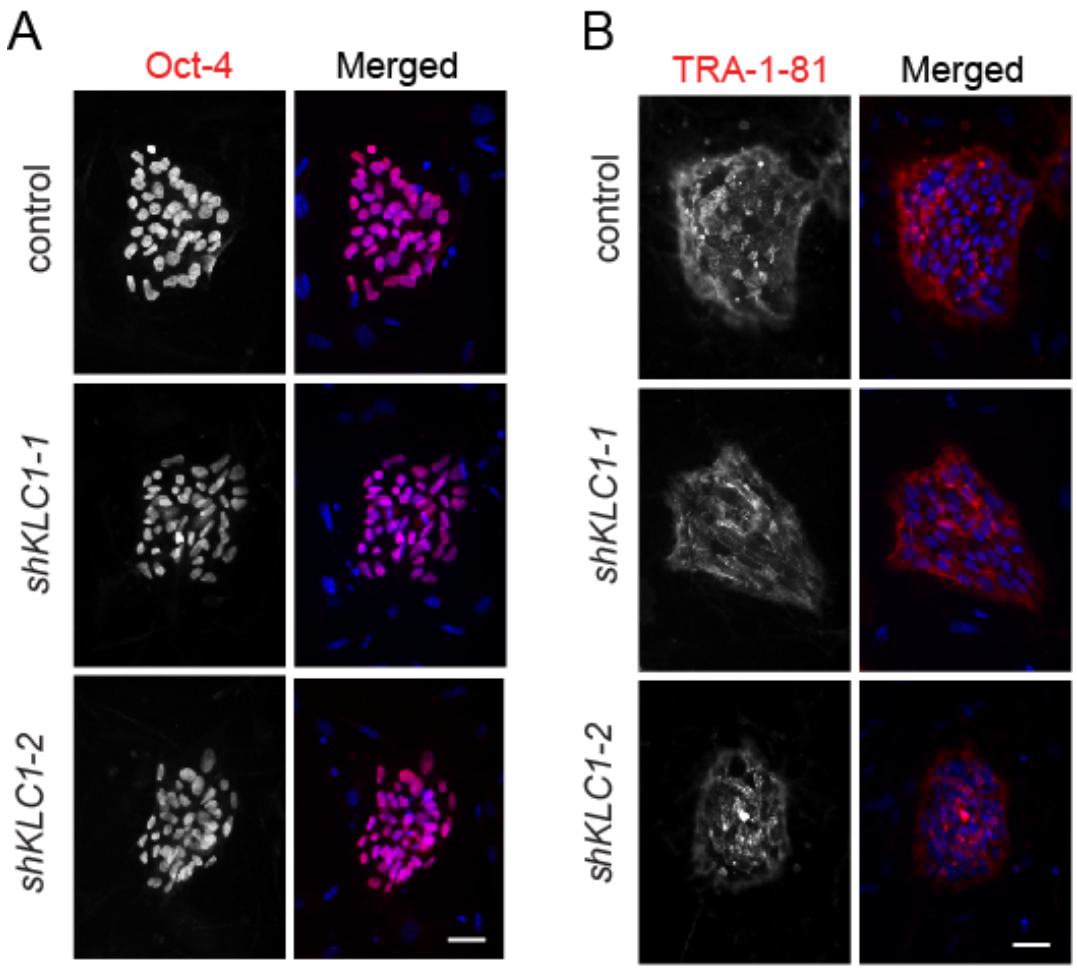


Figure 3.4. Undifferentiated KLC1-reduced hESC display normal localization of pluripotency markers Oct-4 and TRA-1-81. (A-B) Immunofluorescence of undifferentiated control, *shKLC1-1* and *shKLC1-2* cultures for pluripotency markers Oct-4 (A) and TRA-1-81 (B). Merged images show overlay of Oct-4 (A; red) or TRA-1-81 (B; red) and DAPI-stained nuclei (blue). Scale bar 50 micrometers.

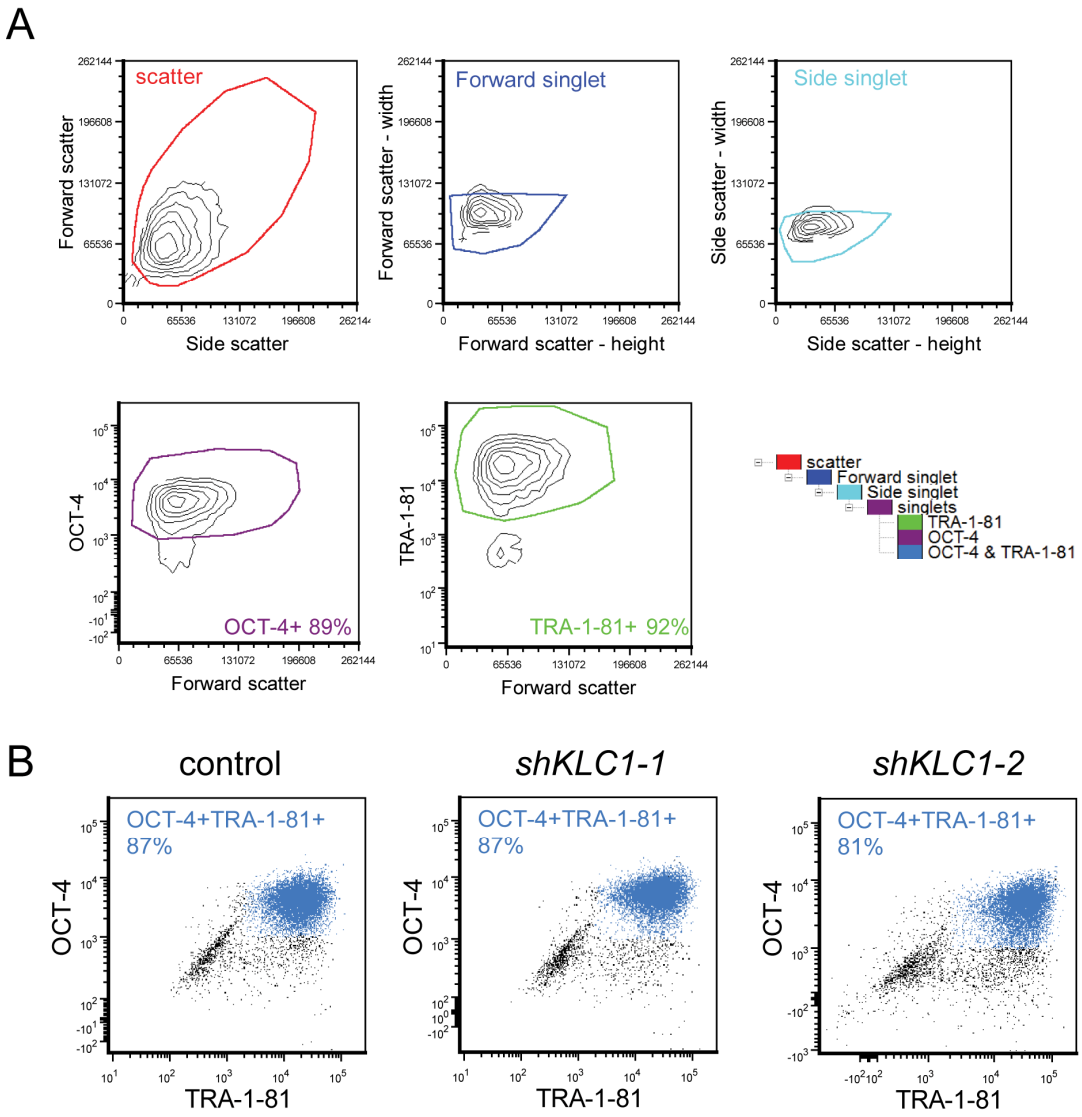
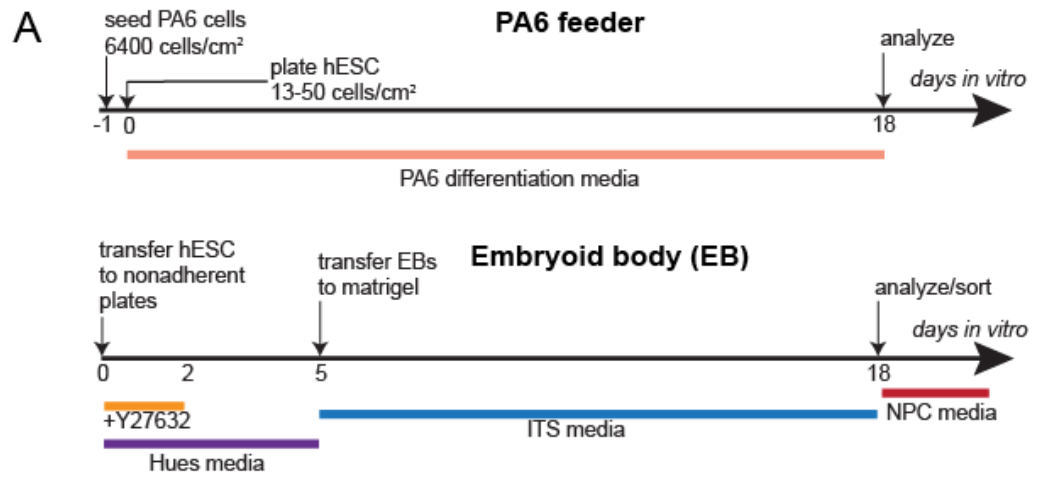
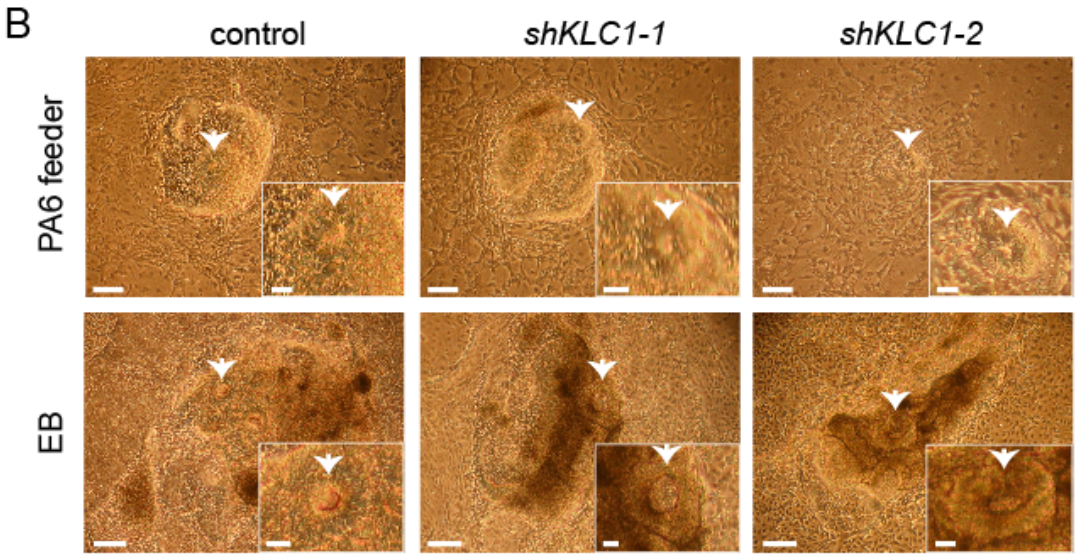


Figure 3.5. Normal proportions of undifferentiated hESC with reduced KLC1 express both pluripotency markers Oct-4 and TRA-1-81. (A) Hues9 percentile contour plots showing gating strategy to exclude coincident events and analyze pluripotency markers TRA-1-81 and Oct-4. (B) Bivariate plots show distribution of cells in control, *shKLC1-1* and *shKLC1-2* undifferentiated cultures Oct-4+TRA-1-81+ (in blue). Data is representative of three experiments.

Figure 3.6. Neural induction cultures derived from hESC with reduced KLC1 form characteristic rosettes, but have reduced cell densities. (A) Timeline of events for PA6 feeder and EB neural induction cultures. (B) Control, *shKLC1-1* and *shKLC1-2* hESC were subjected to neural induction conditions for 18 days using PA6 feeder or EB methods. Bright-field images of neural induction cultures 18 days *in vitro*. Arrowheads point to rosettes. Insets show close-ups of indicated rosettes. Scale bars: 200 μm for main images, 50 μm for insets. (C) Quantification of cell density in EB neural induction cultures. EB cultures 18 days *in vitro* were dissociated enzymatically and counted using a hemocytometer.


A
seed PA6 cells
6400 cells/cm²
plate hESC
13-50 cells/cm²
PA6 feeder
analyze
days in vitro
-1
0
18
PA6 differentiation media
transfer hESC
to nonadherent
plates
transfer EBs
to matrigel
Embryoid body (EB)
analyze/sort
days in vitro
0
2
5
18
+Y27632
Hues media
ITS media
NPC media


B
control
shKLC1-1
shKLC1-2
PA6 feeder
EB

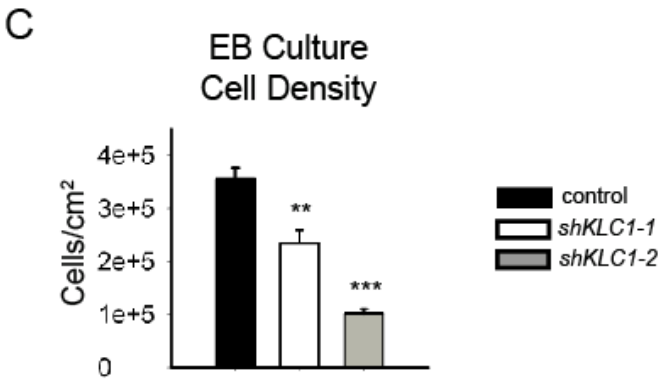
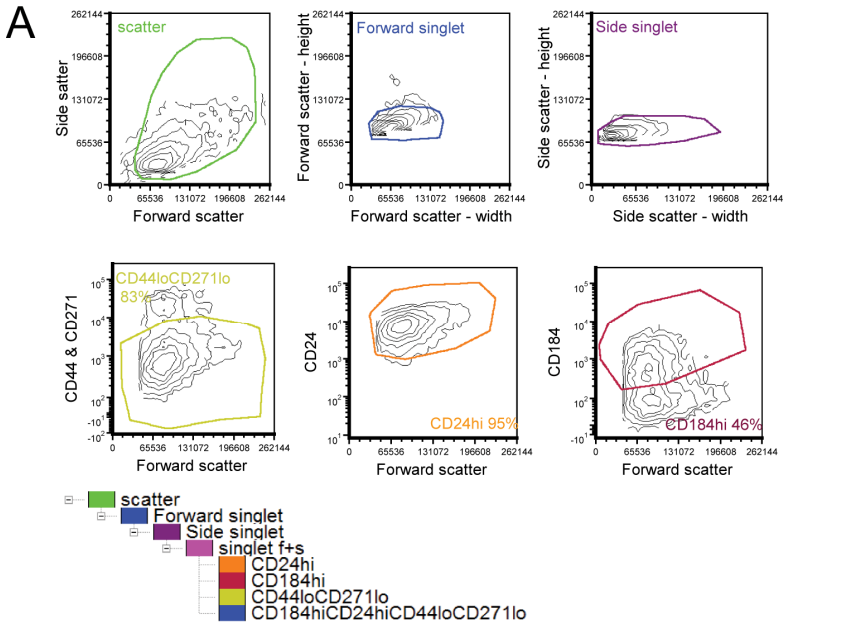
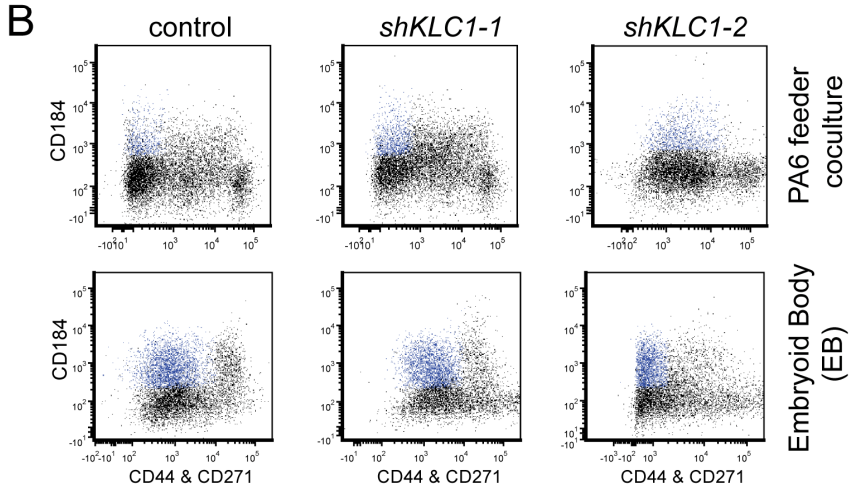
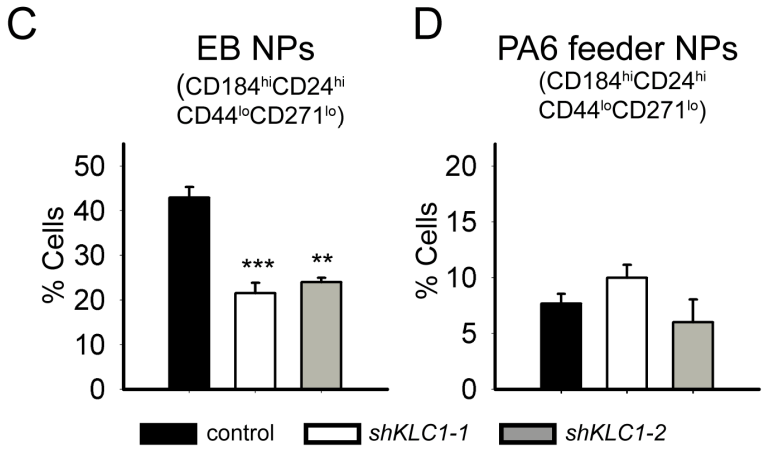

C
EB Culture
Cell Density
Cells/cm²
4e+5
3e+5
2e+5
1e+5
0
**
***
control
shKLC1-1
shKLC1-2

Figure 3.7. NP cell surface signatures of neural induction cultures derived from hESC with reduced KLC1. Control, *shKLC1-1* and *shKLC1-2* hESC were subjected to neural induction conditions for 18 days using PA6 feeder or EB methods. (A) Hues9 control percentile contour plots showing scatter gates for excluding coincident events (top panels) and for both positive (CD184 and CD24) and negative (CD44 and CD271) NP cell markers (bottom panels). The gating hierarchy is shown below contour plots. (B) Back-gating of $CD184^{hi}$ $CD24^{hi}$ $CD271^{lo}$ $CD44^{lo}$ population (shown in blue) on CD184 – CD44 & CD271 bivariate dot plots for control, *shKLC1-1* and *shKLC1-2* PA6 feeder and EB neural induction cultures 18 days *in vitro*. (C-D). Percent of cells within EB (C) or PA6 feeder (D) differentiation cultures exhibiting $CD184^{hi}CD24^{hi}CD44^{lo}CD271^{lo}$ NP cell surface marker signature after 18 days *in vitro.* For (B-C), control n=9, *shKLC1-1* n=6, *shKLC1-2* n=3. For (D), n=3 each line. $^{**}p < 0.01$, $^{***}p<0.001$ by 2-tailed t-test compared to control.


A
scatter
Forward singlet
Side singlet
Side satter
Forward scatter
Forward scatter - height
Forward scatter - width
Side scatter - height
Side scatter - width
CD44loCD271lo
83%
CD24hi 95%
CD184hi 46%
CD44 & CD271
CD24
CD184
scatter
Forward singlet
Side singlet
singlet f+s
CD24hi
CD184hi
CD44loCD271lo
CD184hiCD24hiCD44loCD271lo


B
control
shKLC1-1
shKLC1-2
CD184
CD44 & CD271
PA6 feeder coculture
Embryoid Body (EB)


C
EB NPs
(CD184hiCD24hi
CD44loCD271lo)
% Cells
***
**
control
shKLC1-1
shKLC1-2
D
PA6 feeder NPs
(CD184hiCD24hi
CD44loCD271lo)
% Cells

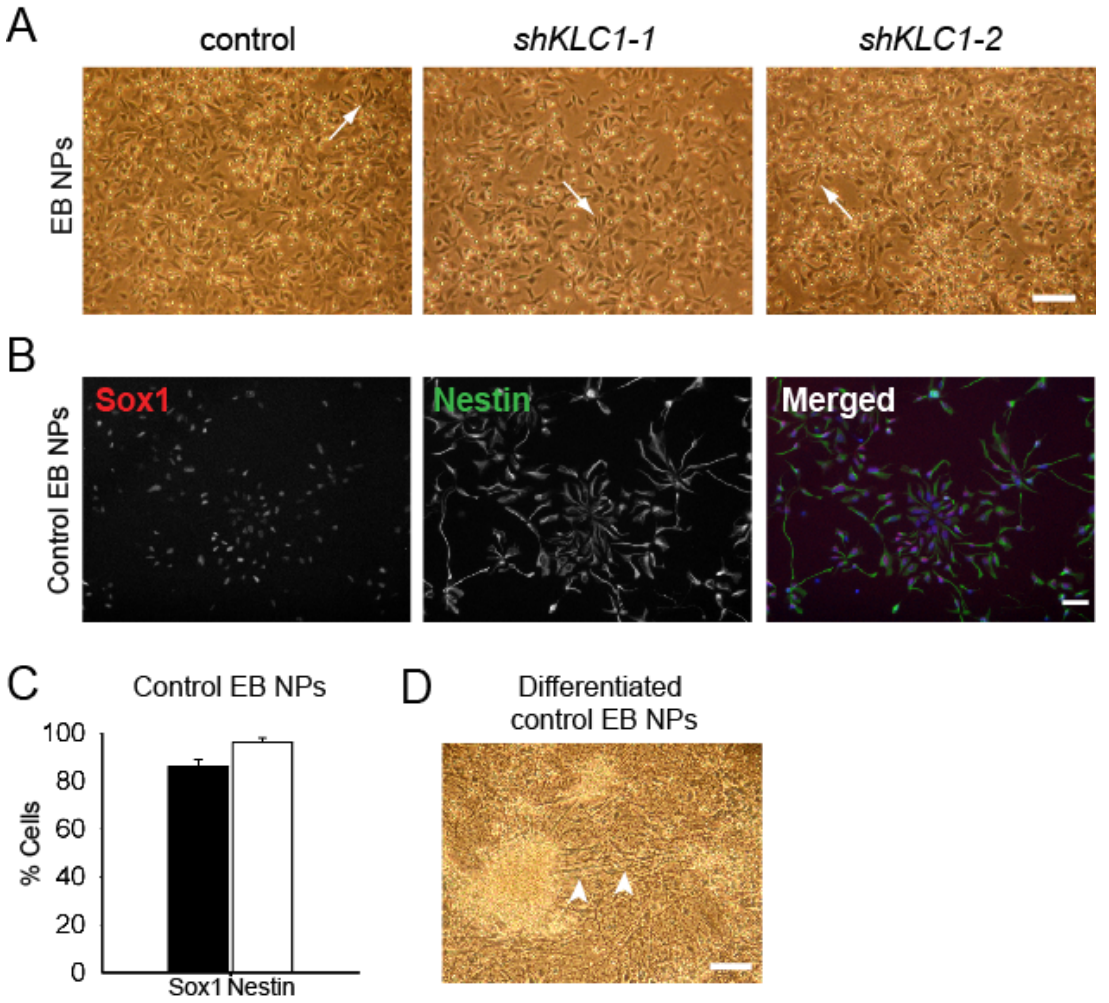


Figure 3.8. Defective proliferation of NPs derived from KLC1 suppressed hESC. (A) Cells exhibiting the NP cell surface signature were sorted by flow cytometry. Representative images of EB derived NP bright field morphology one day post-sort. Arrows point to individual cells with similar morphology. Scale bar 100 μm. (B) Immunofluorescence for NP intracellular markers Sox1 and Nestin in sorted NP cells from control hESC cultures generated using the EB method. Merged image shows overlay of Sox1 (red), Nestin (green) and DAPI stained nuclei (blue). (C) Quantification of percent of cells (=DAPI nuclei) positive for Sox1 or Nestin in control derived NP cells. (D) Representative bright field image of control hESC derived NPs differentiated for a further 10 wks. Arrowheads show neurites extending from cell clusters. Scale bar 100 microns.

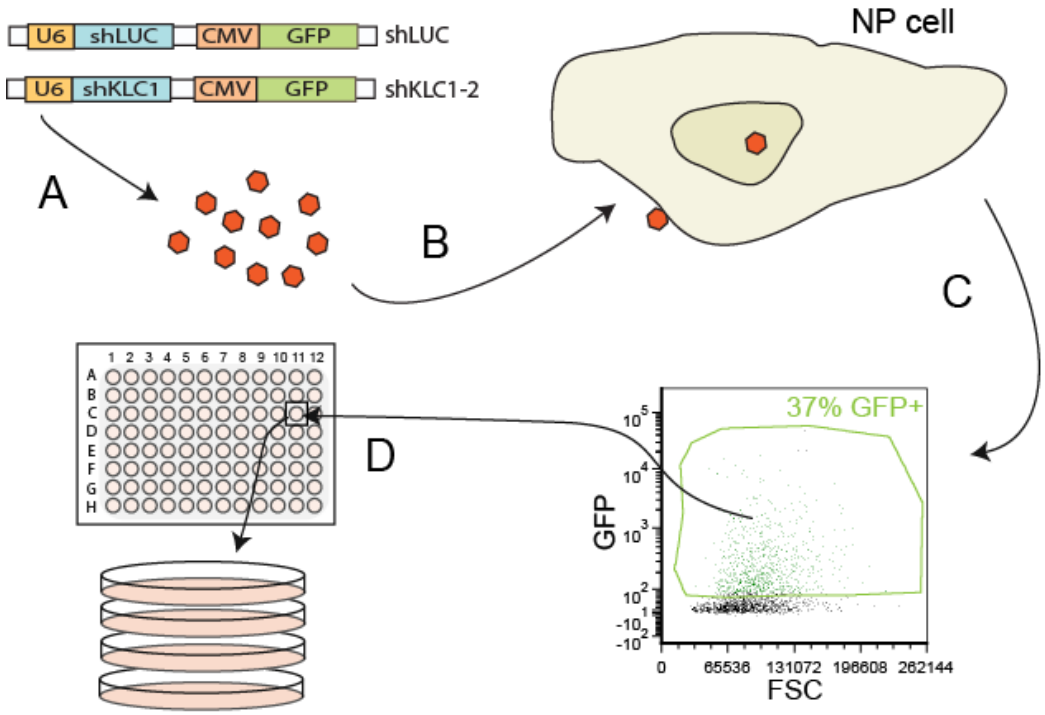


Figure 3.9. Scheme for infection and sorting of NPs with lentivirus expressing shRNA to KLC1 or Luciferase. (A) A lentiviral vector encoding a shRNA targeted to KLC1 (shKLC1) or Luciferase is packaged into lentiviral particles. (B) Dissociated Hues9 derived NP cells are exposed to the virus, (C) sorted by flow cytometry and (D) plated for expansion.

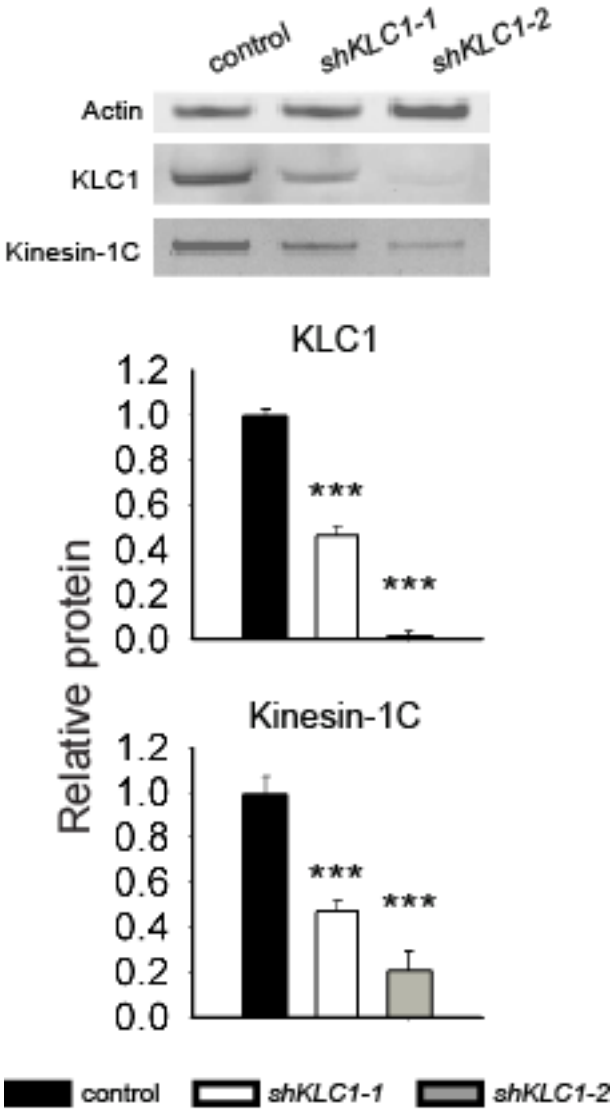


Figure 3.10. KLC1 and KHC Kinesin-1C subunits are reduced in neural cultures derived from KLC1 suppressed hESC. PA6 neural differentiation cultures were harvested after seven weeks *in vitro* and equal protein from control, *shKLC1-1* and *shKLC1-2* cultures analyzed by Western blotting for KLC1, Kinesin-1C and Actin. Bar graphs show relative quantification of KLC1 and Kinesin-1C levels relative to Actin. Based on n=7 control and *shKLC1-1*; n=3 *shKLC1-2*, ***p<0.001 by two-tailed Student's t-test compared to control.

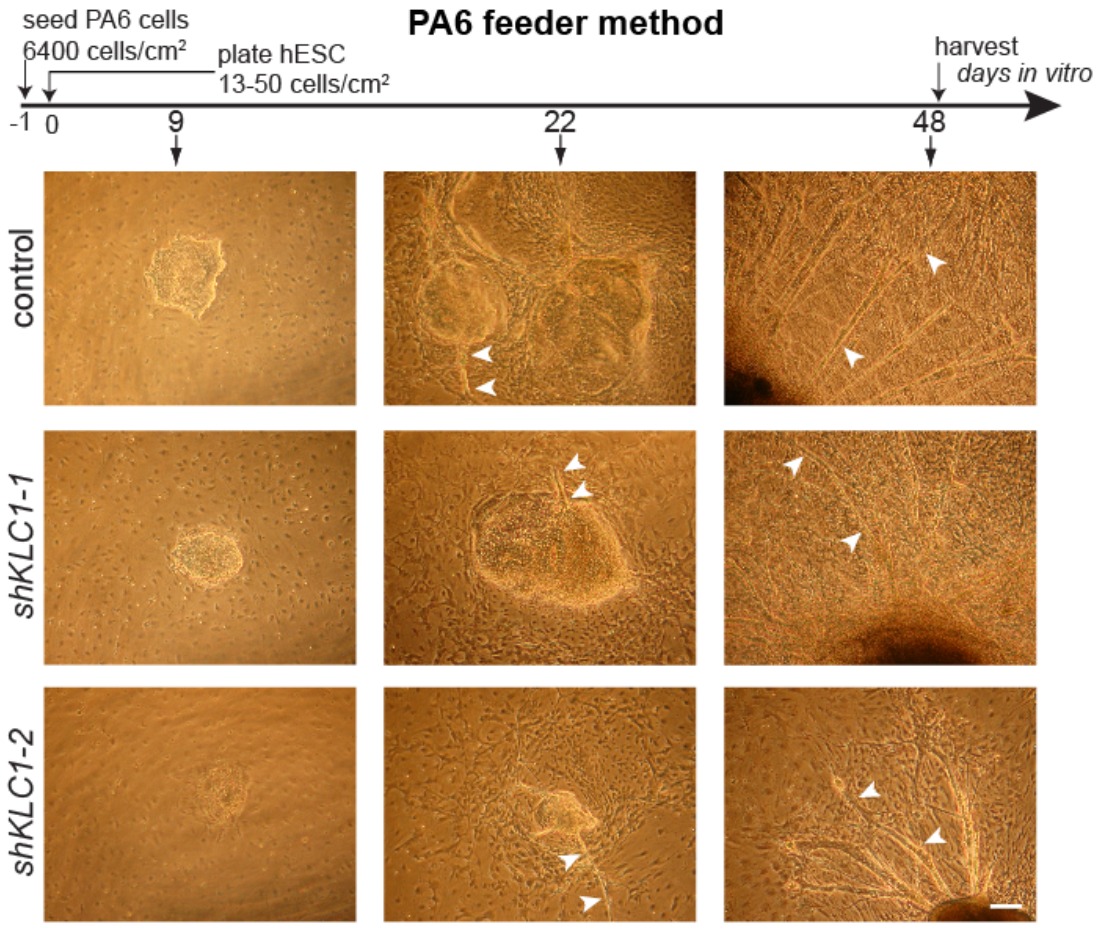


Figure 3.11. Time-course and morphology of neural cultures derived from control and KLC1 suppressed hESC. Control, *shKLC1-1* and *shKLC1-1* hESC were differentiated for seven weeks using the PA6 feeder method. Representative bright field images of control, *shKLC1-1* and *shKLC1-2* PA6 feeder co-cultures collected at 9, 22 and 48 days after plating. Arrowheads denote axon-like projections emanating from hESC derived cell clusters. Scale bar = 200 micrometers.

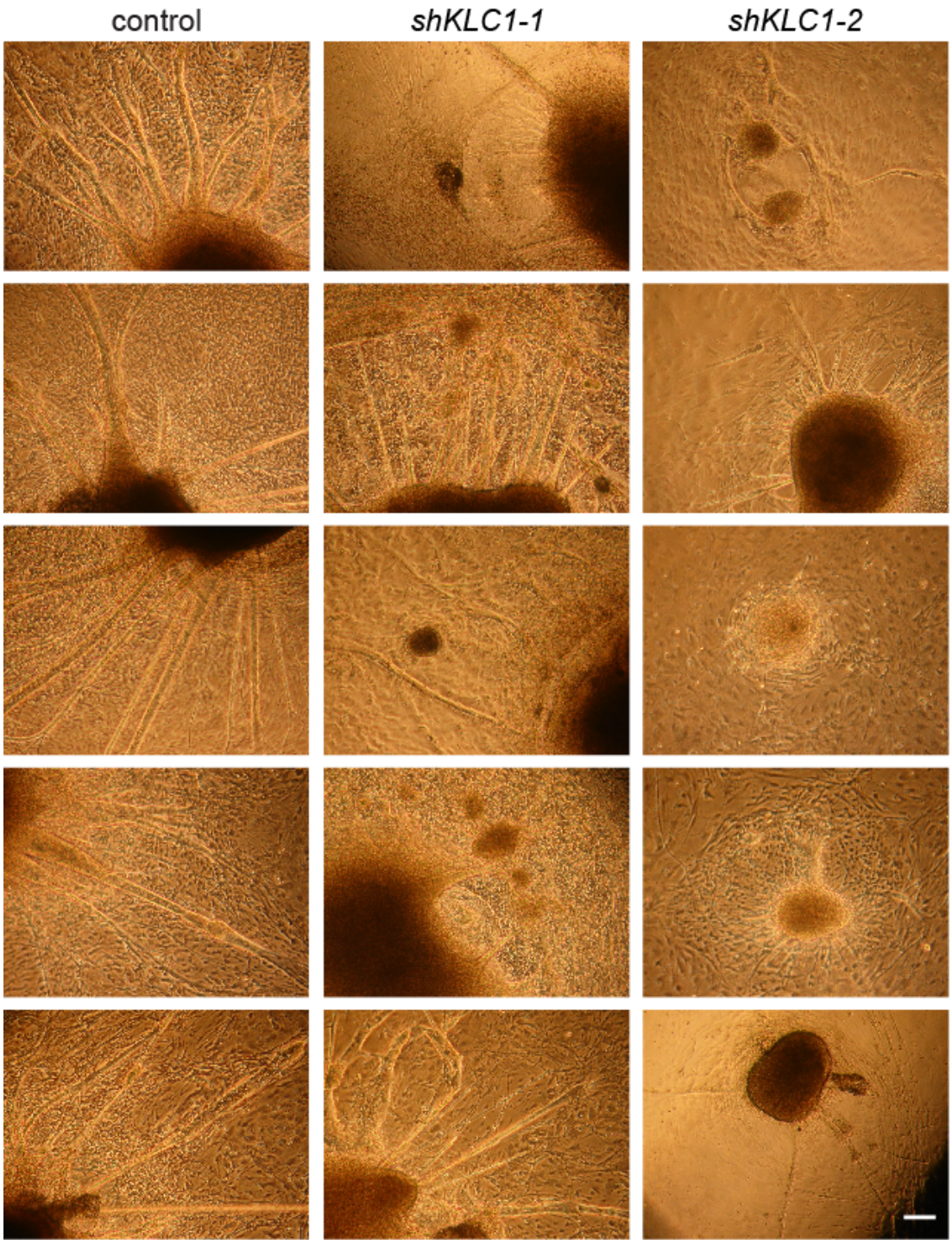


Figure 3.12. Neuron-like cells derived from PA6 feeder differentiation of KLC1-reduced hESC exhibit shorter neurites. Control, shKLC1-1 and shKLC1-1 hESC were differentiated for seven weeks using the PA6 feeder method. Bright-field images of control, *shKLC1-1* and *shKLC1-2* PA6 feeder co-cultures at 48 days since plating. Scale bar = 200 micrometers.

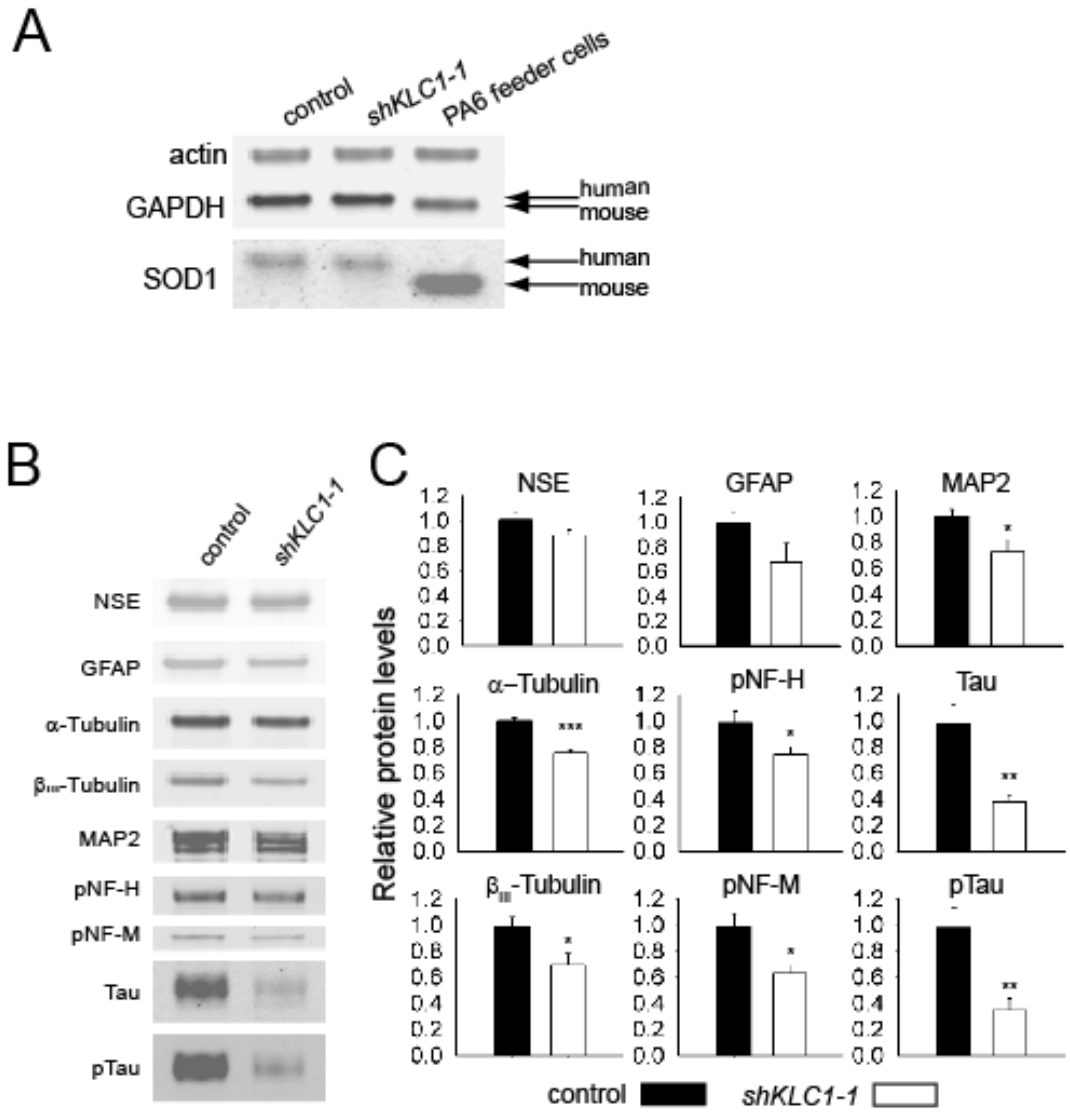
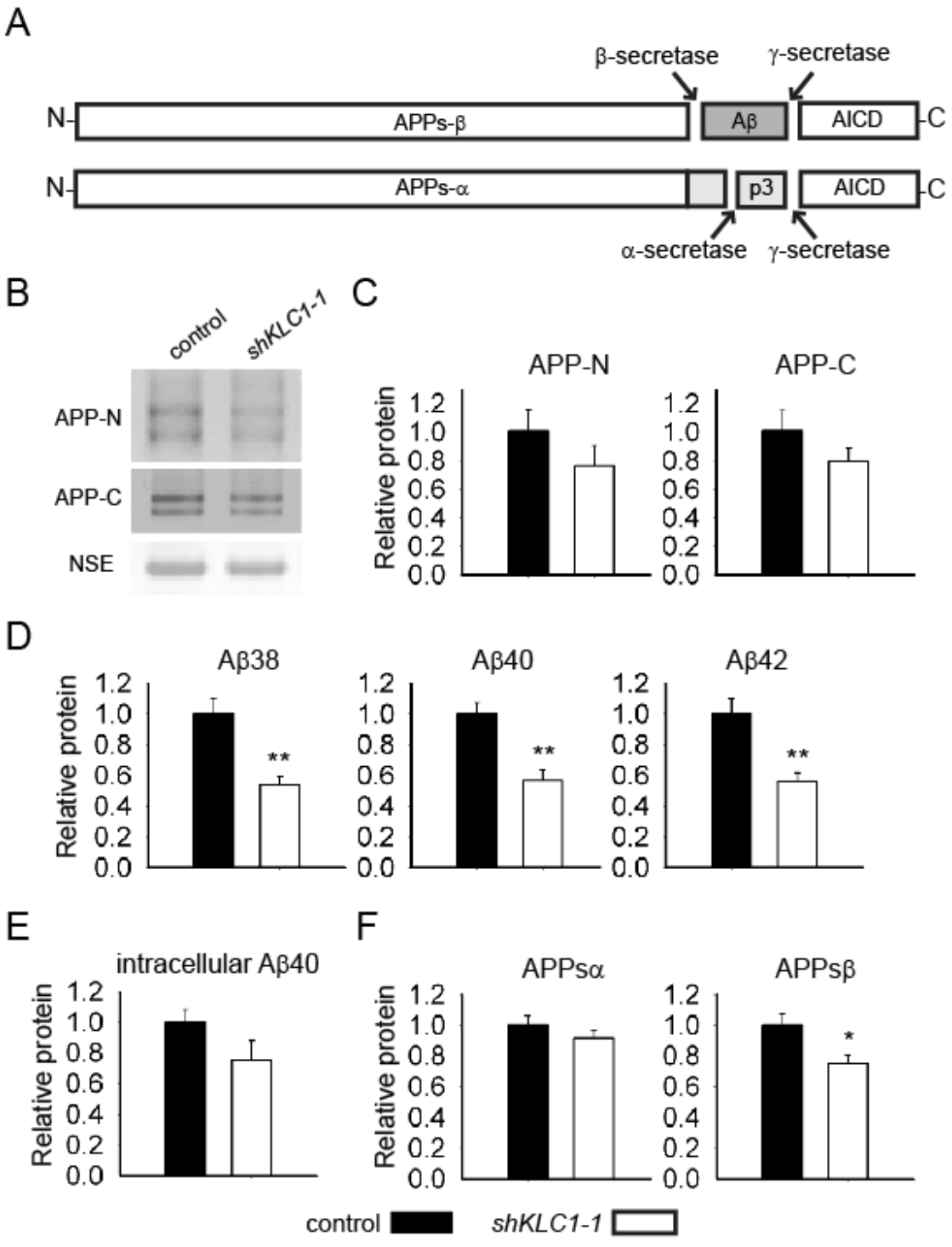


Figure 3.13. Reduced neural microtubule associated markers in neural cultures derived from KLC1-suppressed hESC. (A) Cultures were harvested at seven weeks *in vitro* and equal protein from mouse PA6 feeders cultured with control, *shKLC1-1* or no hESC (PA6 feeder cells lane) were analyzed by western blotting for Actin, GAPDH and SOD1. Note that unlike Actin, mouse and human GAPDH and SOD1 have different electrophoretic mobilities (arrows), suggesting the contribution of mouse PA6 feeder cell protein in hESC differentiation cultures is minimal. (B-C) Control or *shKLC1-1* hESC were cultured for 48 days with PA6 feeder cells and then harvested. Equal protein from control and *shKLC1-1* cultures was analyzed by Western blotting. (B) Representative immunoblots of NSE, GFAP, α-Tubulin, β-III-Tubulin, MAP2, pNF-H, pNF-M, Tau and pTau. (C) Quantification of protein levels relative to control and normalized to Actin. Based on n=6 wells each *$p < 0.05$, **$p < 0.01$ by 2 tailed t-test compared to control.

Figure 3.14. Human neural cultures with reduced KLC1 exhibit altered APP metabolism. (A) APP proteolytic processing by either β-and γ-secretases or α- and γ-secretases produces sAPPβ and Aβ (shaded dark grey) or sAPPα and p3 fragments, respectively. (B-C) PA6 feeder neural differentiation cultures were harvested after 48 days and equal protein from control and *shKLC1-1* cultures were analyzed using Western blots. (B) Representative immunoblots for full length APP in control and *shKLC1-1* neural differentiation lysates. Results for both amino (APP-N; LN27) and carboxyl terminal (APP-C) antibodies are shown. The APP carboxyl terminal cleavage fragments were not reliably detected. (C) Quantification of full length APP levels relative to NSE. (D) Levels of extracellular human Aβ peptides 38, 40 or 42 amino acids in length detected in media conditioned by control or *shKLC1-1* hESC co-cultured with PA6 feeder cells for 48 days. Human Aβ was not detected from PA6 feeder only cultures. (E) Levels of Triton X-100 soluble intracellular human Aβ-40 in control or *shKLC1-1* PA6 feeder differentiation cultures *in vitro* for 48 days. Intracellular Aβ peptides 38 or 42 amino acids long were not detectable. (F) Levels of human extracellular sAPPα and sAPPβ were detected in media conditioned by control or *shKLC1-1* PA6 feeder co-cultures *in vitro* for 48 days. Based on n=6 each line; *$p<0.05$, **$p < 0.01$ by 2-tailed t-test.


A
β-secretase
γ-secretase
N-
APPs-β
Aβ
AICD
-C
N-
APPs-α
p3
AICD
-C
α-secretase
γ-secretase
B
control
shKLC1-1
APP-N
APP-C
NSE
C
APP-N
APP-C
Relative protein
1.2
1.0
0.8
0.6
0.4
0.2
0.0
D
Aβ38
Aβ40
Aβ42
Relative protein
**
E
intracellular Aβ40
Relative protein
F
APPsα
APPsβ
Relative protein
*
control
shKLC1-1

References

1. Vale RD, Reese TS, Sheetz MP (1985) Identification of a Novel Force-Generating Protein, Kinesin, Involved in Microtubule-Based Motility. Cell 42: 39-50.

2. Brady ST (1985) A novel brain ATPase with properties expected for the fast axonal transport motor. Nature 317: 73-75.

3. Hirokawa N, Pfister KK, Yorifuji H, Wagner MC, Brady ST, et al. (1989) Submolecular domains of bovine brain kinesin identified by electron microscopy and monoclonal antibody decoration. Cell 56: 867-878. doi:10.1016/0092-8674(89)90691-0

4. Niclas J, Navone F, Hom-Booher N, Vale RD (1994) Cloning and localization of a conventional kinesin motor expressed exclusively in neurons. Neuron 12: 1059-1072.

5. Cabeza-Arvelaiz Y, Shih LC, Hardman N, Asselbergs F, Bilbe G, et al. (1993) Cloning and genetic characterization of the human kinesin light-chain (KLC) gene. DNA Cell Biol 12: 881-892.

6. Lamerdin JE, Stilwagen SA, Ramirez MH, Stubbs L, Carrano AV (1996) Sequence analysis of the ERCC2 gene regions in human, mouse, and hamster reveals three linked genes. Genomics 34: 399-409. doi:10.1006/geno.1996.0303

7. Xia C, Rahman A, Yang Z, Goldstein LS (1998) Chromosomal localization reveals three kinesin heavy chain genes in mouse. Genomics 52: 209-213. doi:10.1006/geno.1998.5427

8. Rahman A, Friedman DS, Goldstein LS (1998) Two kinesin light chain genes in mice. Identification and characterization of the encoded proteins. J. Biol. Chem 273: 15395-15403.

9. Kanai Y, Okada Y, Tanaka Y, Harada A, Terada S, et al. (2000) KIF5C, a Novel Neuronal Kinesin Enriched in Motor Neurons. J. Neurosci. 20: 6374-6384.

10. Tanaka Y, Kanai Y, Okada Y, Nonaka S, Takeda S, et al. (1998) Targeted disruption of mouse conventional kinesin heavy chain, kif5B, results in abnormal perinuclear clustering of mitochondria. Cell 93: 1147-1158.

11. Saxton WM, Hicks J, Goldstein LS, Raff EC (1991) Kinesin heavy chain is essential for viability and neuromuscular functions in Drosophila, but mutants show no defects in mitosis. Cell 64: 1093-1102.

12. Xia C-H, Roberts EA, Her L-S, Liu X, Williams DS, et al. (2003) Abnormal neurofilament transport caused by targeted disruption of neuronal kinesin heavy chain KIF5A. J. Cell Biol 161: 55-66. doi:10.1083/jcb.200301026

13. Rahman A, Kamal A, Roberts EA, Goldstein LSB (1999) Defective Kinesin Heavy Chain Behavior in Mouse Kinesin Light Chain Mutants. J Cell Biol 146: 1277-1288.

14. Falzone TL, Stokin GB, Lillo C, Rodrigues EM, Westerman EL, et al. (2009) Axonal Stress Kinase Activation and Tau Misbehavior Induced by Kinesin-1 Transport Defects. J. Neurosci. 29: 5758-5767. doi:10.1523/JNEUROSCI.0780-09.2009

15. Ferreira A, Niclas J, Vale RD, Banker G, Kosik KS (1992) Suppression of kinesin expression in cultured hippocampal neurons using antisense oligonucleotides. J. Cell Biol 117: 595-606.

16. Kimura T, Watanabe H, Iwamatsu A, Kaibuchi K (2005) Tubulin and CRMP-2 complex is transported via Kinesin-1. J. Neurochem 93: 1371-1382. doi:10.1111/j.1471-4159.2005.03063.x

17. Konishi Y, Setou M (2009) Tubulin tyrosination navigates the kinesin-1 motor domain to axons. Nat. Neurosci 12: 559-567. doi:10.1038/nn.2314

18. De Vos KJ, Grierson AJ, Ackerley S, Miller CCJ (2008) Role of axonal transport in neurodegenerative diseases. Annu. Rev. Neurosci 31: 151-173. doi:10.1146/annurev.neuro.31.061307.090711

19. Koo EH, Sisodia SS, Archer DR, Martin LJ, Weidemann A, et al. (1990) Precursor of amyloid protein in Alzheimer disease undergoes fast anterograde axonal transport. Proc. Natl. Acad. Sci. U.S.A 87: 1561-1565.

20. Ferreira A, Caceres A, Kosik KS (1993) Intraneuronal compartments of the amyloid precursor protein. J. Neurosci 13: 3112-3123.

21. Matsuda S, Matsuda Y, D'Adamio L (2003) Amyloid beta protein precursor (AbetaPP), but not AbetaPP-like protein 2, is bridged to the kinesin light chain by the scaffold protein JNK-interacting protein 1. J. Biol. Chem 278: 38601-38606. doi:10.1074/jbc.M304379200

22. Kamal A, Stokin GB, Yang Z, Xia CH, Goldstein LS (2000) Axonal transport of amyloid precursor protein is mediated by direct binding to the kinesin light chain subunit of kinesin-I. Neuron 28: 449-459.

23. Utton MA, Noble WJ, Hill JE, Anderton BH, Hanger DP (2005) Molecular motors implicated in the axonal transport of tau and {alpha}-synuclein. J Cell Sci 118: 4645-4654. doi:10.1242/jcs.02558

24. Falzone TL, Gunawardena S, McCleary D, Reis G, Goldstein LSB (2010) Kinesin-1 transport reductions enhance human tau hyperphosphorylation, aggregation and neurodegeneration in animal models of tauopathies. Hum Mol Genet. Available: http://www.ncbi.nlm.nih.gov/pubmed/20817925. Accessed 8 Sep 2010.

25. Stokin GB, Lillo C, Falzone TL, Brusch RG, Rockenstein E, et al. (2005) Axonopathy and Transport Deficits Early in the Pathogenesis of Alzheimer's Disease. Science 307: 1282-1288. doi:10.1126/science.1105681

26. Dvash T, Ben-Yosef D, Eiges R (2006) Human Embryonic Stem Cells as a Powerful Tool for Studying Human Embryogenesis. Pediatric Research 60: 111-117. doi:10.1203/01.pdr.0000228349.24676.17

27. Thomson JA, Itskovitz-Eldor J, Shapiro SS, Waknitz MA, Swiergiel JJ, et al. (1998) Embryonic Stem Cell Lines Derived from Human Blastocysts. Science 282: 1145-1147. doi:10.1126/science.282.5391.1145

28. Ventura A, Meissner A, Dillon CP, McManus M, Sharp PA, et al. (2004) Cre-lox-regulated conditional RNA interference from transgenes. Proc Natl Acad Sci U S A 101: 10380-10385. doi:10.1073/pnas.0403954101

29. Cowan CA, Klimanskaya I, McMahon J, Atienza J, Witmyer J, et al. (2004) Derivation of embryonic stem-cell lines from human blastocysts. N. Engl. J. Med 350: 1353-1356. doi:10.1056/NEJMsr040330

30. Yuan SH, Martin J, Elia J, Flippin J, Paramban RI, et al. (2011) Cell-surface marker signatures for the isolation of neural stem cells, glia and neurons derived from human pluripotent stem cells. PLoS ONE 6: e17540. doi:10.1371/journal.pone.0017540

31. Kodama HA, Amagai Y, Koyama H, Kasai S (1982) Hormonal responsiveness of a preadipose cell line derived from newborn mouse calvaria. J. Cell. Physiol 112: 83-88. doi:10.1002/jcp.1041120113

32. Zeng X (2004) Dopaminergic Differentiation of Human Embryonic Stem Cells. Stem Cells 22: 925-940. doi:10.1634/stemcells.22-6-925

33. Gropp M, Itsykson P, Singer O, Ben-Hur T, Reinhartz E, et al. (2003) Stable genetic modification of human embryonic stem cells by lentiviral vectors. Mol. Ther 7: 281-287.

34. Zhang S-C (2006) Neural Subtype Specification from Embryonic Stem Cells. Brain Pathology 16: 132-142. doi:10.1111/j.1750-3639.2006.00008.x

35. Zhang S-C, Wernig M, Duncan ID, Brustle O, Thomson JA (2001) In vitro differentiation of transplantable neural precursors from human embryonic stem cells. Nat Biotech 19: 1129-1133. doi:10.1038/nbt1201-1129

36. Tárnok A, Ulrich H, Bocsi J (2010) Phenotypes of stem cells from diverse origin. Cytometry A 77: 6-10. doi:10.1002/cyto.a.20844

37. Satoh D, Sato D, Tsuyama T, Saito M, Ohkura H, et al. (2008) Spatial control of branching within dendritic arbors by dynein-dependent transport of Rab5-endosomes. Nat Cell Biol 10: 1164-1171. doi:10.1038/ncb1776

38. Aguirre-Chen C, Bülow HE, Kaprielian Z (2011) C. elegans bicd-1, homolog of the Drosophila dynein accessory factor Bicaudal D, regulates the branching of PVD sensory neuron dendrites. Development 138: 507-518. doi:10.1242/dev.060939

39. Verhey KJ, Lizotte DL, Abramson T, Barenboim L, Schnapp BJ, et al. (1998) Light chain-dependent regulation of Kinesin's interaction with microtubules. J. Cell Biol 143: 1053-1066.

40. Pomp O, Brokhman I, Ziegler L, Almog M, Korngreen A, et al. (2008) PA6-induced human embryonic stem cell-derived neurospheres: a new source of human peripheral sensory neurons and neural crest cells. Brain Research 1230: 50-60. doi:10.1016/j.brainres.2008.07.029

41. Kim J-E, O'Sullivan ML, Sanchez CA, Hwang M, Israel MA, et al. (2011) Investigating synapse formation and function using human pluripotent stem cell-derived neurons. Proceedings of the National Academy of Sciences 108: 3005 - 3010. doi:10.1073/pnas.1007753108

42. Chambers SM, Fasano CA, Papapetrou EP, Tomishima M, Sadelain M, et al. (2009) Highly efficient neural conversion of human ES and iPS cells by dual inhibition of SMAD signaling. Nat Biotech 27: 275-280. doi:10.1038/nbt.1529

43. Chimge N-O, Bayarsaihan D (2010) Generation of neural crest progenitors from human embryonic stem cells. J. Exp. Zool. B Mol. Dev. Evol 314: 95-103. doi:10.1002/jez.b.21321

44. Lim U-M, Sidhu KS, Tuch BE (2006) Derivation of Motor Neurons from three Clonal Human Embryonic Stem Cell Lines. Curr Neurovasc Res 3: 281-288.

45. Rodionov VI, Gyoeva FK, Tanaka E, Bershadsky AD, Vasiliev JM, et al. (1993) Microtubule-dependent control of cell shape and pseudopodial activity is inhibited by the antibody to kinesin motor domain. J. Cell Biol 123: 1811-1820.

46. Jolly AL, Kim H, Srinivasan D, Lakonishok M, Larson AG, et al. (2010) Kinesin-1 heavy chain mediates microtubule sliding to drive changes in cell shape. Proc. Natl. Acad. Sci. U.S.A 107: 12151-12156. doi:10.1073/pnas.1004736107

47. Yamazaki T, Selkoe DJ, Koo EH (1995) Trafficking of cell surface beta-amyloid precursor protein: retrograde and transcytotic transport in cultured neurons. J. Cell Biol 129: 431-442.

48. Thinakaran G, Koo EH (2008) Amyloid Precursor Protein Trafficking, Processing, and Function. Journal of Biological Chemistry 283: 29615 -29619. doi:10.1074/jbc.R800019200

49. Weidemann A, König G, Bunke D, Fischer P, Salbaum JM, et al. (1989) Identification, biogenesis, and localization of precursors of Alzheimer's disease A4 amyloid protein. Cell 57: 115-126. doi:10.1016/0092-8674(89)90177-3

50. Iwata N, Tsubuki S, Takaki Y, Watanabe K, Sekiguchi M, et al. (2000) Identification of the major Abeta1-42-degrading catabolic pathway in brain parenchyma: suppression leads to biochemical and pathological deposition. Nat. Med 6: 143-150. doi:10.1038/72237

51. Lazarov O, Lee M, Peterson DA, Sisodia SS (2002) Evidence that synaptically released beta-amyloid accumulates as extracellular deposits in the hippocampus of transgenic mice. J. Neurosci 22: 9785-9793.

CHAPTER 4

Discussion

Co-regulation of KLC1 and Kinesin-1C protein levels

Kinesin-1 and other microtubule based motors play critical roles in cell function. The expression of all three KHCs (Kinesin-1A, Kinesin-1B and Kinesin-1C) and at least two KLCs (KLC1 and KLC2) in neuronal tissues points to their importance in neurons [1-4]. As a tetramer comprised of two KHCs and two KLCs, Kinesin-1 is theoretically capable of assembling into many potentially distinct holoenzymes. However, several studies suggest the holoenzyme may in fact be comprised of homodimers [1,3,5-7]. Interestingly, all KLC homodimers can interact with any of the KHC homodimers although KLC2 may be more likely to associate with Kinesin-1B while KLC1 interacts more with Kinesin-1A or Kinesin-1C [1,5,6]. However, many questions remain about which heavy and light chain subunits assemble together and the unique function(s) each holoenzyme may perform within

neurons. Previous reports revealed that loss of full length murine Kinesin-1C or KLC1leads to similar phenotypes [4,8,9] and that Kinesin-1C-/- mouse brain tissue has less KLC1 (Chun-Hong Xia doctoral dissertation “Functional analysis of mouse neuronal kinesin heavy chains”, University of California San Diego 2000). Here I report that both genetic reduction of full length KLC1 in murine hippocampal cultures and RNA interference mediated reduction of KLC1 in human neural cultures lower levels of Kinesin-1C, while genetic reduction of Kinesin-1C in murine hippocampal cultures lowers levels of KLC1. Altogether these data support the possibility that the Kinesin-1C and KLC1 subunits may preferentially assemble into functional holoenzymes. The mechanism by which the levels of these subunits are co-regulated is not known, but it could occur at the transcriptional, translational or post-translational levels. One clue may come from the KLC1-/- mouse where, due to the genomic targeting strategy, the KLC1 N-terminal heptad repeat domain which associates with KHC may still be expressed in hippocampal neurons, since it is detectable by Western in KLC1-/- embryonic stem cells, KLC1-/- brain and KLC1-/- sciatic nerve and by immunofluorescence in differentiated KLC1-/- embryonic stem cells, KLC1-/- sciatic nerve and KLC1-/- dorsal root ganglia and a sciatic nerve ligation assay suggests it is transported in axons with KHC (Amena Rahman doctoral dissertation “Analysis of Kinesin Light Chain in Mouse”, University of California, San Diego 1997). If this KLC1 domain is also expressed in KLC1-/- hippocampal neurons (and unfortunately we do not presently have access to an N terminal antibody to test this) it is capable of binding to the Kinesin-1C [10] and potentially stabilizing the holoenzyme and thus

levels of the Kinesin-1C subunit. This may explain why levels of Kinesin-1C in murine KLC1-/- hippocampal cultures (Figure 2.1A, C) are higher than expected given the strong reduction of Kinesin-1C observed in human neuronal cultures derived from KLC1 suppressed hESC (Figure 3.10) and of KLC1 in Kinesin-1C-/- mouse neuron (Figure 2.1 C-E)). Thus the data collected here may point to co-regulatory mechanisms at the translational or post-translational level and suggest the hypothesis that Kinesin-1C and KLC1 homodimers assemble into functional Kinesin-1 holoenzymes. Regardless of the mechanism, it may be an important consideration when designing pharmaceuticals specifically targeting either of the subunits as drugs aimed at one may have consequences to both. It will be interesting to discover whether reduction in levels of other Kinesin-1 subunits are co-regulated as well since this may shed light on unique functions of different Kinesin-1 subunits.

Roles for KLC1 (and Kinesin-1C) in neural development

Several lines of evidence suggest that Kinesin-1 may have important functions in the nervous system. The expression of all three mammalian KHCs (Kinesin-1A, Kinesin-1B and Kinesin-1C) and at least two KLCs (KLC1 and KLC2) Kinesin-1 subunits in neuronal tissues hints at their importance in neurons [1-4]. Further clues are derived from defects in the brain and spinal cord associated with the loss of specific neural Kinesin-1 subunits [3,8,11]. Kinesin-1 may be an important player in neuronal polarization in rodent primary hippocampal neurons. A truncated constitutively active Kinesin-1C-YFP fusion protein localizes to the tip of the neurite

destined to develop into the axon [12]. Suppression of KHCs or KLCs decreases the length of cultured rodent neurons [13-15]. Simultaneous siRNA reduction of all Kinesin-1 motor subunits increases the fraction of neurons with multiple axons [15]. However, it is still unknown which particular subunits are required for these functions, whether such functions are neuron type dependent and whether other subunits can compensate.

I tested whether reduction in full length KLC1 and/or Kinesin-1C affects neurite lengths using rodent mouse hippocampal neurons and human PSC derived neuron-like cells. Interestingly, I found that neuronal cultures derived from KLC1 suppressed compared to control hESC have reduced levels of microtubule associated proteins (Figure 3.13) and apparently shorter neurites (Figures 3.11-12; although due to the complex nature of the cultures and extensive length of control neurites this was not quantifiable on the images) suggesting reduction in human KLC1 may cause reduced neurite length of cells in neuronal cultures derived from KLC1-reduced hESC. However, compared to wildtype, average murine KLC1-/- and Kinesin-1C-/- hippocampal neuron axon lengths were slightly longer (Figure 2.2). These disparate results in the mouse and human *in vitro* cultures systems suggest that KLC1 and Kinesin-1C may not have generalized roles in regulating axon length in all neurons. Rather these subunits may have specialized functions depending on the developmental stage, neuron type and/or species. Alternatively, these different results may be due to the different modes of protein reduction. Acute reduction of KHCs or KLCs using antisense or shRNA leads to shortened axons. Chronic reduction via genetic targeting

of KLC1 or Kinesin-1C results in longer axons. If KLC1-/- and Kinesin-1C-/- hippocampal neurons express more Kinesin-1A, Kinesin-1B and/or KLC2 to compensate for the loss of KLC1 and Kinesin-1C, this may result in increased activity of Kinesin-1A, Kinesin-1B and/or KLC2 and longer neurites. Thus the longer axons in KLC1-/- and Kinesin-1C-/- could be a result of (over-) compensation by other Kinesin-1 subunits.

Mice or flies with reduced or defective Kinesin-1 subunits are abnormal with defects manifesting in the nervous system. *D. melanogaster* has one genetic copy each of KHC and KLC and larvae deficient for either exhibit an abnormal “tail flipping” behavior when crawling [16,17]. Three week old mice lacking Kinesin-1A in neurons are 50% smaller than wildtype and have abnormal hind leg posture [11]. KLC1-/- animals are also smaller than wildtype and are unable to cling to chicken wire as long as wildtype [18]. Kinesin-1C mice have smaller brains [3]. Together these organism level phenotypes might indicate developmental defects, possibly in neural precursors, but this question had not been addressed previously.

To examine this question, I subjected hESC to neural induction conditions to model human neural development. I used two neural induction strategies, referred to as the EB or PA6 feeder methods, to differentiate hESC. Interestingly, the two methods gave rise to quite different proportions of control cells exhibiting the NP cell surface signature, with the EB method producing higher proportions of NPs than the PA6 feeder method (black bars in Figure 3.7C-D). The simplest explanation for this is that the EB method supports the formation of larger or larger numbers of NP

producing environments (Figure 4.1A). A second possibility is that different NP subtypes that develop into distinct neuron types arise under different neural induction conditions. Precursors in EB compared to PA6 feeder cultures may exhibit greater diversity of NP subtypes that add up to a larger proportion of the cell population and these NP subtypes may produce different types of neurons (Figure 4.1B). This latter possibility is supported by reports suggesting PA6 feeder cells produce neurons most resembling neural crest derivatives (which produce peripheral neurons) while EB methods are capable of generating cells similar to forebrain or spinal cord motor neurons [19-21].

To test whether reduced KLC1 affects neural precursor production or function I used both the EB and PA6 feeder methods to differentiated hESC with normal or reduced levels of KLC1. In line with general observations of reduced organs or body sizes in Kinesin-1 mouse mutants, I found that reduction of KLC1 in hESC leads to reduced cell densities of differentiated progeny (Figures 3.6, 3.11), hinting at a possible role for KLC1 in maintaining cell proliferative potential. To assay whether KLC1 reduction impairs production of neural precursors, I examined the proportion of cells derived from control, *shKLC1-1* or *shKLC1-2* EB or PA6 feeder neural induction cultures exhibiting a neural precursor signature. I found that unlike proportions of NPs in PA6 feeder cultures which were unaffected, the proportion of NPs produced by EB cultures is reduced by KLC1 knockdown. I propose that different neural induction methods give rise to different NP subtypes (Figure 4.1B) that differ in their requirements for KLC1 function. PA6 feeder neural induction cultures ultimately give

rise to peripheral nervous system neurons through neural crest precursors whose proliferation within neural induction cultures is not affected by KLC1 reduction (Figure 4.1C top panel). However, EB neural induction cultures give rise to motor and forebrain neuron precursors (perhaps among other NP subtypes not shown; Figure 4.1C, bottom). Reduction of KLC1 is detrimental to some NP subtypes, affecting proliferation of motor neuron, but not neural crest or forebrain neuron precursors (Figure 4.1C). These defects in NPs lead to reduced populations of specific neuron types (Figure 4.1C). If true this may account for why motor neuron numbers in particular are reduced in KLC1 mutant mice [14]

To examine whether NPs with reduced KLC1 are normal, I sorted NPs from control and KLC1-reduced EB neural induction cultures. While control NPs multiplied, I found that sorted NPs with reduced KLC1 did not proliferate. When control EB-derived NPs were infected with lentivirus coding for shRNA targeting KLC1 or luciferase as a control, the NPs infected with KLC1 shRNA again failed to proliferate while the luciferase treated cells were able to multiply and differentiate further into cultures containing highly polarized cells resembling neurons. Thus EB differentiation of hESC with reduced KLC1 yielded lowered proportions of NPs compared to control and when sorted EB-derived control NPs were infected with a KLC1 knockdown construct they were also unable to proliferate, together suggesting normal KLC1 function may be required to maintain this NP population. Using the PA6 feeder differentiation system I found reduction of KLC1 had no affect on the proportion of cells in the culture with the NP signature compared to control (Figure

3.7D). Control PA6 feeder derived NPs infected with lentivirus containing KLC1 sequences also failed to multiply. Since undifferentiated hESC with reduced KLC1 are capable of proliferating, KLC1 reduction does not cause a general defect in the cell cycle. Since the two differentiation methods may produce different types of neural precursors and neurons it is possible that KLC1 may have vital functions in EB-derived but not PA6 feeder derived NPs. If only some NPs require KLC1 for maintenance, loss of KLC1 function may only appear to affect some neuron types derived from those precursors (Figure 4.1C). This notion could explain why, for example, KLC1-/- and Kinesin-1C-/- mice have selective reductions in motor neurons populations [3,8].

What are the molecular and cellular mechanisms governing proliferation that may go awry in NPs with reduced KLC1? Some of the signaling pathways involved in NP self-renewal include Notch, sonic hedgehog and growth factors such as EGFR, FGFR, and TGF-β [22]. Of these, only the TGF-β signaling pathway has thus far been reported to intersect with Kinesin-1 function. In *Xenopus*, zebrafish and immortalized human keratinocytes, inhibition of Kinesin-1 prevents TGF-β/activin/nodal signaling by blocking the phosphorylation and subsequent nuclear localization of Smad2 in response to TGF signaling [23]. The authors used both expression of dominant negative KLC2 and drugs targeting KHC to reach their conclusions, so it is not known whether reduction of the neuronal subunits KLC1 or Kinesin-1C specifically would also interfere with Smad2 signaling. Also unknown is whether the EB-derived NPs that fail to proliferate when challenged with shRNA targeting KLC1 are utilizing the

TGFβ signaling pathway to control self-renewal. Further, interruption of TGFβ signaling would be expected to increase proliferation, not decrease it [24].

As indicated above, NPs require signals to proliferate (Figure 4.2A, stars). Such signals may originate from the NPs themselves or other cell types present in the cultures (Figure 4.2B). I propose that these signaling molecules are derived from both the NPs and other cell types present in neural induction cultures (Figure 4.2C). When control NPs are isolated from neural induction cultures, they are capable of self-renewal but KLC1-suppressed NPs are not (Figure 4.2D), Thus these NPs with reduced KLC1 lack the capacity to proliferate when isolated from neural induction cultures. I propose two possible models for how KLC1 reduction impairs proliferation. In the first, KLC1 is required for proper secretion of the proliferation signal from NPs (Figure 4.2E). In the second, KLC1 is needed for the transport of components necessary for the receipt and transmission of the signal (Figure 4.2F). Future experiments using control and KLC1 reduced NPs will be required to both elucidate the signals responsible for self-renewal in these NPs and to determine how disruptions in KLC1-based Kinesin-1 transport impairs proliferation of these cells.

Tau and Kinesin-1 subunits KLC1 and Kinesin-1C

Since the discovery that hyperphosphorylated Tau, a microtubule associate protein that promotes the assembly and stability of axonal microtubules [25-27], is the principle component of neurofibrillary tangles in AD brains [28-32], many studies have focused on how Tau may be misregulated in disease. One study suggests axonal

Tau transport in rat cortical neurons may be Kinesin-1 dependent [33]. Disruption of Kinesin-1 transport in the KLC1-/- mouse leads to axonopathies in the spinal cord of adult mice containing hyperphosphorylated Tau. Very recently it was reported that KLC1+/- adult mice expressing transgenic mutant human Tau exhibit higher proportions of cell bodies in the hippocampus and spinal cord with pTau [34], suggesting reduced Kinesin-1 function may lead to increased hyperphosphorylated Tau. However much remains unknown about this connection. Are increased phosphorylated Tau levels only apparent in aged animals or is the effect detectible earlier? Are changes in Tau levels more apparent in human neurons expressing endogenous Tau? Is the neuronal Kinesin-1C subunit responsible for any observed differences in Tau levels?

To embark on studies to answer some of these questions, I prepared mouse and human tissue cultures systems to examine the affect of reduced Kinesin-1 subunits KLC1 and Kinesin-1C on pTau levels. To test for changes in endogenous murine Tau due to reductions in KLC1 or Kinesin-1C I compared Tau and pTau in lysates from mouse wildtype, KLC1-/- and Kinesin-1C-/- primary hippocampal cultures. I observed no statistically significant difference in Tau or pTau levels between KLC1-/- , Kinesin-1C-/- and wildtype neurons, or in the proportion of pTau to non-phosphorylated Tau (Figure 2.3), suggesting no large effect on endogenous Tau due to loss of KLC1 or Kinesin-1C in young primary mouse hippocampal neurons. However, this result doesn’t rule out changes in the localization of Tau or pTau in these cells,

especially given the very recent finding of increased pTau+ cell bodies in the hippocampus of aged mice [34].

To investigate whether KLC1 impairment alters human endogenous Tau, I engineered hESC to constitutively express shRNA to KLC1, neuronally differentiated these hESC and tested levels of Tau and pTau relative to control. I found that both Tau and pTau were both substantially reduced in these cultures. Interestingly there was no difference in the proportion of pTau relative to non-phosphorylated Tau in shKLC1-1 compared to control cultures, suggesting that KLC1 (and possibly Kinesin-1C since it is also reduced) affects Tau itself and not its phosphorylation. Thus Kinesin-1 subunits KLC1 and Kinesin-1C affect Tau levels in human neural differentiation cultures, but not in hippocampal neurons derived from KLC1-/- or Kinesin-1C-/- mice. It is interesting to note, however the trend in the Kinesin-1C-/- neurons to reduced overall levels of Tau and pTau, which is in line with the observation in the human system. A second interesting point is the different responses of full length KLC1 reduction between the aged mice where Tau is increased and the hESC derived neural cultures where Tau is reduced. Possible reasons for these dissimilarities between the human and mouse model systems could include differences in maturity or neuron subtypes between the cultures, differences in behavior of human and mouse Tau, a requirement for organism aging or physiological structures not present in vitro and/or the means of modulating levels of the motor subunits – via genetic or shRNA targeting. Nevertheless, my data support the notion of a functional relationship between Kinesin-1 and Tau.

Given that Tau is hyperphosphorylated and mislocalized to neuronal cell bodies in AD it is important to understand how Tau is transported in normal and diseased neurons. Both my data in human and the mislocalization of pTau in aged mice with impaired KLC1 support a causal role for KLC1 in regulating Tau in human neural differentiation cultures. It is therefore important to probe further the nature of this putative functional relationship between Tau and Kinesin-1. Tau is localized to the axon and Kinesin-1 is an axonal motor. Does Kinesin-1 transport Tau? Tau associates and colocalizes with Kinesin-1 [33,35-37], suggesting this may be the case, but more direct data is needed. If involved, does Kinesin-1 transport Tau regardless of post-translational modifications or a subset –perhaps pTau or Tau phosphorylated at particular sites – a possibility suggested by data that Kinesin-1 may prefer to associate with pTau rather than non-phosphorylated Tau [37]. Which Kinesin-1 subunits participate in the transport of Tau or do the subunits function redundantly? If specific, can this knowledge be used to devise treatment strategies for clearing cell body pTau without disrupting all Kinesin-1 cargos? Is Tau transported by a similar mechanism in all neuron types? Future work in both human and mouse neuronal cultures will address these issues.

Does Kinesin-1C regulate APP levels and metabolism by controlling APP transport?

Since the discoveries pointing to the role of APP in producing the amyloid plaques associated with AD [39-43], the study of APP trafficking and metabolism has

been the focus of intense research. Many studies suggest Kinesin-1 transports APP into the axons of primary rodent neurons [8,44-47]. Disruption in this transport in KLC1+/- mice also expressing a FAD mutant APP transgene causes earlier and accentuated brain Aβ levels in adult animals, suggesting disruptions in Kinesin-1 mediated APP transport may affect Aβ levels [47], although whether this effect is due to changes in production, secretion or degradation is unknown. Also unknown is whether increased Aβ levels are evident only in aged animals or are detectible earlier? Are the changes in Aβ levels exclusive to the human mutant APP transgene or is this a more general phenomenon equally applicable to endogenous mouse APP? Does Kinesin-1 reduction alter Aβ levels in human cells expressing normal endogenous APP? Is the neuronal Kinesin-1C subunit responsible for any observed differences in Aβ levels?

To begin to address these issues I set up mouse and human tissue cultures systems to test the affect of reduced Kinesin-1 subunits KLC1 and Kinesin-1C on extracellular Aβ levels. To examine murine extracellular production of Aβ, I extracted mouse neurons from the hippocampus of wildtype, KLC1-/- and Kinesin-1C-/- embryonic day 18-21 mice. Using this well established system, I noted no difference in levels of γ–secretase products Aβ and p3 (the assay used does not discriminate between the two murine APP fragments) in KLC1-/- neurons, but in Kinesin-1C-/- neurons, less extracellular Aβ and p3 was detectable. (Figure 2.4) Upon examination of the protein in the cell lysates, I discovered full length APP levels tracked with extracellular Aβ and p3 levels across genotypes (Figure 2.4C-D), suggesting that the

difference in extracellular levels of APP γ–secretase products Aβ and p3 observed in the Kinesin-1C-/- compared to wildtype neurons may be due to a concomitant reduction in overall APP levels in the Kinesin-1C-/- neurons. Thus differences in Aβ observed in whole brains of aged KLC1-/- APP transgenic mice are not evident in young hippocampal neurons of KLC1-/- mice expressing endogenous APP, suggesting that either transgenic human mutant APP, aging, intracellular stores of Aβ or cell types not present in the hippocampal in vitro cultures may lead to higher Aβ levels in brains of adult animals.

To test whether levels of human endogenous Aβ levels are affected by KLC1 reduction in human cells, I inserted a constitutively expressed shRNA construct targeting KLC1 into human embryonic stem cells, differentiated these pluripotent cells into cultures containing neurons and measured levels of extracellular Aβ. Interestingly, I observed significantly less extracellular Aβ and sAPP-α in KLC1-reduced compared to control human neural cultures (Figure 3.13D, F). While not reaching statistical significance, it is interesting to note trends toward less full length APP and less intracellular Aβ in shKLC1-1 compared to control cultures (Figure 3.14C), which suggests that the reduction in extracellular Aβ may be due in part to less overall APP. Indeed if extracellular Aβ is “normalized” to full length APP in the corresponding lysate, no statistically significant differences are evident between shKLC1 and control neural cultures. Thus it appears that reduction of KLC1 in human neural cultures leads to less extracellular Aβ compared to control and that this difference my be due to reduced levels of APP. Interestingly this result parallels that in

the mouse Kinesin-1C-/- neuronal cultures, where KLC1 is also reduced to 25% of wildtype (Figure 2.1D). Recall that Kinesin-1C levels in the human shKLC1 neuronal cultures were reduced to ~50% control. Thus reductions in both subunits may be responsible for this change in full length APP. It is unclear why the murine KLC1-/- neuronal cultures do not also exhibit similarly less APP and extracellular γ–secretase products. One potential explanation is the possible presence of a truncated KLC1 product which could interrupt the normal function of the remaining KHCs. My data in human neural cultures expressing shRNA to KLC1 and in mouse Kinesin-1C-/- neurons suggest that while in brains of aged KLC1+/- mice expressing transgenic mutant APP, in young human or mouse neuronal cultures expressing endogenous APP, reduced Kinesin-1 function lessens extracellular Aβ by reducing overall levels of APP. However, it is also possible that the different cellular compositions of the brain compared to *in vitro* hippocampal or neural differentiation cultures mediate different effects on extracellular Aβ levels. Cell types differ in their ability to produce, secrete or degrade Aβ and the measurement of extracellular Aβ is the sum of these processes. It is possible for example that an equivalent amount of transgenic human Aβ are produced in aged KLC1+/- compared to KLC1+/+ murine brains, but the KLC1+/- brains have a reduced capacity to clear the Aβ, leading to an overall increase in Aβ levels.

My data suggest that reduced function of specific Kinesin-1 subunits KLC1 and Kinesin-1C may reduce neuronal levels of APP, a key protein involved in AD pathogenesis. If this result is to be of any use in potentially treating this disease, it is

essential to understand the mechanism by which this proposed regulation occurs. Toward that end, many questions remain. Are KLC1 and Kinesin-1C the only Kinesin-1 subunits capable of mediating this effect or does reduction in Kinesin-1A, Kinesin-1B or KLC2 also lower APP levels? This is important because if the effects are specific to Kinesin-1C or KLC1, treatment strategies targeting these proteins may be ultimately more useful as they may be less prone to side effects than ones perturbing the ubiquitously expressed Kinesin-1B and KLC2 subunits.

What is the mechanism by which reduced KLC1 and Kinesin-1C lowers APP levels? Does reduced Kinesin-1 transport of APP lead to less cellular APP overall? Is APP transported axonally by Kinesin-1A, Kinesin-1B or Kinesin-1C or some/all of them? Does KLC2 participate in the transport of APP? Previous work in rodent primary hippocampal neurons suggest that antisense oligonucleotides targeting Kinesin-1B substantially reduces endogenous mouse APP cell surface and axonal staining compared to sense treated cells [44,45]. No reports have described the effect on APP of loss of Kinesin-1A or KLC2. Reductions in full length KLC1 reduces anterograde transport of transfected APP-YFP in hippocampal neurons [34,47], but it doesn't stop all anterograde moving APP traffic. So what subset of APP vesicles is KLC1 associated with? The APP carboxyl-terminal domain immunoprecipitates the KLC TPR domain, likely through the scaffold JNK (c-jun N terminal kinase)-interacting protein (JIP1b) [6,48,49]. Muresan and Muresan (2005) propose that APP phosphorylated on the C terminal domain is transported using KLC [50]. Other data suggest APP may be transported axonally independent of the C terminal domain by

Kinesin-1C in a Rab3A dependent manner [51], raising the interesting possibility that not all APP containing vesicles are transported by the same mechanism. Since APP metabolism is likely regulated in part by its location within the cell it is important to understand the modes of APP localization [52].

Although it seems likely that reduced Kinesin-1C and KLC1 lowers APP levels which in turn reduces extracellular amyloid, it is also possible that there are other factors which could contribute to the differences in extracellular Aβ levels especially given the APP's complex metabolism. As mentioned previously, APP cellular location is thought to be a key factor regulating APP secretase cleavage pathways. The particular cargos of Kinesin-1C and KLC1 are largely unknown, but it is possible that the location of the secretase components could be perturbed by impaired Kinesin-1, thereby affecting substrate cleavage [53]. Once cleaved, APP fragments may be transported separately [54] and it is possible that various Kinesin-1 subunits may be responsible for secretion of these products. Thus reduction in Kinesin-1 may in this way reduce the secretion of the Aβ. Finally, Aβ is normally turned over by proteases like Neprilysin in the extracellular space [55] and it is possible that transport perturbations could affect this process as well. Regardless of the mechanism, taken together with already published results, my data suggest Kinesin-1 subunits KLC1 and Kinesin-1C regulate extracellular Aβ levels.

Model for KLC1 functions in neural development and in regulating neuronal Tau and Aβ levels.

Altogether my data suggest a model where KLC1 based Kinesin-1 transport is important for proper function of some cell types, including NPs and neurons. While KLC1 appears not to play a crucial role in undifferentiated pluripotent stem cells (Figure 4.3A), it does function in maintaining cell numbers in neural induction cultures and in proliferation of at least some NPs (Figure 4.3B), by affecting cell signaling regulating proliferation. This defect in NPs leads to reduced proportions of some neuron types (Figure 4.3C). In some neuron types, KLC1 together with Kinesin-1C, affects axon lengths (Figure 4.3C) and axonal transport of Tau and APP (Figure 4.3D). Impaired axonal transport of Tau and APP leads to misregulation of intracellular Tau and extracellular Aβ levels.

This model makes a number of testable predictions.

1. *Undifferentiated pluripotent stem cells with reduced KLC1 have normal pluripotency gene expression*. To test this prediction, perform a comparative analysis of undifferentiated control, *shKLC1-1* and *shKLC1-2* cells by mRNA expression array for genes associated with pluripotency.
2. *NPs with reduced KLC1 exhibit disruptions in cell signaling pathways associated with proliferation*. First, determine which cell signaling pathways are active in control and shKLC1 expressing NPs by mRNA expression analysis of control and shKLC1 expressing NPs. Second, verify hits by experimentally perturbing the indicated cell signaling pathways in the control

NPs. For example, withdraw or inhibit the indicated ligands or receptors and verify loss of proliferation. Next, identify the KLC1-dependent step(s) in the cell signaling pathway. Finally, rescue the proliferation defect in shKLC1 expressing NPs.

3. *Reduced function of KLC1 in motor neuron NPs leads to reduced motor neuron populations.* To test this hypothesis, first import/establish methods for differentiation of both hESC and NPs to motor and peripheral (as a control) neurons. Test whether hESC or NPs with reduced KLC1 can differentiate to these neuron types. Quantify and compare the number of motor and peripheral NP cells in control compared to cultures derived from stem cells with reduced KLC1. For the cultures originating with undifferentiated hESC, parallel cultures must be assessed for motor and peripheral NP cells prior to the generation of neurons. Identify the proportions of motor and peripheral neurons relative to control and relative to the appropriate NP populations.
4. *Reduced function of Kinesin-1C/KLC1 containing Kinesin-1 complexes impairs axonal development of some neuron types*. To test this possibility, compare axon lengths between mouse wildtype, KLC1-/- and Kinesin-1C-/- dissociated primary neurons from the brain cortex and midbrain, spinal cord motor neurons and dorsal root ganglia.
5. *In some neuron types, reduced function of Kinesin-1C/KLC1 containing Kinesin-1 complexes impairs the axonal transport of Tau and APP, leading to misregulation of Tau and Aβ levels*. To test this hypothesis, first analyze live

transport of fluorescent APP and Tau in dissociated primary mouse neurons from murine wildtype, KLC1-/- and Kinesin-1C-/- brain cortex, midbrain, spinal cord (motor) and dorsal root ganglia. Quantify intracellular Tau and extracellular Aβ in these cultures. Ask if there is a correlation between any observed impairments in APP and Tau transport and altered levels of Tau or Aβ.

Prospects for human pluripotent stem cell based systems for modeling human development, biology and disease

Since the first successful adaptation of human embryonic stem cells to *in vitro* culture [56], and the subsequent reprogramming of somatic to pluripotent cells [57,58], the use of pluripotent stem cells (PSC) to model disease and development has increased dramatically. Their utility is two-fold: they can self-renew and give rise to virtually any human cell type. In practice, controlling PSC self-renewal is straightforward and while withdrawal of self-renewal signals induces differentiation, the continual challenge is in obtaining a well characterized cell type (or cell types) of interest. The first requirement to meet this challenge is the identification markers to specifically distinguish cell types of interest. Good markers are crucial to any successful attempt to characterize differentiation progeny. Such markers may include a distinctive cellular morphology, miRNAs and cell surface and/or intracellular proteins unique to the cell type of interest. Such markers should ideally identify features related

to cellular maturity and function that is not also expressed in the precursors or other related cell types.

A second requirement for successful exploitation of PSC differentiation capacity is to understand and provide PSC the appropriate cues over the course of differentiation to induce them to adopt a particular lineage, subtype and mature cell type of interest. Substantial progress has been made in the differentiation of pluripotent cells to specific lineages using clues derived from human development [59]. Related to this goal is improving the efficiency of differentiation schemes as well as the *in vitro* conditions necessary for maintaining functional mature cell types – research areas that will likely remain active for some time.

An example of an important methodological advance which addresses both of these requirements is reported in Yuan et al (2011) [60]. In this paper we generated neural induction cultures, manually enriched for NPs and performed a large flow cytometry cell surface marker screen to discover a cell surface marker signature that recognizes NPs. This cell surface signature was subsequently used to flow sort NPs from neural induction cultures. Once sorted these NPs self renewed and differentiated into neurons and glia. Using imaging and flow cytometry screens, we also identified cell surface signatures characteristic of neurons and glia and used them to flow sort these cell types. In developing methods to produce, identify, sort and differentiate NPs, neurons and glia this paper represents an important advancement in the production of human neural types useful for regenerative medicine. The next steps will be to use such screens to identify other key cell types. For example, cell surface

markers uniquely labeling germ layer stem cells early in the course of PSC differentiation would be useful not only for applying cell sorting strategies to enrich for cells of a specific germ layer but also for monitoring the efficiency of various differentiation strategies in producing cell preparations composed of specific proportions of representatives of all three germ layers.

To demonstrate the utility of PSC for modeling human neural development and disease, I analyzed the neural differentiation progeny of hESC engineered to express reduced levels of the Kinesin-1 subunit KLC1. KLC1 was chosen because phenotypes associated with defective KLC1 have been described in animal models [8,17,18] and reduction in full length KLC1 has been shown to exacerbate Aβ and Tau pathology in adult mice [8,34,47]. Using these phenotypes of Kinesin-1 mutant animals as a guide, I analyzed KLC1-reduced hESC, NPs and neural cultures.

Neural cultures differentiated from hESC with reduced KLC1 compared to control contained neuron like cells with apparently shorter projections and less neuronal microtubule-associated markers, including Tau, suggesting that reduction in KLC1 (and possibly Kinesin-1C which is also reduced) may impair neurite outgrowth in some human neurons. Primary rodent hippocampal cultures with either reduced Kinesin-1B or KLC1 and KLC2 also develop shortened neurites [13,14], but my data from KLC1-/- and Kinesin-1C-/- hippocampal neurons suggest that genetic reduction in full length KLC1 either has either no effect (KLC1-/-) or lengthens (Kinesin-1C-/-) axons developing in culture. Why might modulating KLC1 and Kinesin-1C shorten human and lengthen mouse hippocampal neurons? One possibility is that Kinesin-1

subunits have different functions in different neuron types. This idea is supported by the fact that KLC1-/- , Kinesin-1A-/- and Kinesin-1C-/- mice exhibit different neuronal phenotypes [3,8,11,18]. One present challenge with use of human PSC derived neural cultures is that the cell types and their expected development and maturation patterns are not yet known, making interpretation of results problematic. In the rodent system, neurons are collected from a specific area of the brain and the stepwise process by which axons and dendrites are re-formed in such cultures has been known for two decades [61]. As yet there is currently no such frame of reference for human PSC derived neurons, illustrating the critical need for an improved understanding of the development, maturation and markers associated with hPSC derived cell types, including neurons.

Complex human diseases don't develop in a single isolated cell type. The well described pathology of AD occurs in the human brain, an organ which is laced with blood vessels and in which neurons are the minority cell type [62]. Since AD and control human brains cannot be fully studied, mouse strains modeling aspects of AD, though imperfect, are still valuable sources of information on how AD might develop. Amazing progress has been made in producing hPSC lines and in using them to generate individual cell types. The next challenge for regenerative medicine will be to harness human PSC for the production of more complex multi-cellular structures that mimic human tissue and organ systems. Such models will be an invaluable source of information for understanding and treating human diseases.

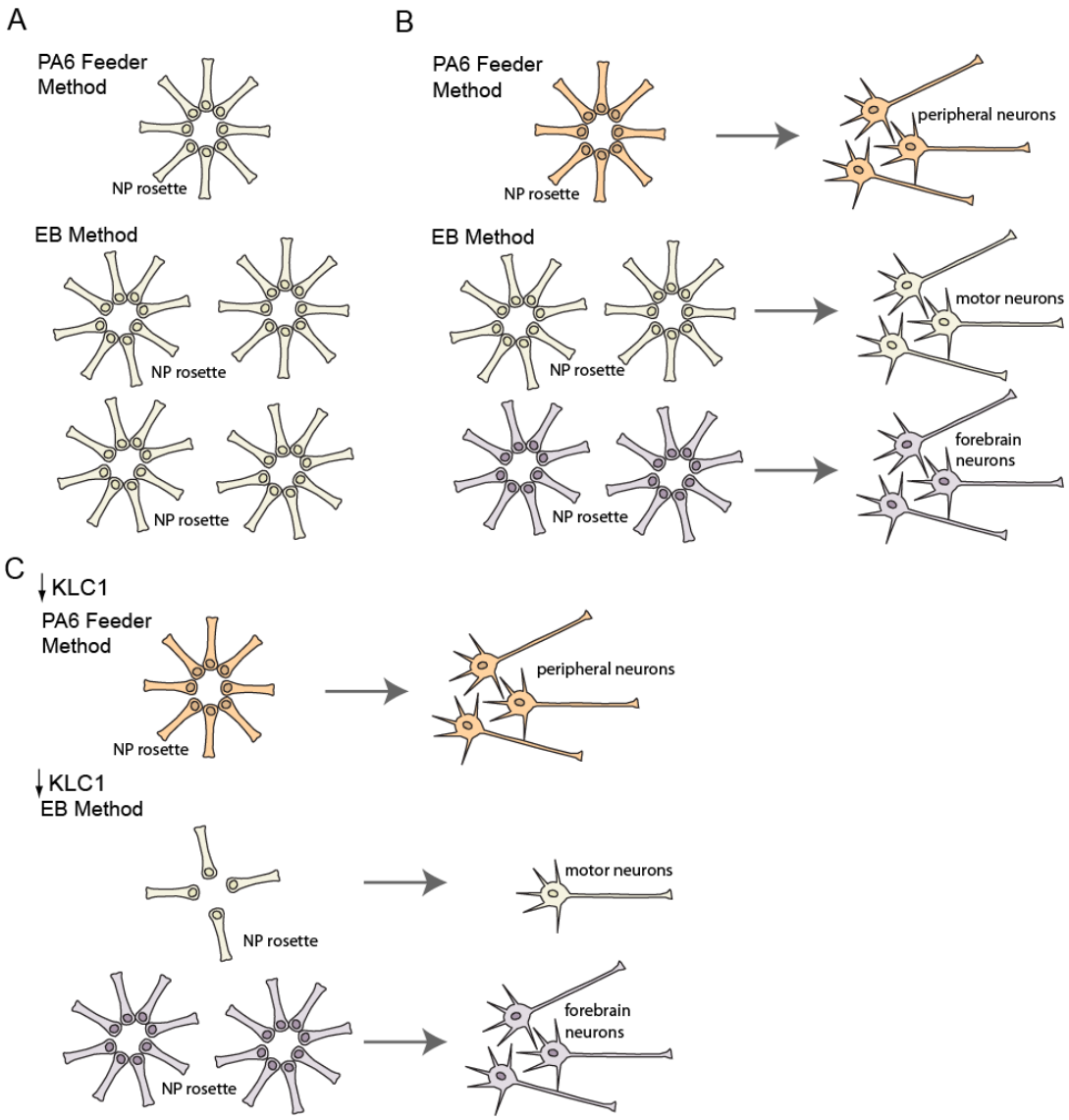


Figure 4.1. Model for how KLC1 reduction in pluripotent stem cells may affect production of specific NP and neuron subtypes. Different neural induction methods (e.g., PA6 feeder compared to EB) produce different proportions of NPs (A, left-most on B). The EB compared to the PA6 method may produce more or larger NP-producing environments (A) or, alternatively, multiple different NP subtypes (represented by different colors) that add up to higher overall proportions of NPs (B, NP rosettes). (B) Different NP subtypes give rise to different neuron subtypes (shown in different colors). (C) Different NPs and neuron subtypes have different requirements for KLC1, thus reduction in KLC1 leads to reduced populations of some (e.g. motor neuron) but not all NP and neuron subtypes.

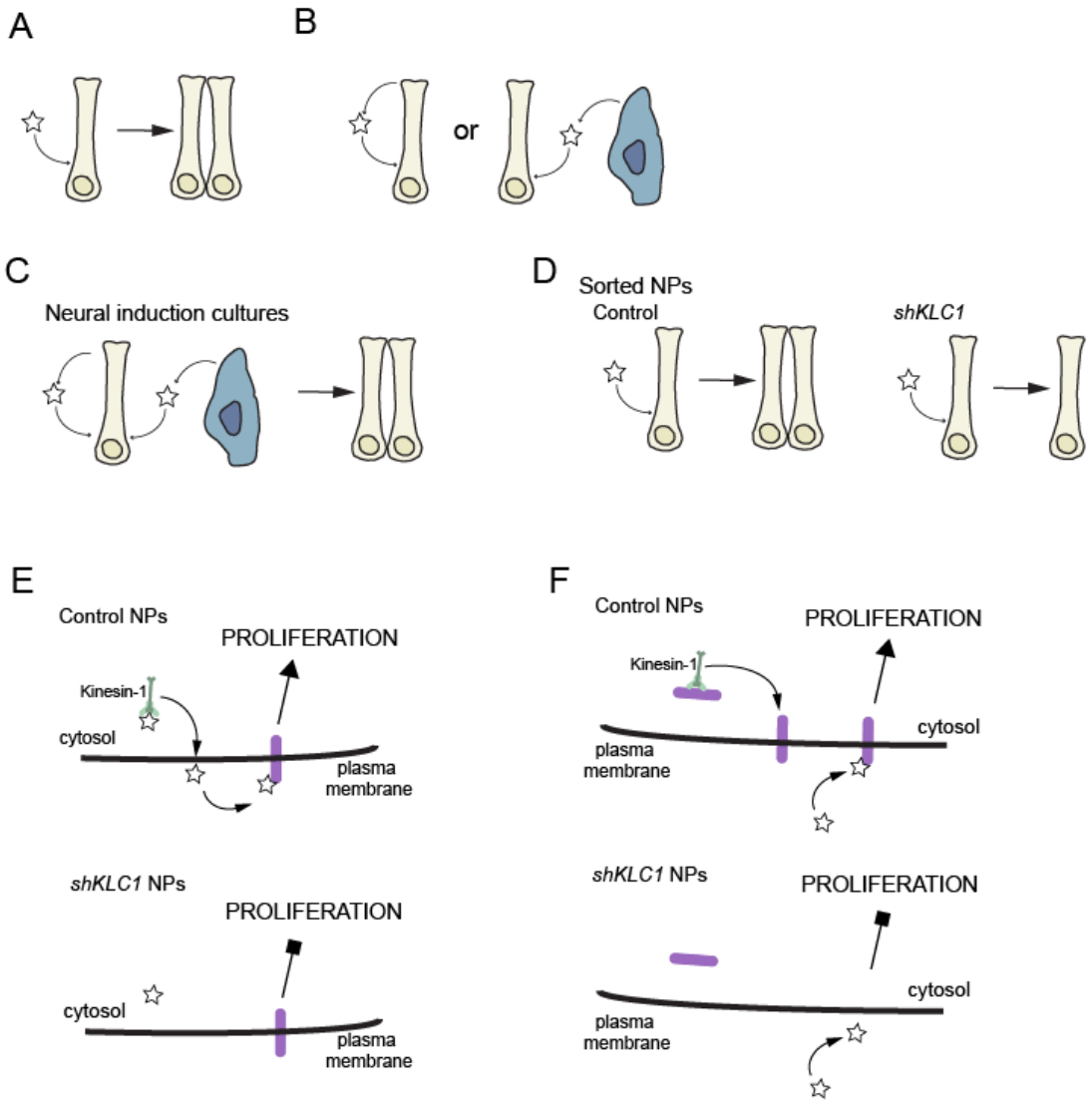
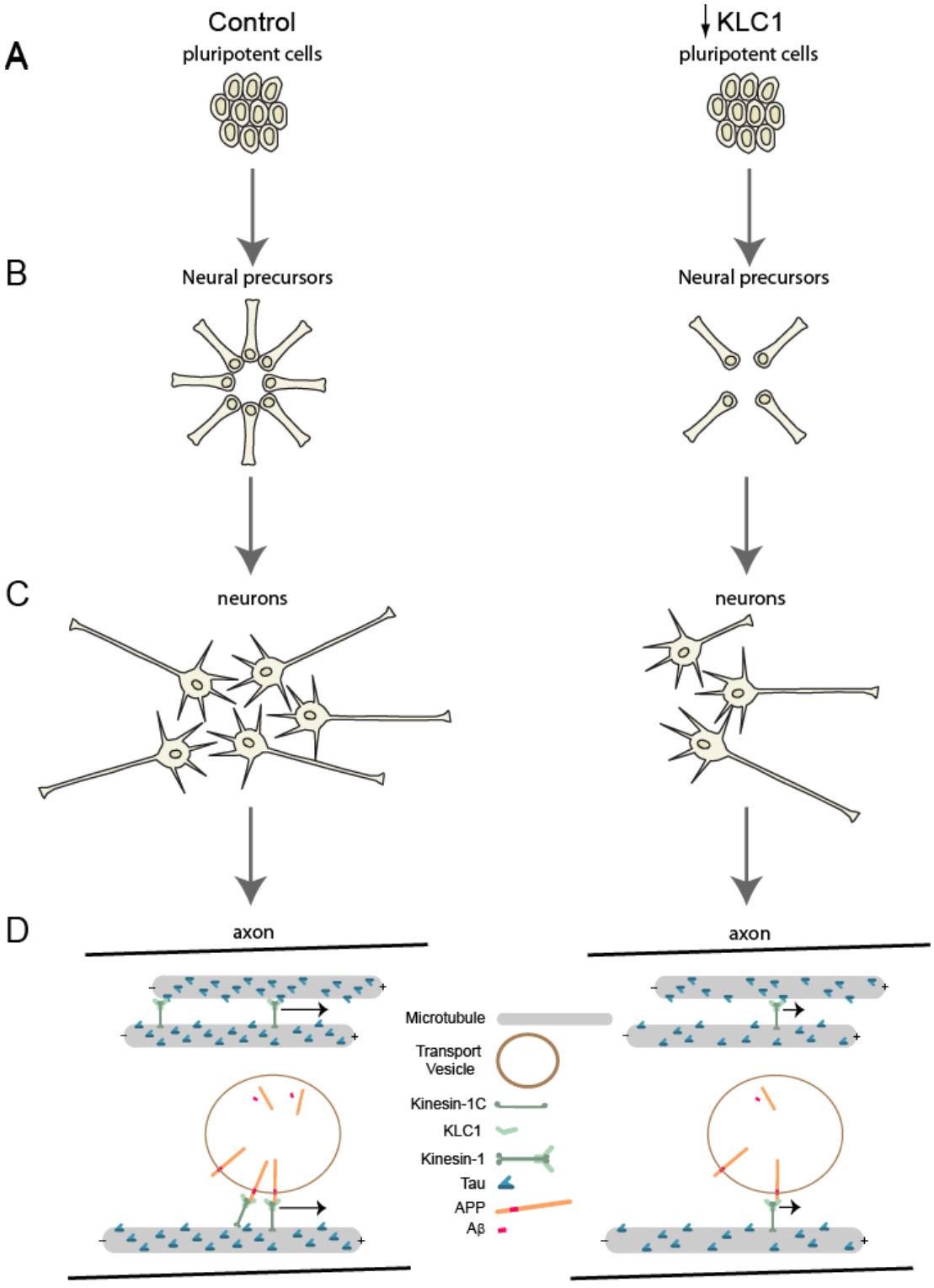


Figure 4.2. Cell signaling pathways governing proliferation in control and shKLC1 expressing NPs. (A) Molecular signals (represented by a star in A-F) induce NPs to proliferate. (B) These signals may be derived from the NPs or from other cell types, shown in blue. (C) Signals originating from both NPs and other cell types are likely present in unsorted neural induction cultures. (D) Signals from the sorted NPs are sufficient to induce proliferation of control, but not NPs with reduced KLC1. (E) Sorted NPs require KLC1 to secrete the proliferation signal. Reduced KLC1 impairs proliferation by limiting availability of the signal. (F) Sorted NPs require KLC1 to transport component(s) of the signaling apparatus, depicted here as a cell surface receptor (in purple). Reduced KLC1 interferes with the cells ability to respond to the signal and leads to reduced proliferation.

Figure 4.3. Model of KLC1 Kinesin-1 subunit functions in neural cells. (A). Undifferentiated pluripotent cells with reduced KLC1 function normally. (B) During neural induction of pluripotent stem cells, KLC1 functions to maintain cellular densities and to control proliferation potential of some NP subtypes by positively regulating cell signal pathway(s) governing NP proliferation. Reduction in KLC1 therefore leads to lower proportions of some neural progeny. (C) KLC1 has divergent functions in different neuron types, affecting axon length or (D) axonal transport of Tau and APP in some but not all neuron types. Faulty axonal transport of Tau and APP (represented by a shortened arrow) leads to misregulation of intracellular Tau and extracellular Aβ levels in affected neurons.


A
Control
pluripotent cells
KLC1
pluripotent cells
B
Neural precursors
Neural precursors
C
neurons
neurons
D
axon
axon
Microtubule
Transport Vesicle
Kinesin-1C
KLC1
Kinesin-1
Tau
APP
Aβ

References

1. Rahman A, Friedman DS, Goldstein LS (1998) Two kinesin light chain genes in mice. Identification and characterization of the encoded proteins. J. Biol. Chem 273: 15395-15403.

2. Xia C, Rahman A, Yang Z, Goldstein LS (1998) Chromosomal localization reveals three kinesin heavy chain genes in mouse. Genomics 52: 209-213. doi:10.1006/geno.1998.5427

3. Kanai Y, Okada Y, Tanaka Y, Harada A, Terada S, et al. (2000) KIF5C, a Novel Neuronal Kinesin Enriched in Motor Neurons. J. Neurosci. 20: 6374-6384.

4. Tanaka Y, Kanai Y, Okada Y, Nonaka S, Takeda S, et al. (1998) Targeted disruption of mouse conventional kinesin heavy chain, kif5B, results in abnormal perinuclear clustering of mitochondria. Cell 93: 1147-1158.

5. DeBoer SR, You Y, Szodorai A, Kaminska A, Pigino G, et al. (2008) Conventional kinesin holoenzymes are composed of heavy and light chain homodimers. Biochemistry 47: 4535-4543. doi:10.1021/bi702445j

6. Kamal A, Stokin GB, Yang Z, Xia CH, Goldstein LS (2000) Axonal transport of amyloid precursor protein is mediated by direct binding to the kinesin light chain subunit of kinesin-I. Neuron 28: 449-459.

7. Niclas J, Navone F, Hom-Booher N, Vale RD (1994) Cloning and localization of a conventional kinesin motor expressed exclusively in neurons. Neuron 12: 1059-1072.

8. Falzone TL, Stokin GB, Lillo C, Rodrigues EM, Westerman EL, et al. (2009) Axonal Stress Kinase Activation and Tau Misbehavior Induced by Kinesin-1 Transport Defects. J. Neurosci. 29: 5758-5767. doi:10.1523/JNEUROSCI.0780-09.2009

9. Encalada SE, Szpankowski L, Xia C-H, Goldstein LSB (2011) Stable Kinesin and Dynein assemblies drive the axonal transport of Mammalian prion protein vesicles. Cell 144: 551-565. doi:10.1016/j.cell.2011.01.021

10. Gauger AK, Goldstein LS (1993) The Drosophila kinesin light chain. Primary structure and interaction with kinesin heavy chain. J. Biol. Chem 268: 13657-13666.

11. Xia C-H, Roberts EA, Her L-S, Liu X, Williams DS, et al. (2003) Abnormal neurofilament transport caused by targeted disruption of neuronal kinesin heavy chain KIF5A. J. Cell Biol 161: 55-66. doi:10.1083/jcb.200301026

12. Jacobson C, Schnapp B, Banker GA (2006) A Change in the Selective Translocation of the Kinesin-1 Motor Domain Marks the Initial Specification of the Axon. Neuron 49: 797-804. doi:10.1016/j.neuron.2006.02.005

13. Ferreira A, Niclas J, Vale RD, Banker G, Kosik KS (1992) Suppression of kinesin expression in cultured hippocampal neurons using antisense oligonucleotides. J. Cell Biol 117: 595-606.

14. Kimura T, Watanabe H, Iwamatsu A, Kaibuchi K (2005) Tubulin and CRMP-2 complex is transported via Kinesin-1. J. Neurochem 93: 1371-1382. doi:10.1111/j.1471-4159.2005.03063.x

15. Konishi Y, Setou M (2009) Tubulin tyrosination navigates the kinesin-1 motor domain to axons. Nat. Neurosci 12: 559-567. doi:10.1038/nn.2314

16. Hurd DD, Saxton WM (1996) Kinesin mutations cause motor neuron disease phenotypes by disrupting fast axonal transport in Drosophila. Genetics 144: 1075-1085.

17. Gindhart JG, Desai CJ, Beushausen S, Zinn K, Goldstein LS (1998) Kinesin light chains are essential for axonal transport in Drosophila. J. Cell Biol 141: 443-454.

18. Rahman A, Kamal A, Roberts EA, Goldstein LSB (1999) Defective Kinesin Heavy Chain Behavior in Mouse Kinesin Light Chain Mutants. J Cell Biol 146: 1277-1288.

19. Pomp O, Brokhman I, Ziegler L, Almog M, Korngreen A, et al. (2008) PA6-induced human embryonic stem cell-derived neurospheres: a new source of human peripheral sensory neurons and neural crest cells. Brain Research 1230: 50-60. doi:10.1016/j.brainres.2008.07.029

20. Kim J-E, O'Sullivan ML, Sanchez CA, Hwang M, Israel MA, et al. (2011) Investigating synapse formation and function using human pluripotent stem cell-derived neurons. Proceedings of the National Academy of Sciences 108: 3005 - 3010. doi:10.1073/pnas.1007753108

21. Lim U-M, Sidhu KS, Tuch BE (2006) Derivation of Motor Neurons from three Clonal Human Embryonic Stem Cell Lines. Curr Neurovasc Res 3: 281-288.

22. Yun SJ, Byun K, Bhin J, Oh J-H, Nhung LTH, et al. (2010) Transcriptional regulatory networks associated with self-renewal and differentiation of neural stem cells. J. Cell. Physiol 225: 337-347. doi:10.1002/jcp.22294

23. Batut J, Howell M, Hill CS (2007) Kinesin-mediated transport of Smad2 is required for signaling in response to TGF-beta ligands. Dev. Cell 12: 261-274. doi:10.1016/j.devcel.2007.01.010

24. Golestaneh N, Mishra B (2005) TGF-beta, neuronal stem cells and glioblastoma. Oncogene 24: 5722-5730. doi:10.1038/sj.onc.1208925

25. Witman GB, Cleveland DW, Weingarten MD, Kirschner MW (1976) Tubulin requires tau for growth onto microtubule initiating sites. Proc. Natl. Acad. Sci. U.S.A 73: 4070-4074.

26. Cleveland DW, Hwo SY, Kirschner MW (1977) Purification of tau, a microtubule-associated protein that induces assembly of microtubules from purified tubulin. J. Mol. Biol 116: 207-225.

27. Cleveland DW, Hwo SY, Kirschner MW (1977) Physical and chemical properties of purified tau factor and the role of tau in microtubule assembly. J. Mol. Biol 116: 227-247.

28. Grundke-Iqbal I, Iqbal K, Tung YC, Quinlan M, Wisniewski HM, et al. (1986) Abnormal phosphorylation of the microtubule-associated protein tau (tau) in Alzheimer cytoskeletal pathology. Proc. Natl. Acad. Sci. U.S.A 83: 4913-4917.

29. Ihara Y, Nukina N, Miura R, Ogawara M (1986) Phosphorylated tau protein is integrated into paired helical filaments in Alzheimer's disease. J. Biochem 99: 1807-1810.

30. Nukina N, Ihara Y (1986) One of the antigenic determinants of paired helical filaments is related to tau protein. J. Biochem 99: 1541-1544.

31. Kosik KS, Joachim CL, Selkoe DJ (1986) Microtubule-associated protein tau (tau) is a major antigenic component of paired helical filaments in Alzheimer disease. Proc. Natl. Acad. Sci. U.S.A 83: 4044-4048.

32. Wood JG, Mirra SS, Pollock NJ, Binder LI (1986) Neurofibrillary tangles of Alzheimer disease share antigenic determinants with the axonal microtubule-associated protein tau (tau). Proc. Natl. Acad. Sci. U.S.A 83: 4040-4043.

33. Utton MA, Noble WJ, Hill JE, Anderton BH, Hanger DP (2005) Molecular motors implicated in the axonal transport of tau and {alpha}-synuclein. J Cell Sci 118: 4645-4654. doi:10.1242/jcs.02558

34. Falzone TL, Gunawardena S, McCleary D, Reis G, Goldstein LSB (2010) Kinesin-1 transport reductions enhance human tau hyperphosphorylation, aggregation and neurodegeneration in animal models of tauopathies. Hum Mol Genet. Available: http://www.ncbi.nlm.nih.gov/pubmed/20817925. Accessed 8 Sep 2010.

35. Jancsik V, Filliol D, Rendon A (1996) Tau proteins bind to kinesin and modulate its activation by microtubules. Neurobiology (Bp) 4: 417-429.

36. Dubey M, Chaudhury P, Kabiru H, Shea TB (2008) Tau inhibits anterograde axonal transport and perturbs stability in growing axonal neurites in part by displacing kinesin cargo: neurofilaments attenuate tau-mediated neurite instability. Cell Motil. Cytoskeleton 65: 89-99. doi:10.1002/cm.20243

37. Cuchillo-Ibanez I, Seereeram A, Byers HL, Leung K-Y, Ward MA, et al. (2008) Phosphorylation of tau regulates its axonal transport by controlling its binding to kinesin. FASEB J. 22: 3186-3195. doi:10.1096/fj.08-109181

38. Nizzardo M, Simone C, Falcone M, Locatelli F, Riboldi G, et al. (2010) Human motor neuron generation from embryonic stem cells and induced pluripotent stem cells. Cell. Mol. Life Sci 67: 3837-3847. doi:10.1007/s00018-010-0463-y

39. Glenner GG, Wong CW (1984) Alzheimer's disease and Down's syndrome: sharing of a unique cerebrovascular amyloid fibril protein. Biochem. Biophys. Res. Commun 122: 1131-1135.

40. Goldgaber D, Lerman MI, McBride OW, Saffiotti U, Gajdusek DC (1987) Characterization and chromosomal localization of a cDNA encoding brain amyloid of Alzheimer's disease. Science 235: 877-880.

41. Kang J, Lemaire HG, Unterbeck A, Salbaum JM, Masters CL, et al. (1987) The precursor of Alzheimer's disease amyloid A4 protein resembles a cell-surface receptor. Nature 325: 733-736. doi:10.1038/325733a0

42. Robakis NK, Ramakrishna N, Wolfe G, Wisniewski HM (1987) Molecular cloning and characterization of a cDNA encoding the cerebrovascular and the neuritic plaque amyloid peptides. Proc. Natl. Acad. Sci. U.S.A 84: 4190-4194.

43. Tanzi RE, Gusella JF, Watkins PC, Bruns GA, St George-Hyslop P, et al. (1987) Amyloid beta protein gene: cDNA, mRNA distribution, and genetic linkage near the Alzheimer locus. Science 235: 880-884.

44. Ferreira A, Caceres A, Kosik KS (1993) Intraneuronal compartments of the amyloid precursor protein. J. Neurosci 13: 3112-3123.

45. Yamazaki T, Selkoe DJ, Koo EH (1995) Trafficking of cell surface beta-amyloid precursor protein: retrograde and transcytotic transport in cultured neurons. J. Cell Biol 129: 431-442.

46. Kaether C, Skehel P, Dotti CG (2000) Axonal membrane proteins are transported in distinct carriers: a two-color video microscopy study in cultured hippocampal neurons. Mol. Biol. Cell 11: 1213-1224.

47. Stokin GB, Lillo C, Falzone TL, Brusch RG, Rockenstein E, et al. (2005) Axonopathy and Transport Deficits Early in the Pathogenesis of Alzheimer's Disease. Science 307: 1282-1288. doi:10.1126/science.1105681

48. Inomata H, Nakamura Y, Hayakawa A, Takata H, Suzuki T, et al. (2003) A scaffold protein JIP-1b enhances amyloid precursor protein phosphorylation by JNK and its association with kinesin light chain 1. J. Biol. Chem 278: 22946-22955. doi:10.1074/jbc.M212160200

49. Matsuda S, Matsuda Y, D'Adamio L (2003) Amyloid beta protein precursor (AbetaPP), but not AbetaPP-like protein 2, is bridged to the kinesin light chain by the scaffold protein JNK-interacting protein 1. J. Biol. Chem 278: 38601-38606. doi:10.1074/jbc.M304379200

50. Muresan Z, Muresan V (2005) Coordinated transport of phosphorylated amyloid-beta precursor protein and c-Jun NH2-terminal kinase-interacting protein-1. J. Cell Biol 171: 615-625. doi:10.1083/jcb.200502043

51. Szodorai A, Kuan Y-H, Hunzelmann S, Engel U, Sakane A, et al. (2009) APP anterograde transport requires Rab3A GTPase activity for assembly of the transport vesicle. J. Neurosci 29: 14534-14544. doi:10.1523/JNEUROSCI.1546-09.2009

52. Thinakaran G, Koo EH (2008) Amyloid Precursor Protein Trafficking, Processing, and Function. Journal of Biological Chemistry 283: 29615 -29619. doi:10.1074/jbc.R800019200

53. Kamal A, Almenar-Queralt A, LeBlanc JF, Roberts EA, Goldstein LS (2001) Kinesin-mediated axonal transport of a membrane compartment containing beta-secretase and presenilin-1 requires APP. Nature 414: 643-648. doi:10.1038/414643a

54. Muresan V, Varvel NH, Lamb BT, Muresan Z (2009) The cleavage products of amyloid-beta precursor protein are sorted to distinct carrier vesicles that are independently transported within neurites. J. Neurosci 29: 3565-3578. doi:10.1523/JNEUROSCI.2558-08.2009

55. Iwata N, Tsubuki S, Takaki Y, Watanabe K, Sekiguchi M, et al. (2000) Identification of the major Abeta1-42-degrading catabolic pathway in brain parenchyma: suppression leads to biochemical and pathological deposition. Nat. Med 6: 143-150. doi:10.1038/72237

56. Thomson JA, Itskovitz-Eldor J, Shapiro SS, Waknitz MA, Swiergiel JJ, et al. (1998) Embryonic Stem Cell Lines Derived from Human Blastocysts. Science 282: 1145-1147. doi:10.1126/science.282.5391.1145

57. Takahashi K, Tanabe K, Ohnuki M, Narita M, Ichisaka T, et al. (2007) Induction of Pluripotent Stem Cells from Adult Human Fibroblasts by Defined Factors. Cell 131: 861-872. doi:10.1016/j.cell.2007.11.019

58. Yu J, Vodyanik MA, Smuga-Otto K, Antosiewicz-Bourget J, Frane JL, et al. (2007) Induced Pluripotent Stem Cell Lines Derived from Human Somatic Cells. Science 318: 1917-1920. doi:10.1126/science.1151526

59. Irion S, Nostro MC, Kattman SJ, Keller GM (2008) Directed differentiation of pluripotent stem cells: from developmental biology to therapeutic applications. Cold Spring Harb. Symp. Quant. Biol 73: 101-110. doi:10.1101/sqb.2008.73.065

60. Yuan SH, Martin J, Elia J, Flippin J, Paramban RI, et al. (2011) Cell-surface marker signatures for the isolation of neural stem cells, glia and neurons derived from human pluripotent stem cells. PLoS ONE 6: e17540. doi:10.1371/journal.pone.0017540

61. Dotti CG, Sullivan CA, Banker GA (1988) The establishment of polarity by hippocampal neurons in culture. J. Neurosci 8: 1454-1468.

62. Nolte J (2002) The Human Brain: An Introduction to Its Functional Anatomy. 5th ed. Mosby. p.